In Vitro Selectivity of an Acyclic Cucurbit[n]uril Molecular Container towards Neuromuscular Blocking Agents Relative to Commonly Used Drugs

By Shweta Ganapati,[a] Peter Y. Zavalij,[a] Matthias Eikermann[b,] and Lyle Isaacs[a,]**

[a]Department of Chemistry and Biochemistry, University of Maryland, College Park, MD 20742;
[b]Department of Anesthesia, Critical Care and Pain Medicine, Massachusetts General Hospital and Harvard Medical School, 55 Fruit Street, Boston, Massachusetts 02114

Supporting Information

Table of Contents **Pages**

General experimental details. Drugs used for measuring binding constants with **2** were purchased from commercial suppliers and used without further purification. Compound **2** was prepared according to the literature procedure.[1] ^{1}H NMR spectra were measured on commercial spectrometers operating at 400 or 600 MHz. UV-Vis absorbance was measured on a Varian Cary 100 UV spectrophotometer.

Determination of K_a between Host 2 with various drugs using UV/Vis spectroscopy. K_a values up to 10^4 M^{-1} can be measured reliably by ^{1}H NMR spectroscopic methods. For values that exceed this level it is necessary to use other techniques such as UV/Vis, fluorescence, or isothermal titration calorimetry. UV/Vis spectroscopy was used in this work.

The K_a between **2** and **4** (tetracycline, UV/Vis active drug) was determined by direct titration of a fixed concentration of **4** with increasing concentrations of **2**. The K_a value was determined by fitting the change in absorbance as a function of host concentration to a 1:1 binding model. In order to determine the K_a value for **2** toward guests which were not UV/Vis active, an indicator displacement assay involving the addition of guest to a solution of **2** and dye Rhodamine 6G was used. The change in UV/Vis absorbance as a function of guest concentration was fitted to a competitive binding model which allowed determination of the K_a values based on the known total concentrations of **2**, Rhodamine 6G, and drug. The known K_a value of the **2**•Rhodamine 6G complex (2.3×10^6 M^{-1}) was used as input in the competitive binding model.[2]

References: 1) D. Ma, G. Hettiarachchi, D. Nguyen, B. Zhang, J. B. Wittenberg, P. Y. Zavalij, V. Briken, L. Isaacs *Nat. Chem.* 2012, **4**, 503-510. 2) D. Ma, B. Zhang, U. Hoffmann, M. G. Sundrug, M. Eikermann, L. Isaacs *Angew. Chem. Int. Ed.* 2012, **51**, 11358-11362.

Binding Models Used to Determine Values of K_a with Micromath Scientist

1:1 Binding Model for UV/Vis.

```
// Micromath Scientist Model File
// 1:1 Host:Guest binding model
//This model assumes the guest concentration is fixed and host concentration is varied
IndVars: ConcHostTot
DepVars: SpectroscopicSignal
Params: Ka, ConcGuestTot, SpectroscopicSignalMin, SpectroscopicSignalMax
Ka = ConcHostGuest/(ConcHostFree*ConcGuestFree)
ConcHostTot=ConcHostFree + ConcHostGuest
ConcGuestTot=ConcGuestFree + ConcHostGuest
SpectroscopicSignal = SpectroscopicSignalMin + (SpectroscopicSignalMax - SpectroscopicSignalMin)
* (ConcHostGuest/ConcGuestTot)
//Constraints
0 < ConcHostFree < ConcHostTot
0 < Ka
0 < ConcGuestFree < ConcGuestTot
0 < ConcHostGuest < ConcHostTot
```

Competitive Binding (Indicator Displacement) Models.

Competitive Model Fitting Absorbance at One Wavelength.

```
// MicroMath Scientist Model File
IndVars: ConcAntot
DepVars: Absorb
Params: ConcHtot, ConcGtot, Khg, Kha, AbsorbMax, AbsorbMin
Khg = ConcHG / (ConcH * ConcG)
Kha = ConcHAn / (ConcH * ConcAn)
Absorb = AbsorbMin + (AbsorbMax-AbsorbMin)*(ConcHG/ConcGtot)
ConcHtot = ConcH + ConcHG + ConcHAn
ConcGtot = ConcHG + ConcG
ConcAntot = ConcAn + ConcHAn
0 < ConcHG < ConcHtot
0 < ConcH < ConcHtot
0 < ConcG < ConcGtot
0 < ConcAn < ConcAntot
***
```

Competitive Model Fitting Absorbance at Two Wavelengths.

```
// MicroMath Scientist Model File
IndVars: ConcAntot
DepVars: Absorb1, Absorb2
Params:Khg, Kha, AbsorbMax1, AbsorbMin1, AbsorbMax2, AbsorbMin2
Khg = ConcHG / (ConcH * ConcG)
```

Kha = ConcHAn / (ConcH * ConcAn)
Absorb1 = AbsorbMin1 + (AbsorbMax1-AbsorbMin1)*(ConcHG/0.00001)
Absorb2 = AbsorbMin2 + (AbsorbMax2-AbsorbMin2)*(ConcHG/0.00001)
0.00001 = ConcH + ConcHG + ConcHAn
0.00001= ConcHG + ConcG
ConcAntot = ConcAn + ConcHAn
0 < ConcHG < 0.00001
0 < ConcH < 0.00001
0 < ConcG < 0.00001
0 < ConcAn < ConcAntot
***

(A)

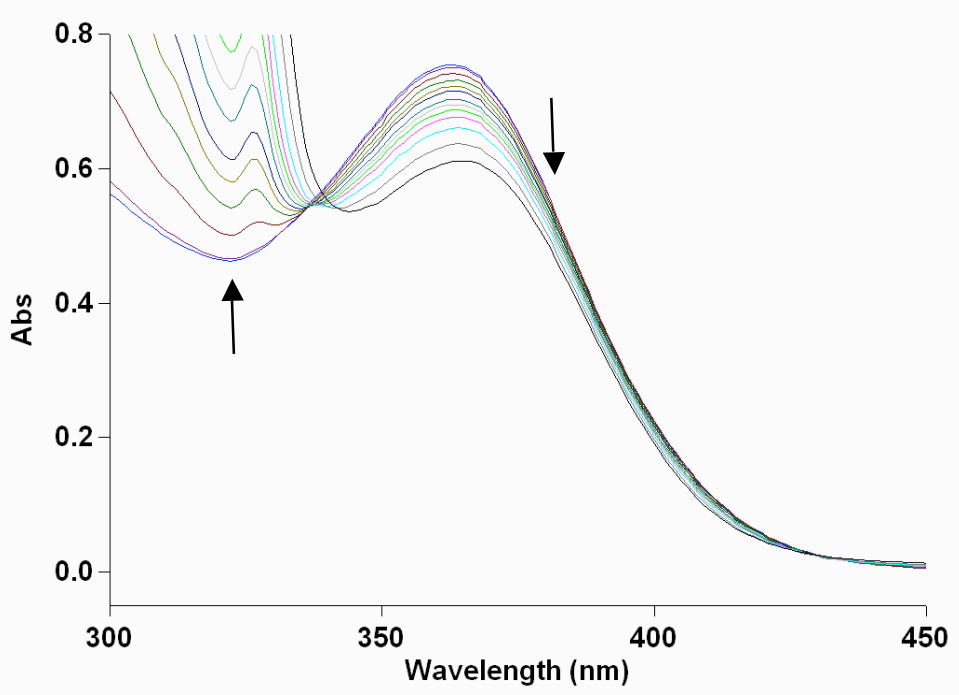

(B)

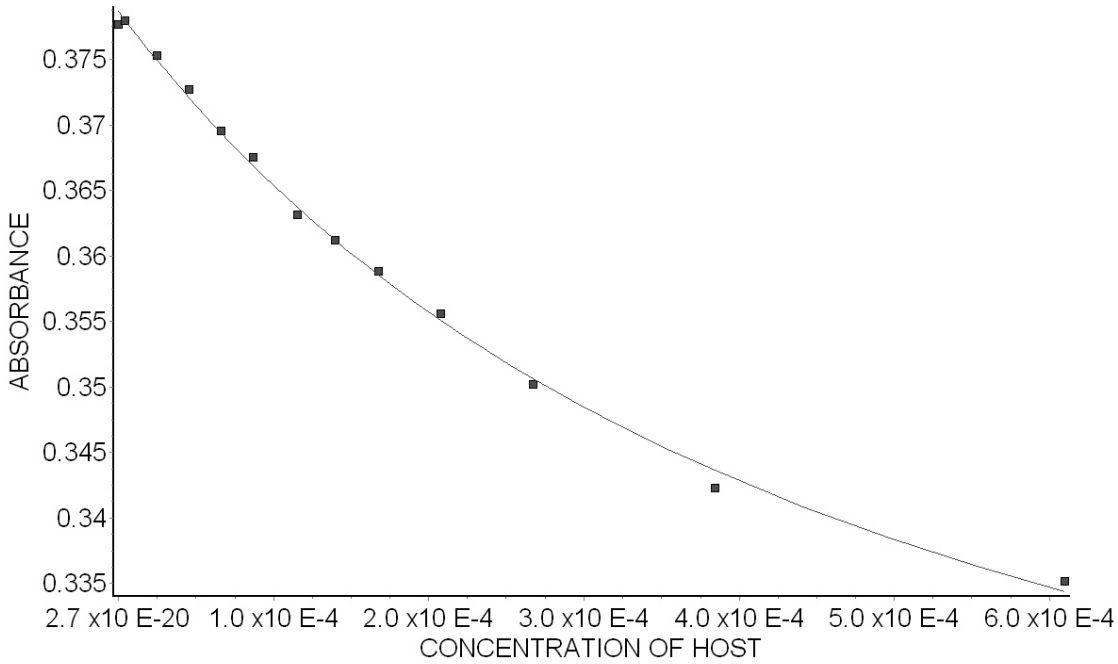

Figure S1. (A) UV/Vis spectra from the titration of **2** (0–610 μM) with guest **4** (57.3 μM) in 20 mM NaH_2PO_4 buffer (pH = 7.4); (B) plot of the A_{390} as a function of the concentration of **2**. The solid line represents the best non-linear fit of the data to a 1:1 binding model ($K_a = (2.3 \pm 0.2) \times 10^3\ M^{-1}$).

(A)

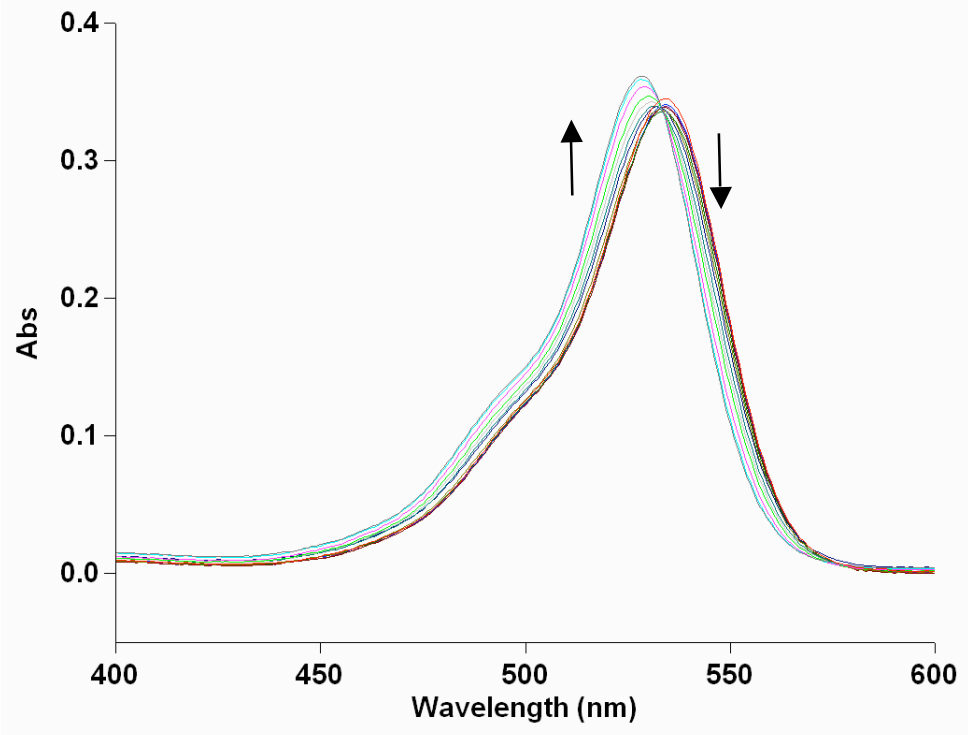

(B)

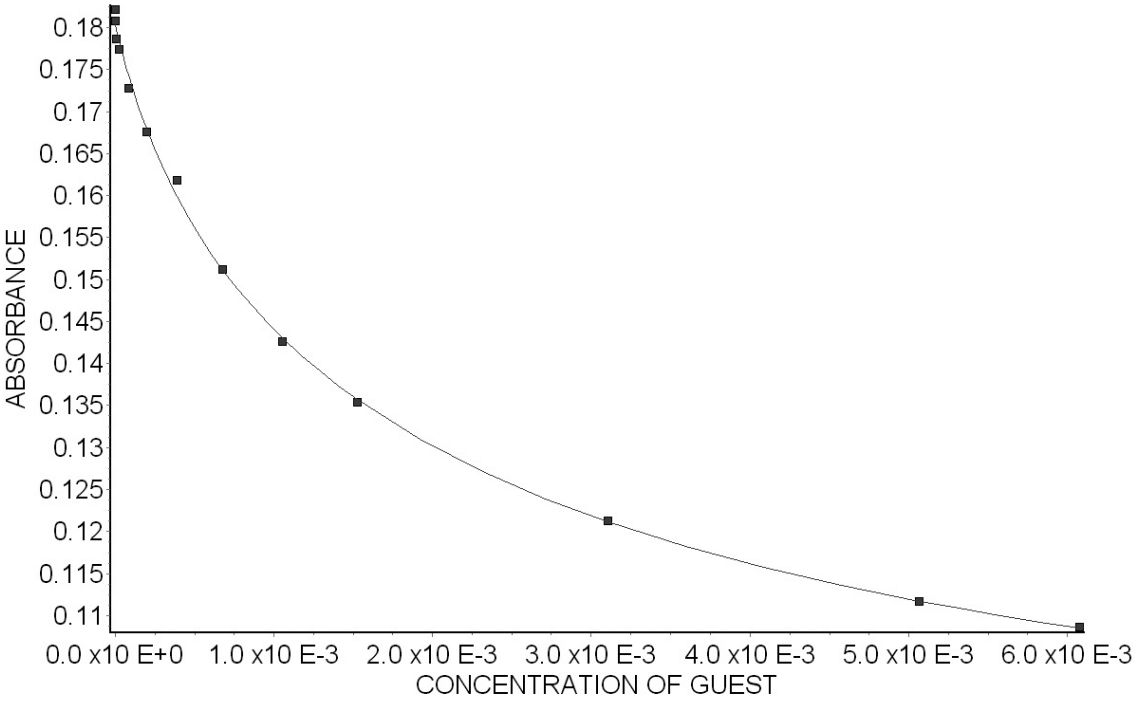

Figure S2. (A) UV/Vis spectra from the titration of **2** (5.07 μM) and Rhodamine 6G (5.01 μM) with guest **8** (0 – 6.08 mM) in 20 mM NaH_2PO_4 buffer (pH = 7.4); (B) plot of the A_{550} as a function of the concentration of **8**. The solid line represents the best non-linear fit of the data to a competitive binding model ($K_a = (5.9 \pm 0.5) \times 10^3$ M^{-1}).

(A)

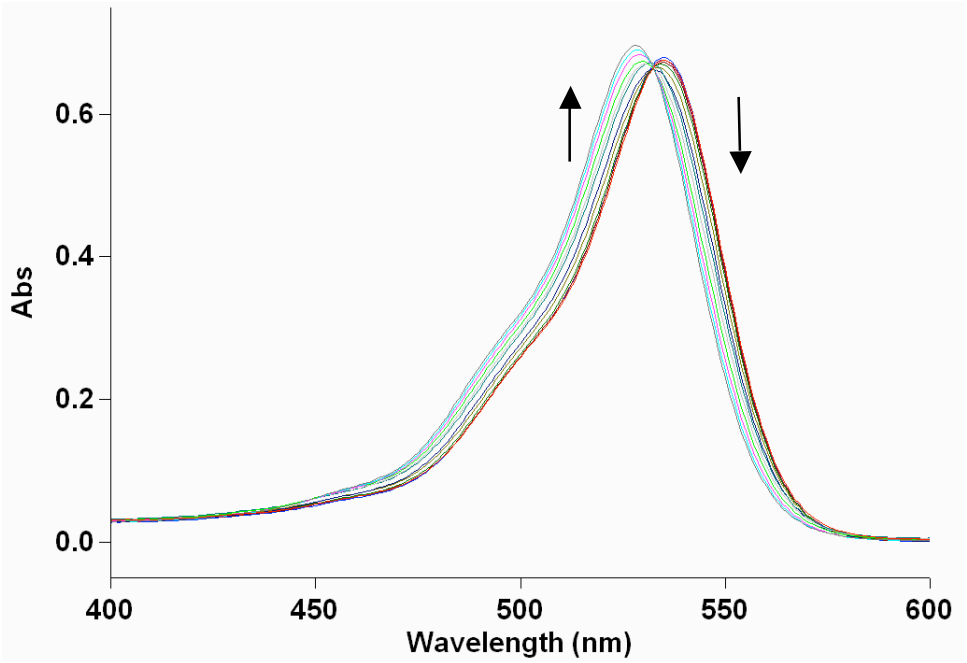

(B)

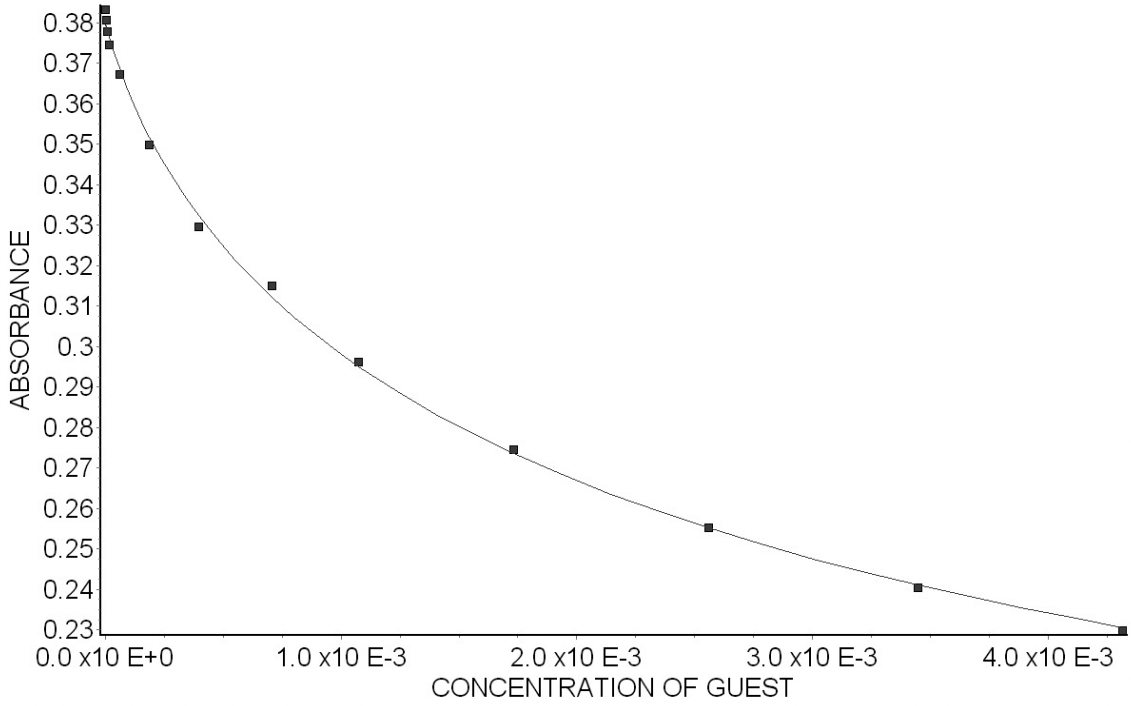

Figure S3. (A) UV/Vis spectra from the titration of **2** (10.1 μM) and Rhodamine 6G (9.96 μM) with guest **10** (0 – 4.32 mM) in 20 mM NaH_2PO_4 buffer (pH = 7.4); (B) plot of the A_{550} as a function of the concentration of **10**. The solid line represents the best non-linear fit of the data to a competitive binding model ($K_a = (8.6 \pm 0.8) \times 10^3\ M^{-1}$).

(A)

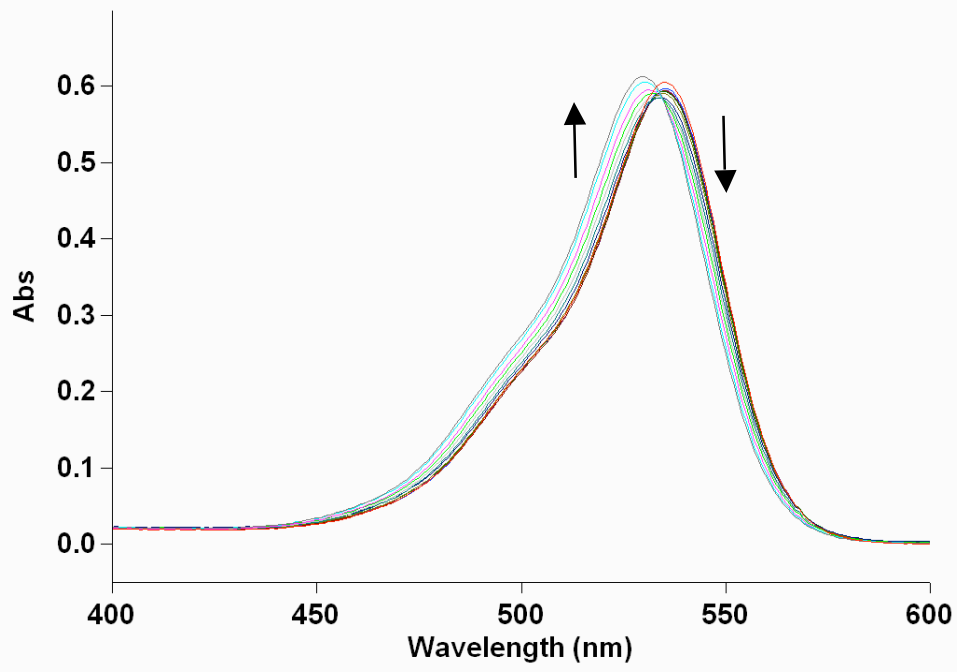

(B)

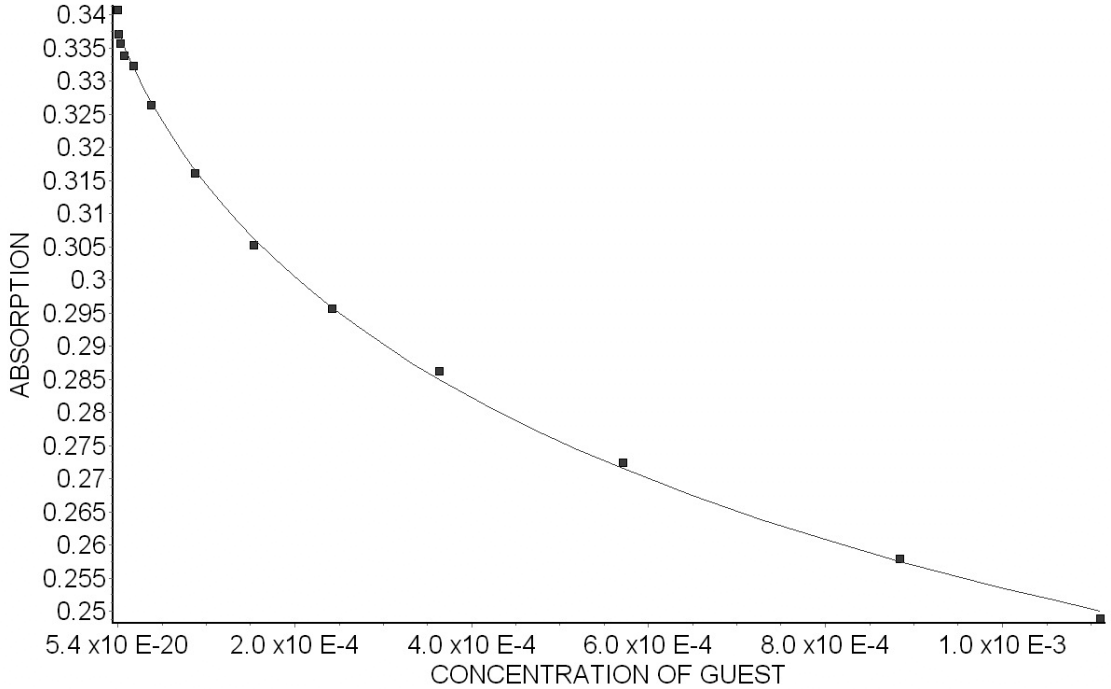

Figure S4. (A) UV/Vis spectra from the titration of **2** (9.98 μM) and Rhodamine 6G (9.96 μM) with guest **12** (0 – 1.11 mM) in 20 mM NaH_2PO_4 buffer (pH = 7.4); (B) plot of the A_{550} as a function of the concentration of **12**. The solid line represents the best non-linear fit of the data to a competitive binding model ($K_a = (2.1 \pm 0.2) \times 10^4\ M^{-1}$).

(A)

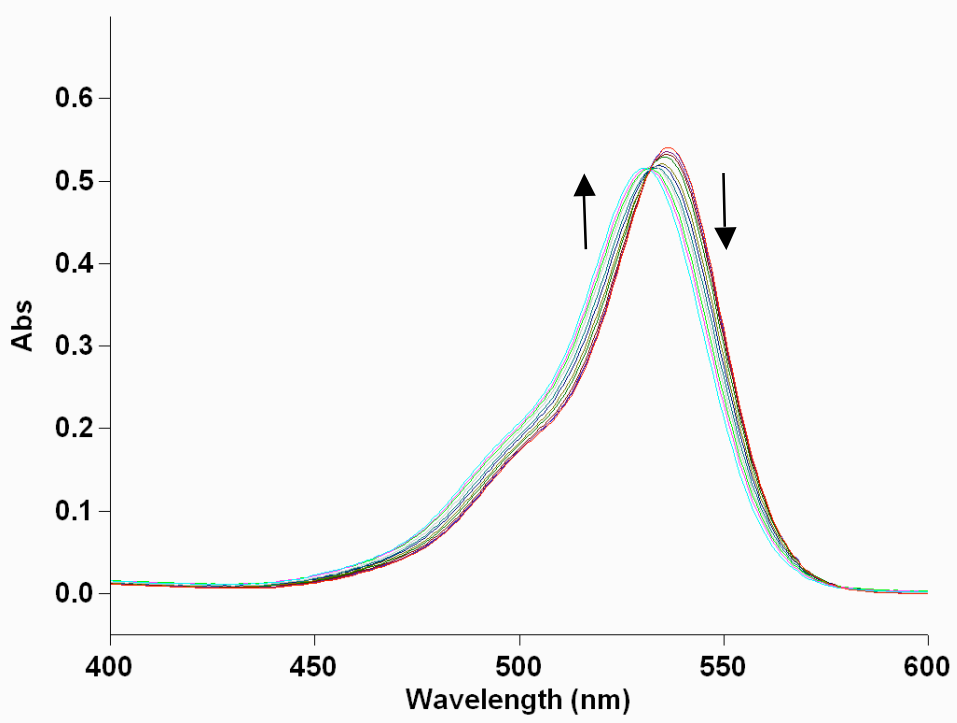

(B)

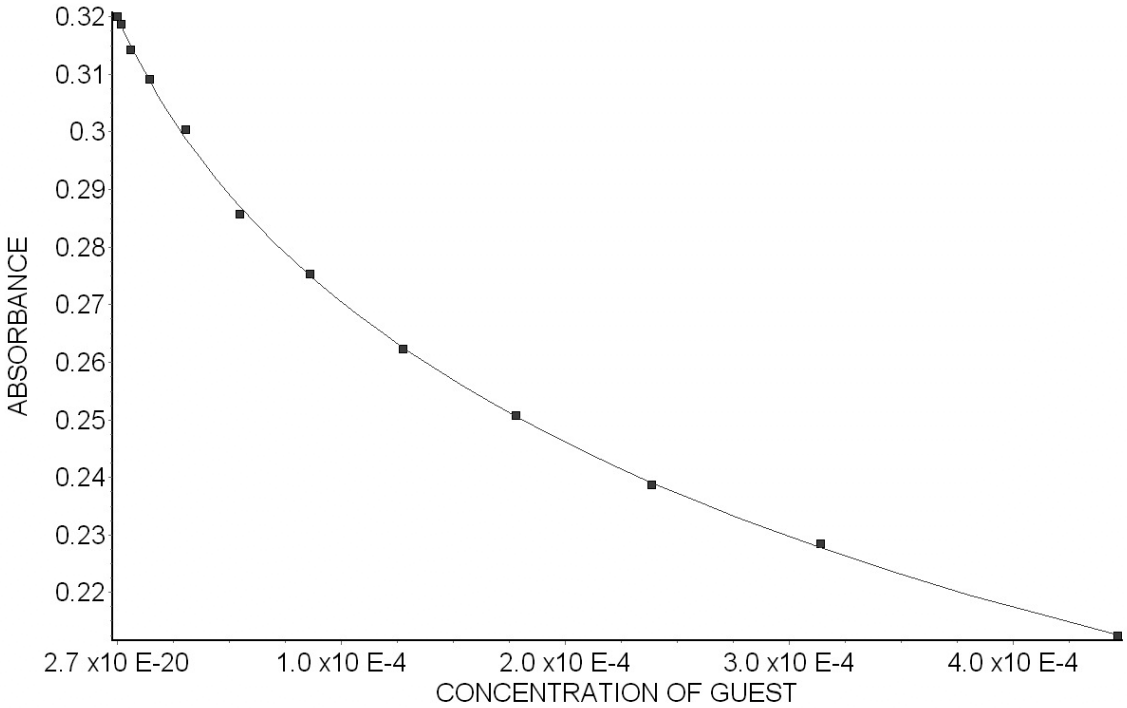

Figure S5. (A) UV/Vis spectra from the titration of **2** (10.2 μM) and Rhodamine 6G (9.96 μM) with guest **14** (0 – 447 μM) in 20 mM NaH_2PO_4 buffer (pH = 7.4); (B) plot of the A_{550} as a function of the concentration of **14**. The solid line represents the best non-linear fit of the data to a competitive binding model ($K_a = (4.4 \pm 0.3) \times 10^4\ M^{-1}$).

(A)

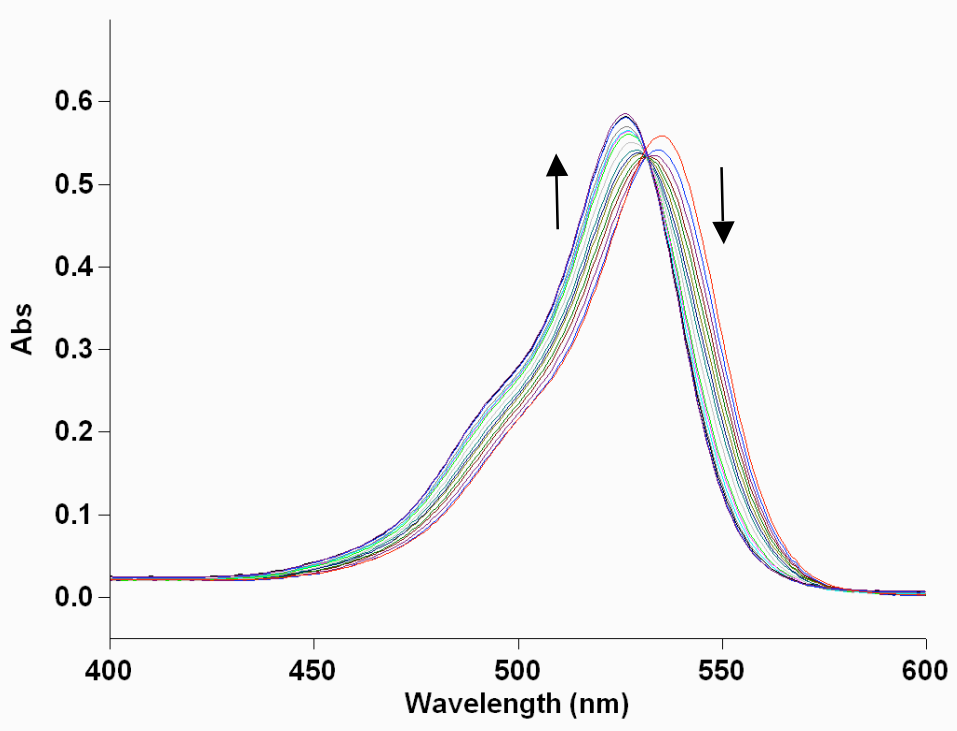

(B)

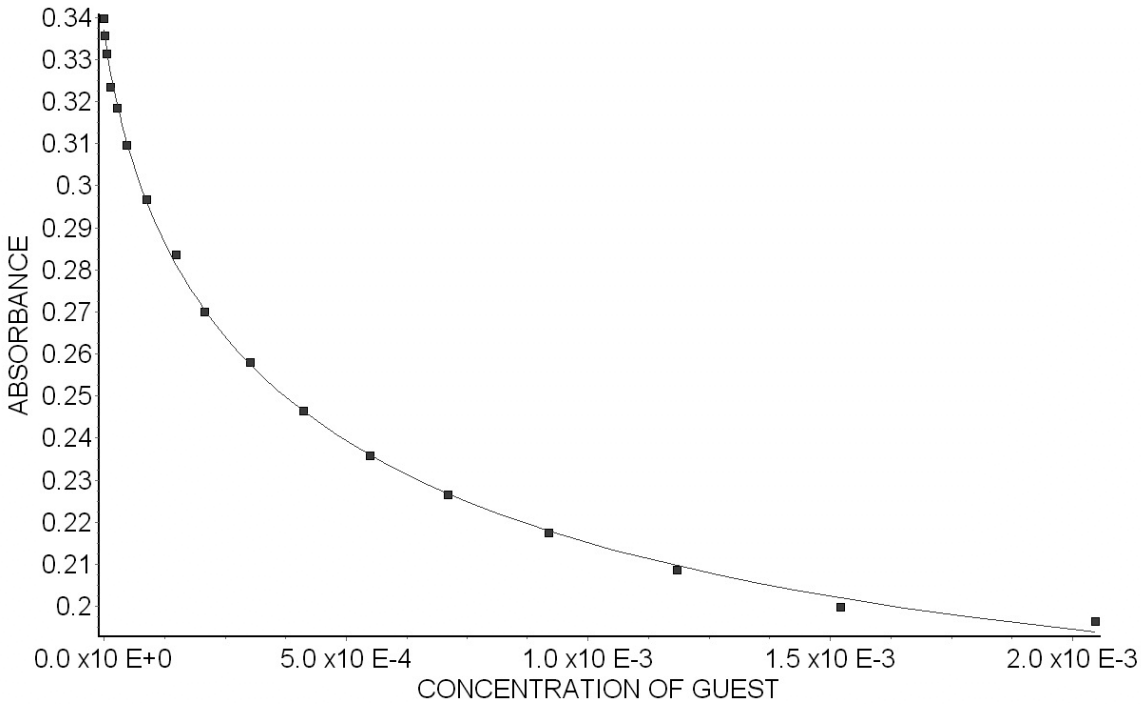

Figure S6. (A) UV/Vis spectra from the titration of **2** (9.92 μM) and Rhodamine 6G (10.0 μM) with guest **15** (0 – 2.05 mM) in 20 mM NaH_2PO_4 buffer (pH = 7.4); (B) plot of the A_{550} as a function of the concentration of **15**. The solid line represents the best non-linear fit of the data to a competitive binding model ($K_a = (4.8 \pm 0.3) \times 10^4\ M^{-1}$)

(A)

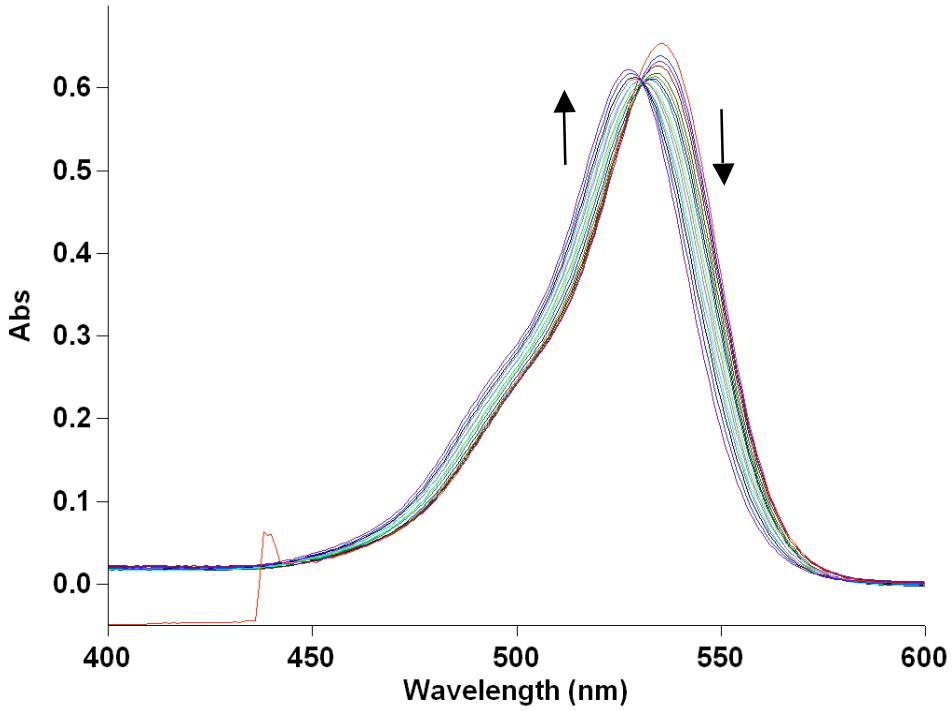

(B)

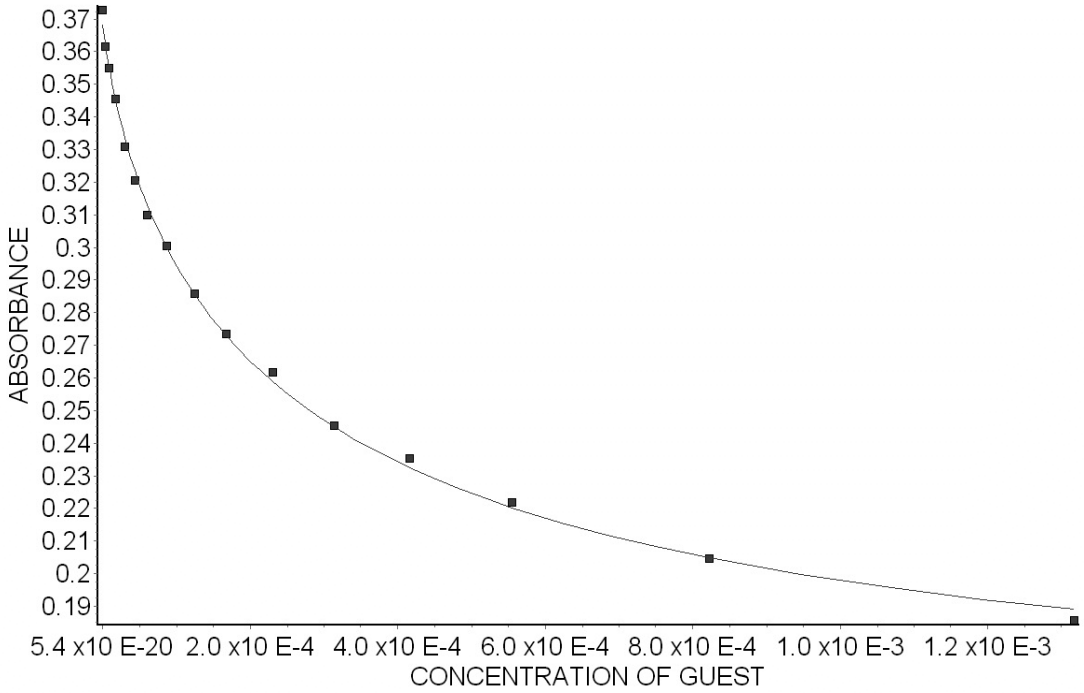

Figure S7. (A) UV/Vis spectra from the titration of **2** (9.92 μM) and Rhodamine 6G (10.0 μM) with guest **16** (0 – 1.32 mM) in 20 mM NaH_2PO_4 buffer (pH = 7.4); (B) plot of the A_{550} as a function of the concentration of **16**. The solid line represents the best non-linear fit of the data to a competitive binding model ($K_a = (8.3 \pm 0.6) \times 10^4\ M^{-1}$).

(A)

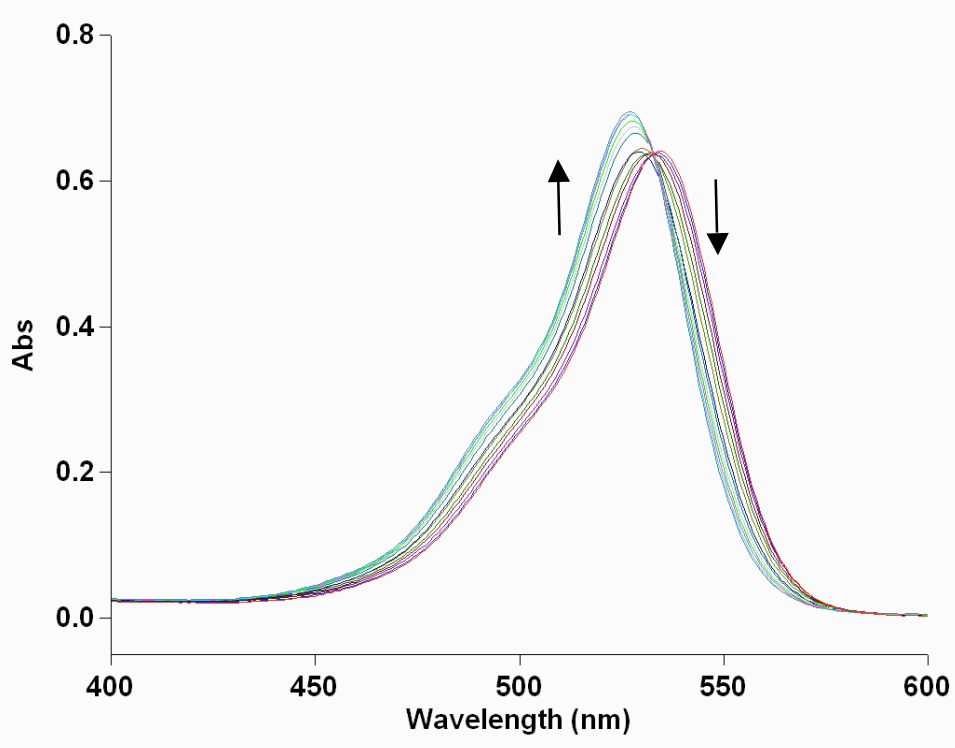

(B)

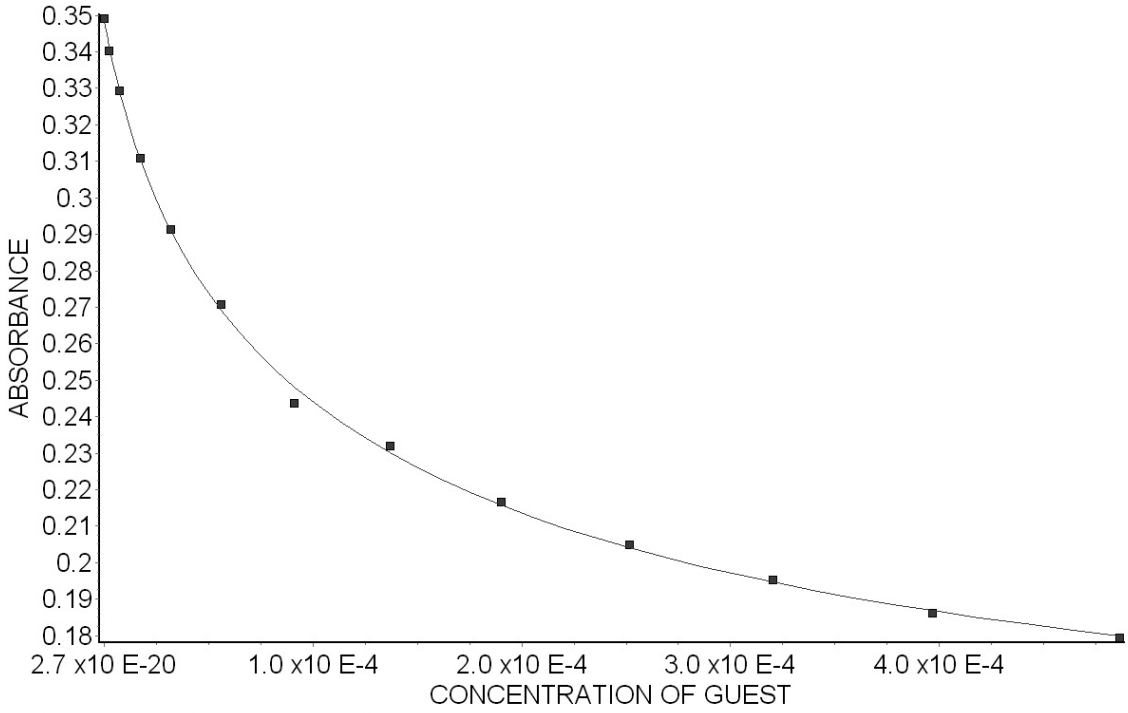

Figure S8. (A) UV/Vis spectra from the titration of **2** (10.1 μM) and Rhodamine 6G (9.96 μM) with guest **17** (0 – 486 μM) in 20 mM NaH_2PO_4 buffer (pH = 7.4); (B) plot of the A_{550} as a function of the concentration of **17**. The solid line represents the best non-linear fit of the data to a competitive binding model ($K_a = (1.9 \pm 0.1) \times 10^5\ M^{-1}$).

(A)

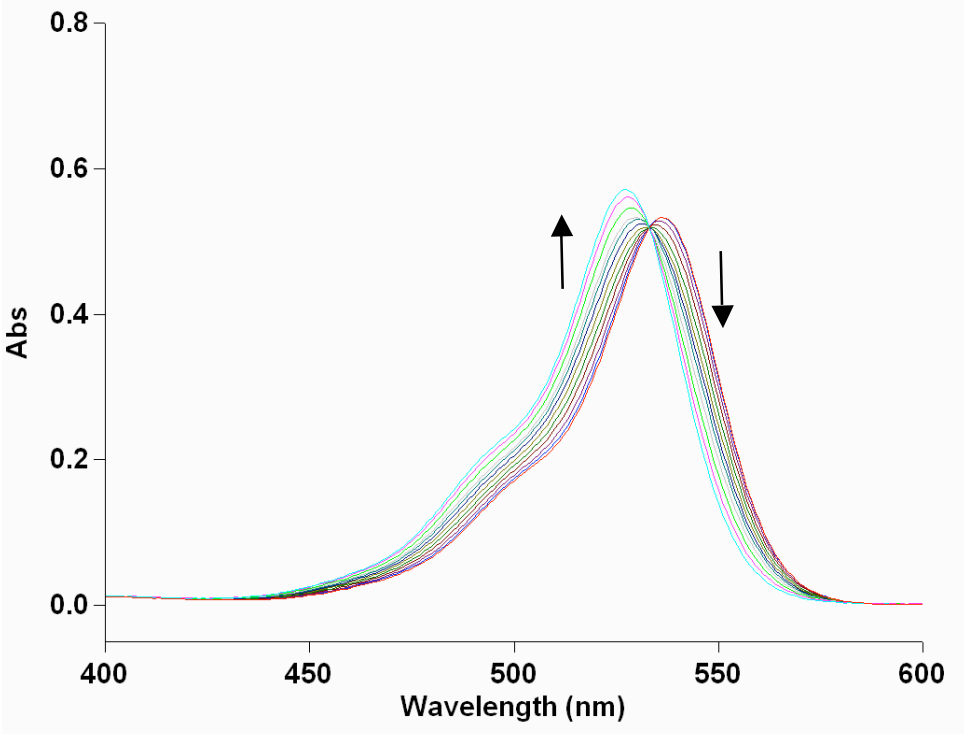

(B)

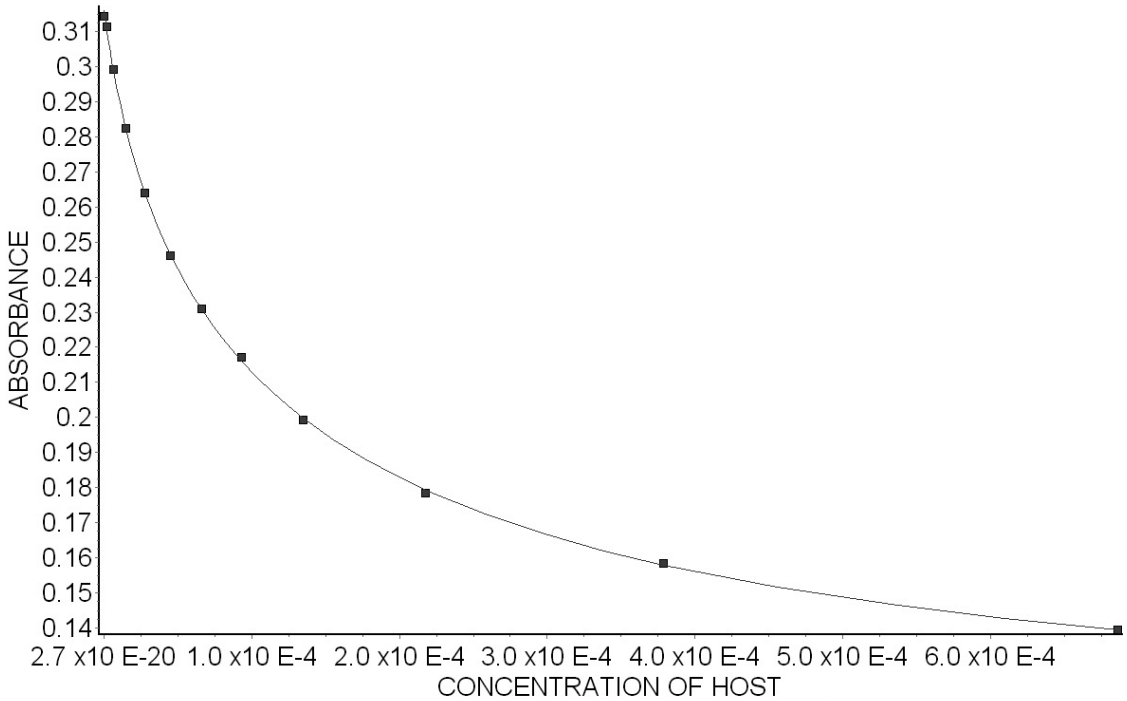

Figure S9. (A) UV/Vis spectra from the titration of **2** (10.2 μM) and Rhodamine 6G (9.96 μM) with guest **18** (0 – 686 μM) in 20 mM NaH_2PO_4 buffer (pH = 7.4); (B) plot of the A_{550} as a function of the concentration of **18**. The solid line represents the best non-linear fit of the data to a competitive binding model ($K_a = (1.9 \pm 0.6) \times 10^5\ M^{-1}$).

(A)

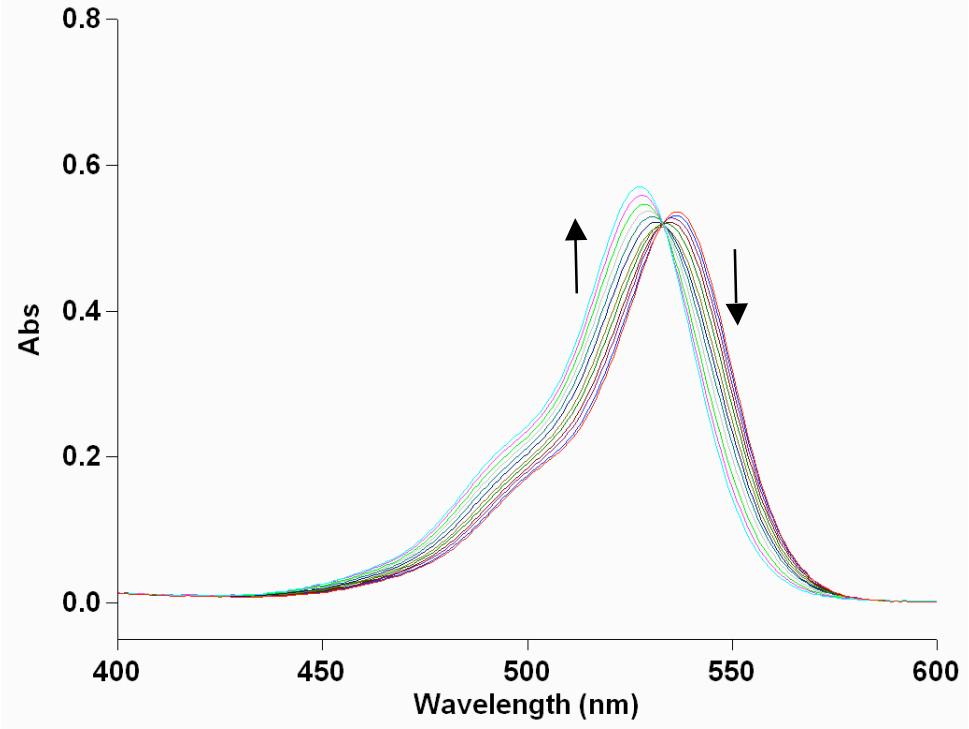

(B)

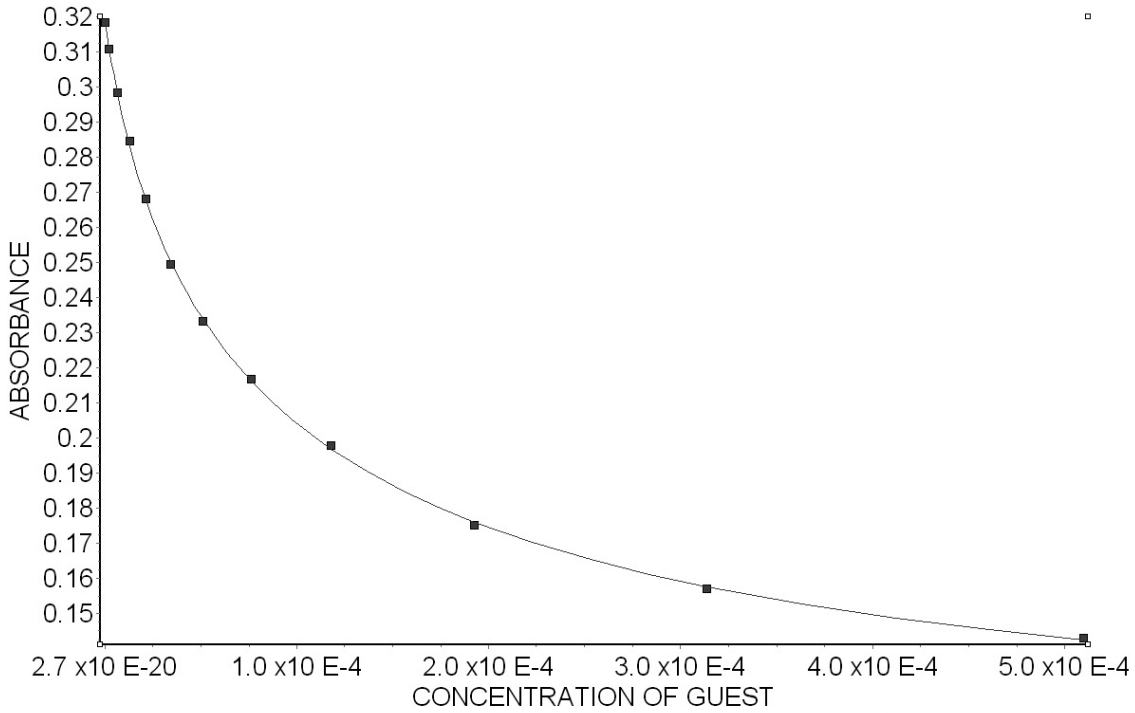

Figure S10. (A) UV/Vis spectra from the titration of **2** (10.2 μM) and Rhodamine 6G (10.3 μM) with guest **19** (0 – 510 μM) in 20 mM NaH_2PO_4 buffer (pH = 7.4); (B) plot of the A_{550} as a function of the concentration of **19**. The solid line represents the best non-linear fit of the data to a competitive binding model ($K_a = (2.5 \pm 0.7) \times 10^5\ M^{-1}$).

(A)

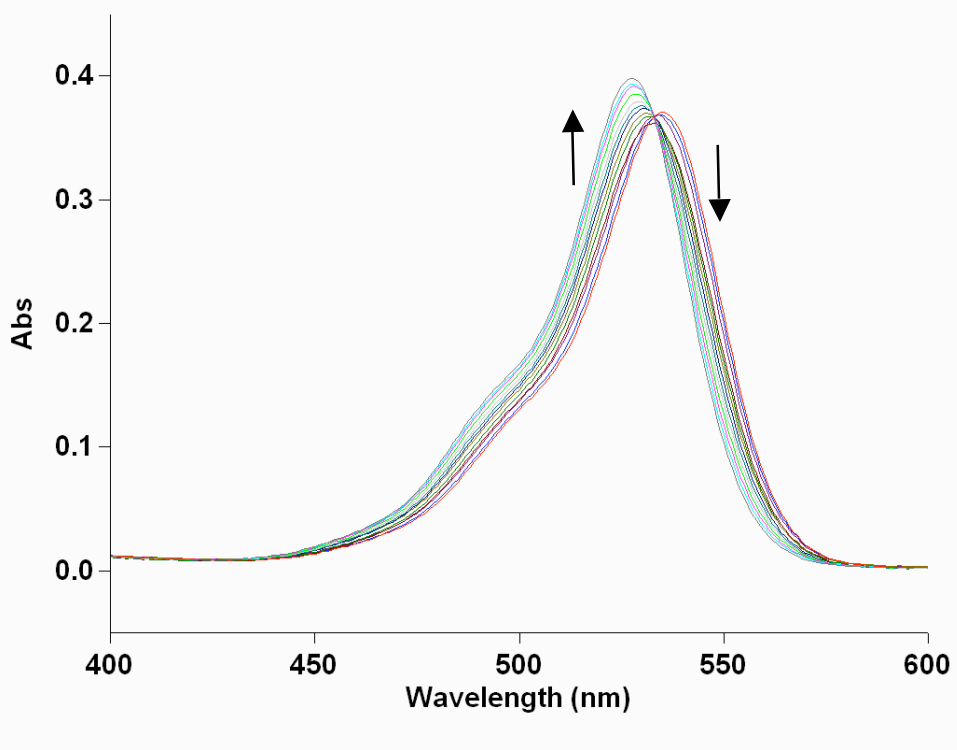

(B)

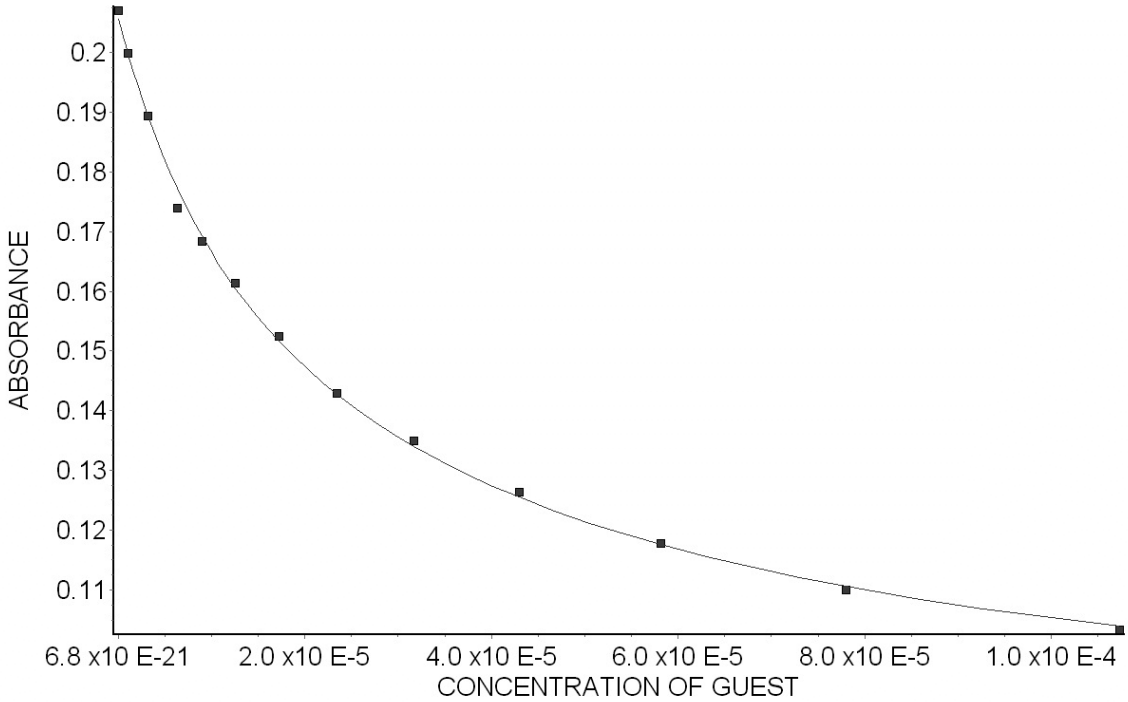

Figure S11. (A) UV/Vis spectra from the titration of **2** (5.07 μM) and Rhodamine 6G (5.01 μM) with guest **20** (0 – 107 μM) in 20 mM NaH_2PO_4 buffer (pH = 7.4); (B) plot of the A_{550} as a function of the concentration of **20**. The solid line represents the best non-linear fit of the data to a competitive binding model ($K_a = (5.3 \pm 0.4) \times 10^5\ M^{-1}$).

(A)

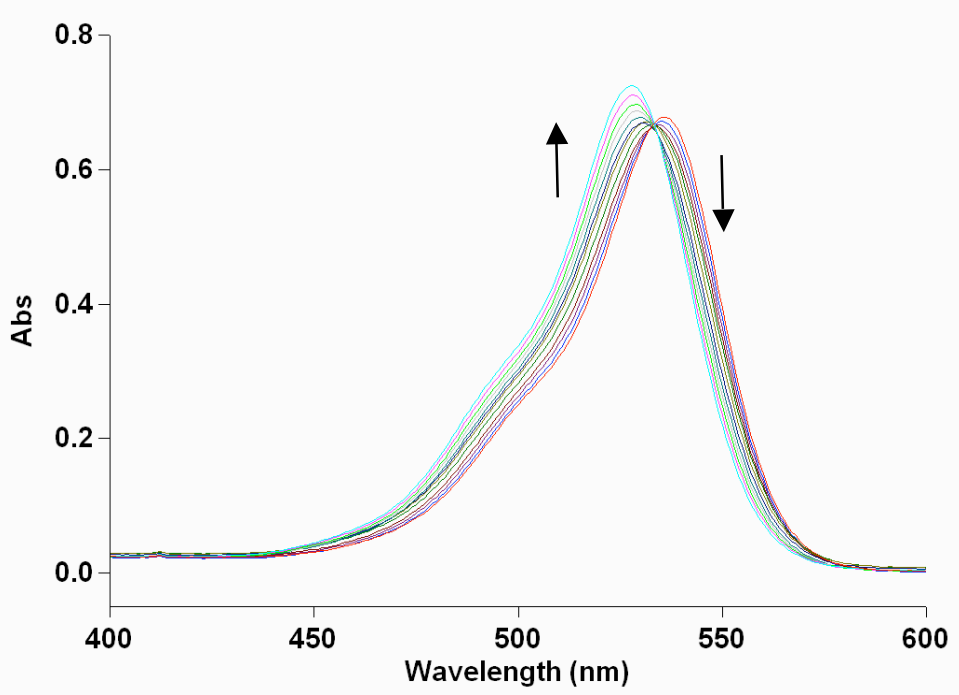

(B)

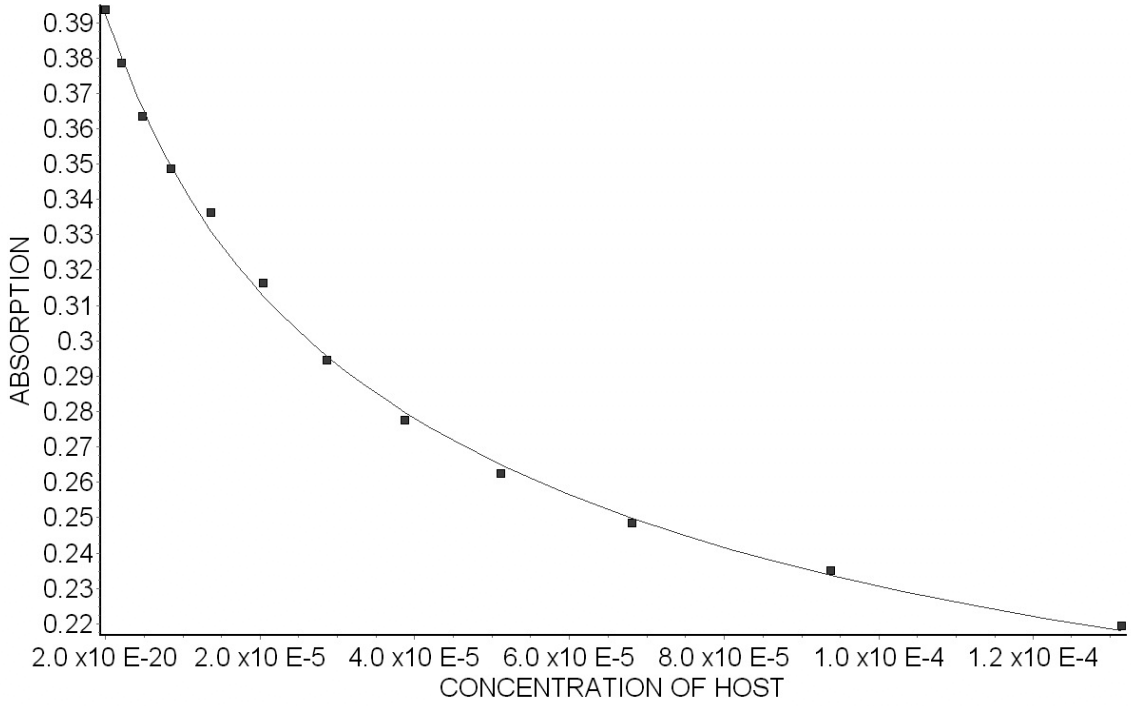

Figure S12. (A) UV/Vis spectra from the titration of **2** (12.5 μM) and Rhodamine 6G (12.4 μM) with guest **21** (0 –131μM) in 20mM NaH_2PO_4 buffer (pH = 7.4); (B) plot of the A_{550} as a function of the concentration of **21**. The solid line represents the best non-linear fit of the data to a competitive binding model ($K_a = (5.9 \pm 0.7) \times 10^5\ M^{-1}$).

(A)

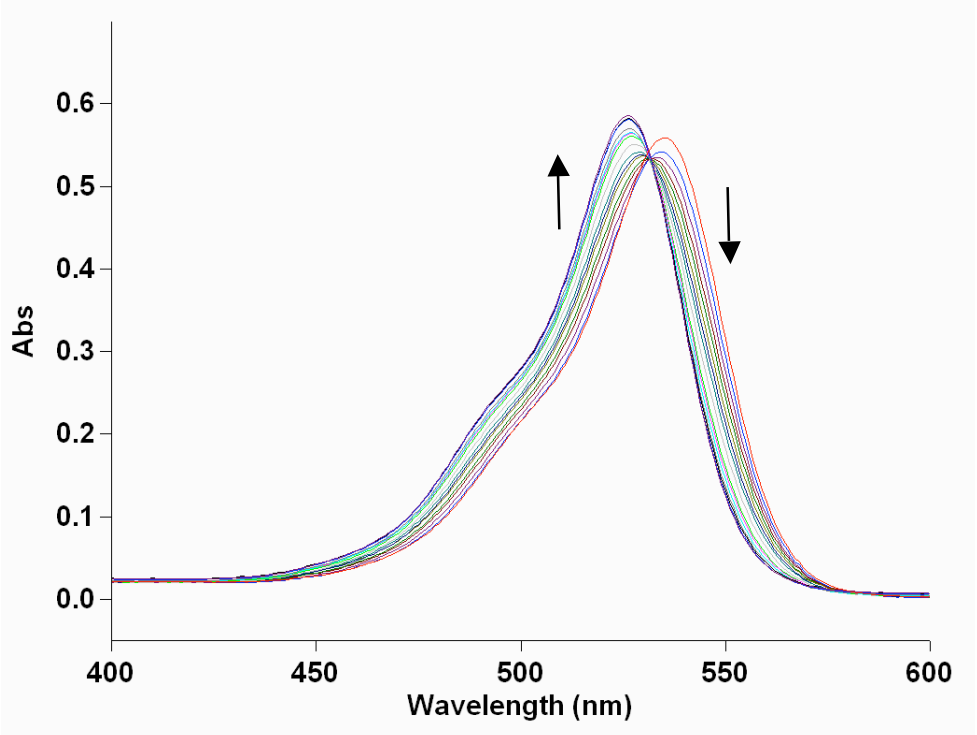

(B)

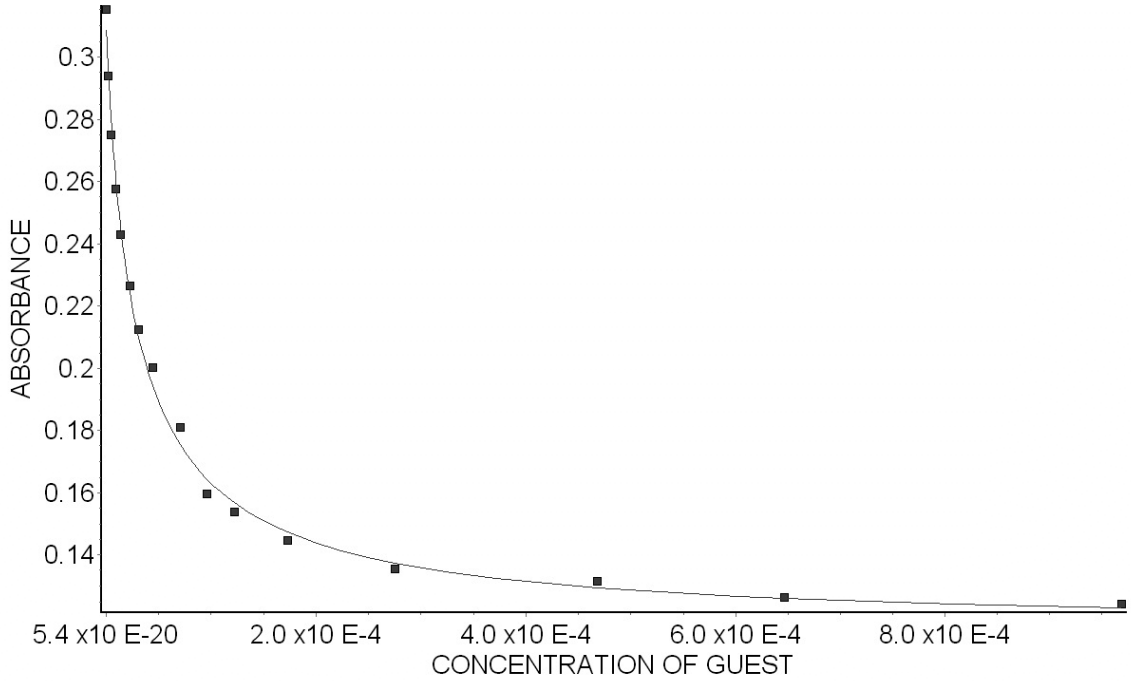

Figure S13. (A) UV/Vis spectra from the titration of **2** (9.92 μM) and Rhodamine 6G (10.0 μM) with guest **22** (0 – 968 μM) in 20 mM NaH_2PO_4 buffer (pH = 7.4); (B) plot of the A_{550} as a function of the concentration of **22**. The solid line represents the best non-linear fit of the data to a competitive binding model ($K_a = (8.0 \pm 0.7) \times 10^5\ M^{-1}$).

(A)

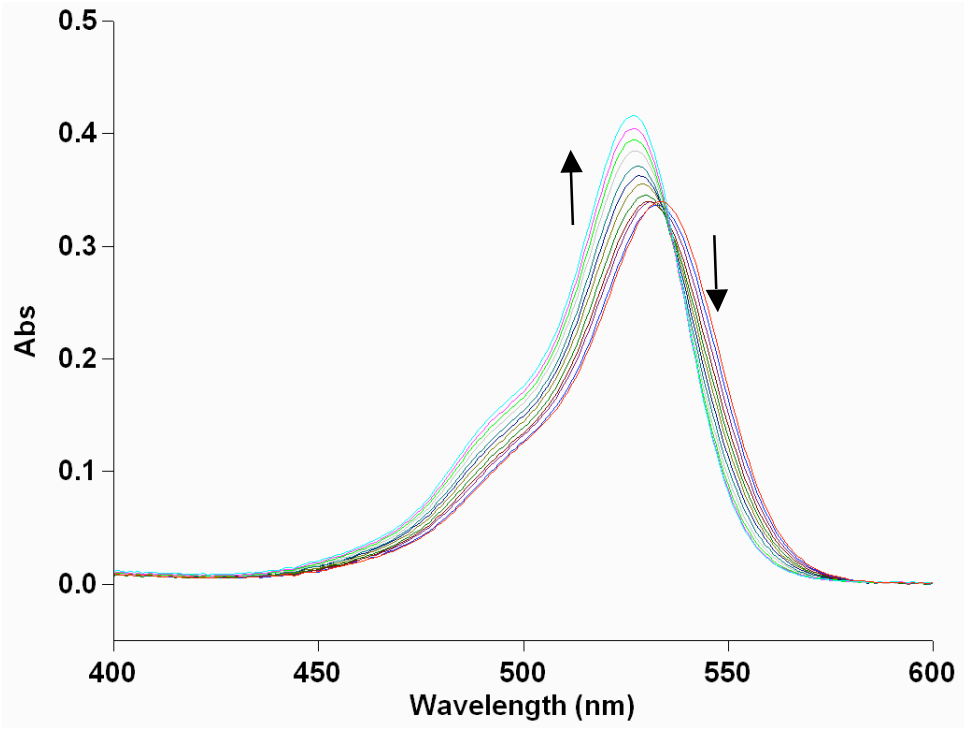

(B)

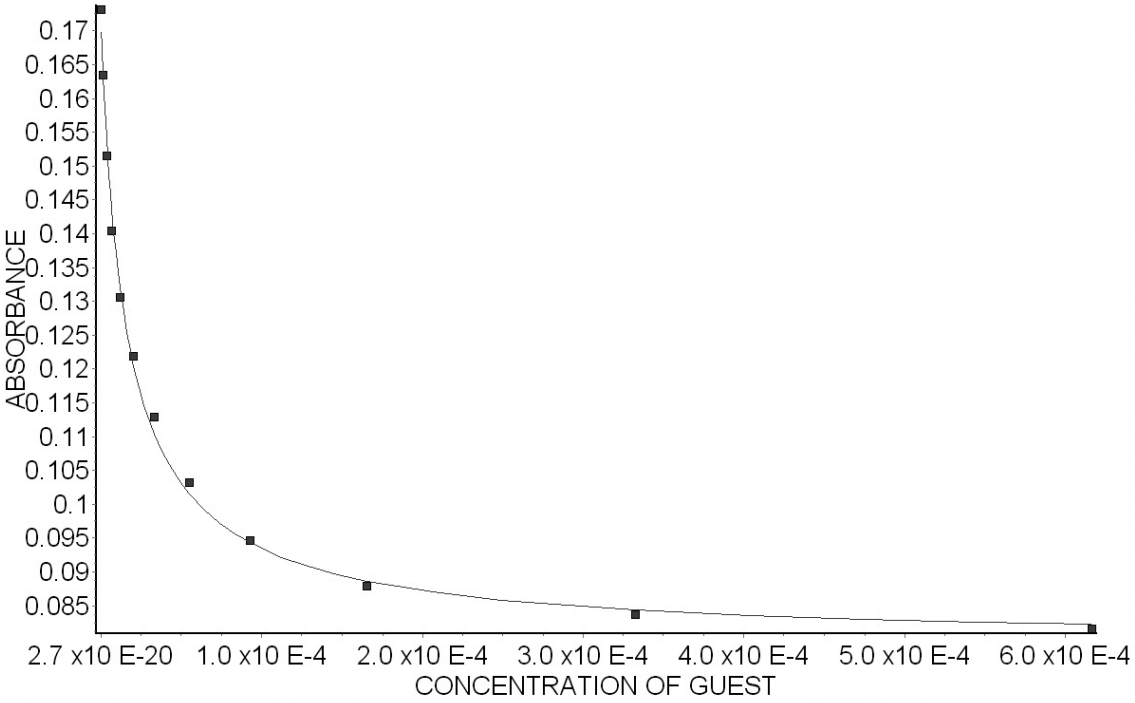

Figure S14. (A) UV/Vis spectra from the titration of **2** (5.07 μM) and Rhodamine 6G (5.01 μM) with guest **23** (0 – 616 μM) in 20 mM NaH_2PO_4 buffer (pH = 7.4); (B) plot of the A_{550} as a function of the concentration of **23**. The solid line represents the best non-linear fit of the data to a competitive binding model ($K_a = (8.2 \pm 0.9) \times 10^5\ M^{-1}$).

(A)

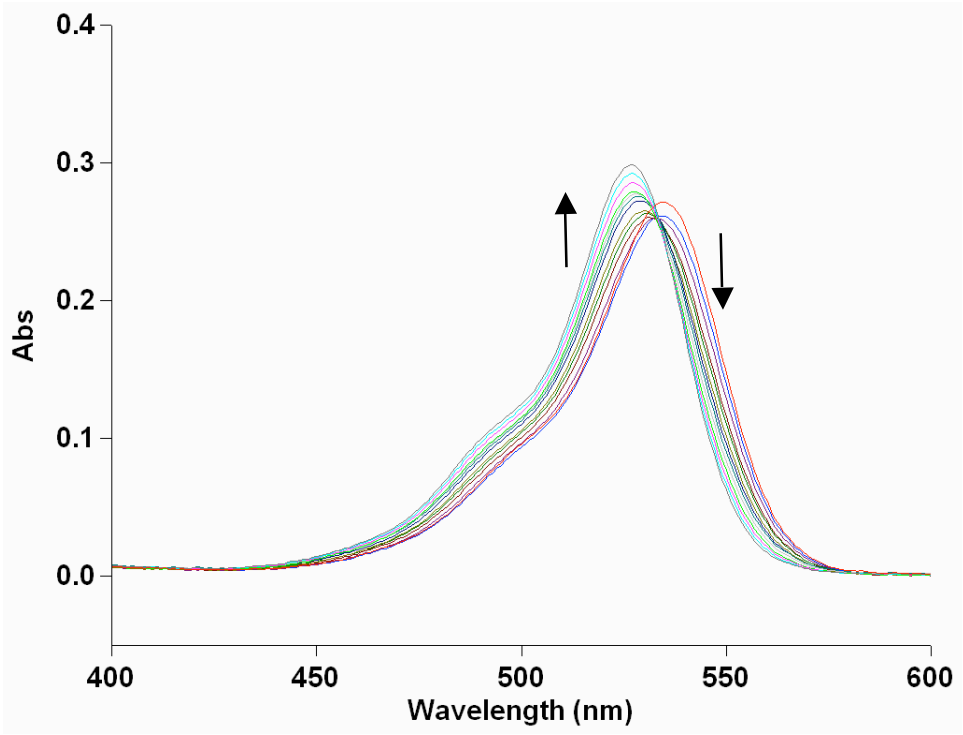

(B)

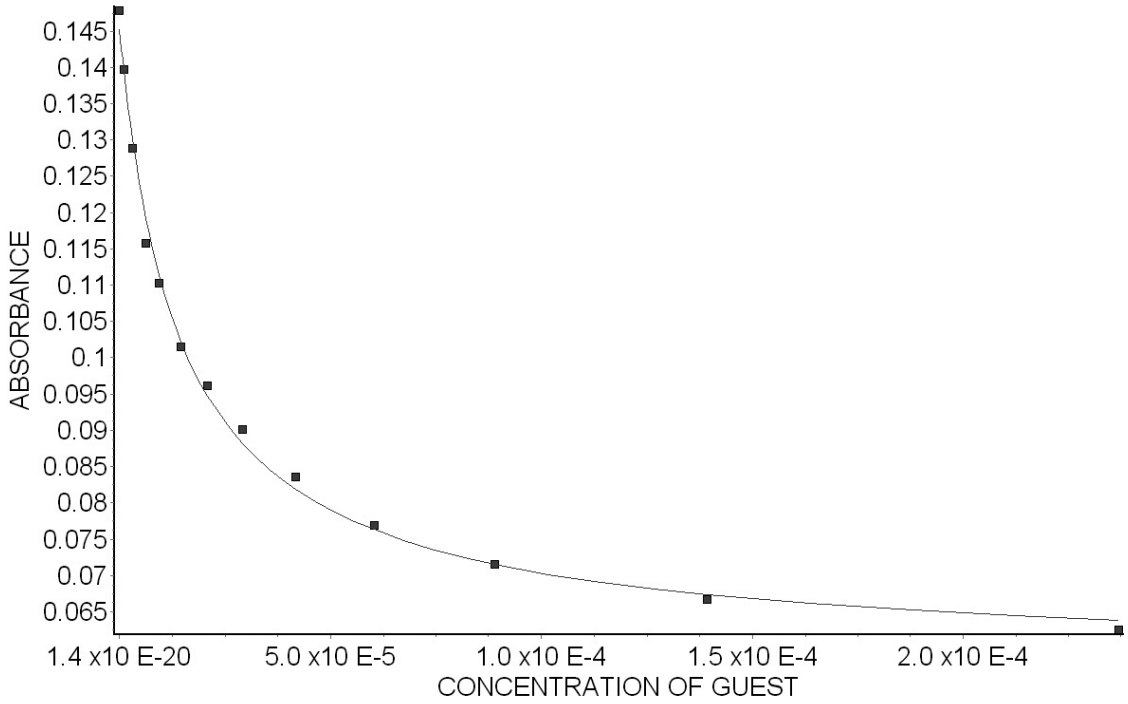

Figure S15. (A) UV/Vis spectra from the titration of **2** (5.07 μM) and Rhodamine 6G (5.01 μM) with guest **24** (0 – 237 μM) in 20 mM NaH_2PO_4 buffer (pH = 7.4); (B) plot of the A_{550} as a function of the concentration of **24**. The solid line represents the best non-linear fit of the data to a competitive binding model ($K_a = (9.3 \pm 0.9) \times 10^5\ M^{-1}$).

(A)

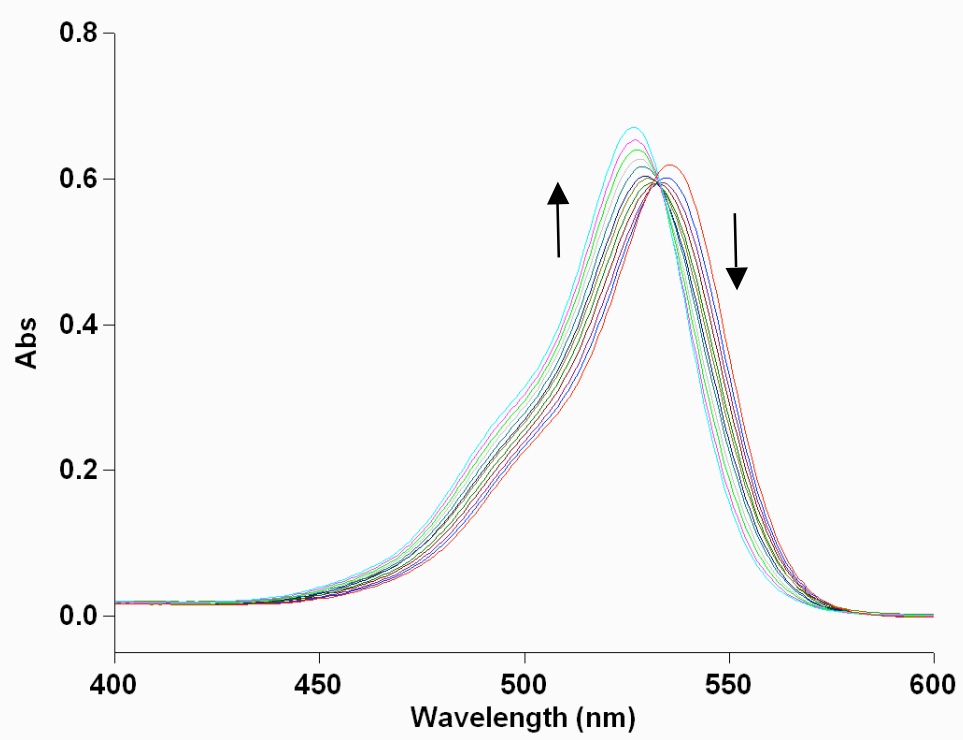

(B)

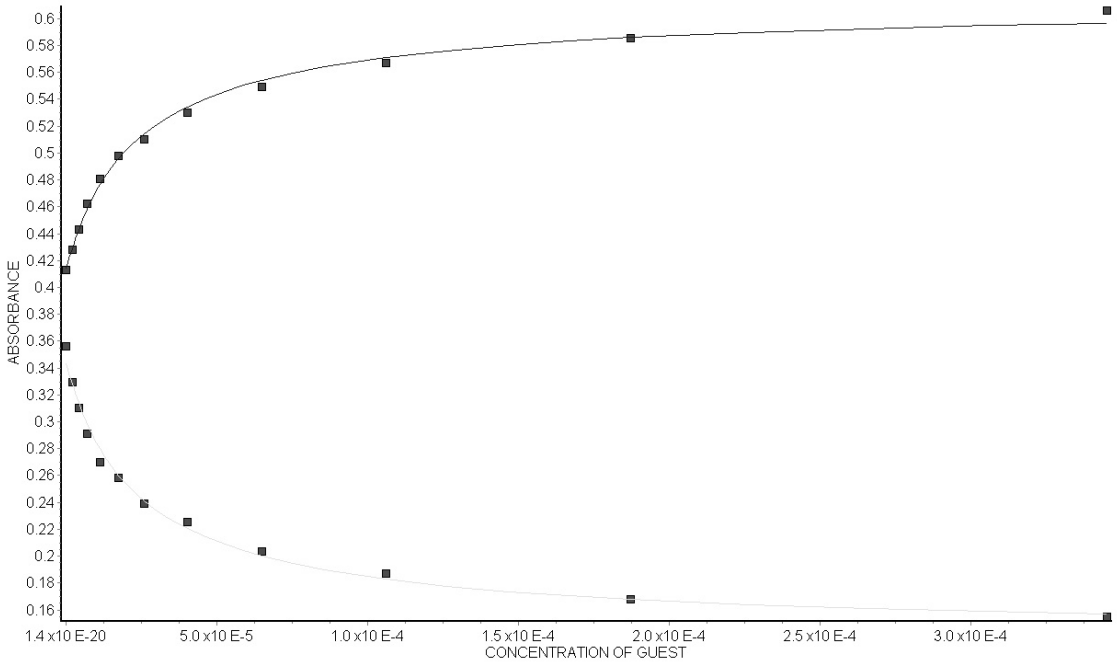

Figure S16. (A) UV/Vis spectra from the titration of **2** (10.1 μM) and Rhodamine 6G (9.96 μM) with guest **25** (0 – 345 μM) in 20 mM NaH_2PO_4 buffer (pH = 7.4); (B) plot of the A_{550} as a function of the concentration of **25**. The solid line represents the best non-linear fit of the data to a competitive binding model ($K_a = (9.7 \pm 1.1) \times 10^5\ M^{-1}$

(A)

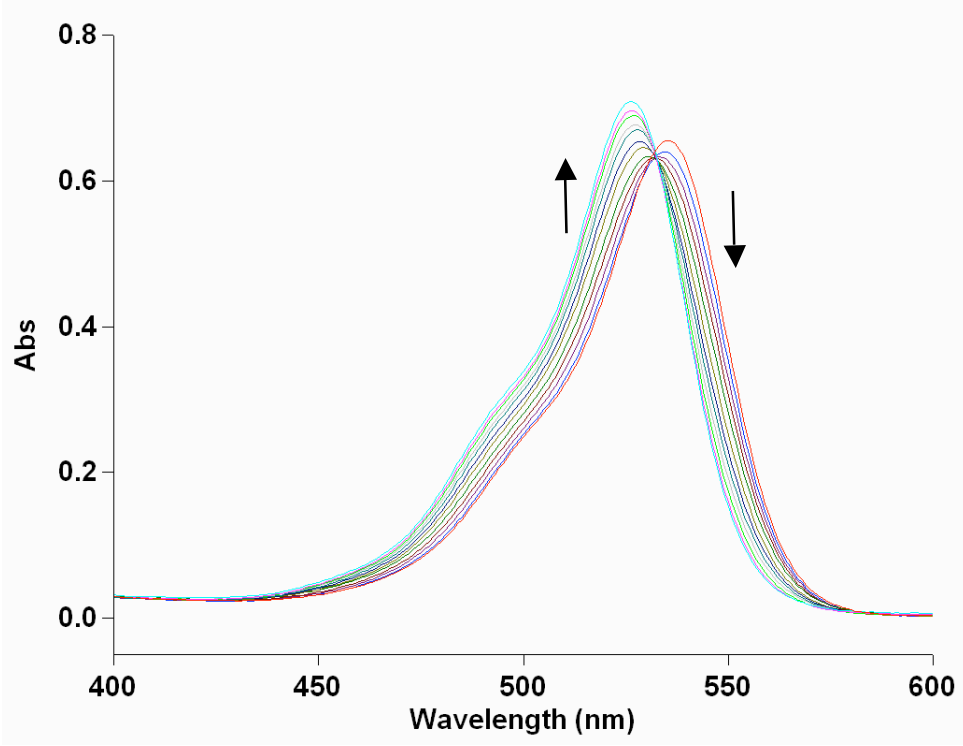

(B)

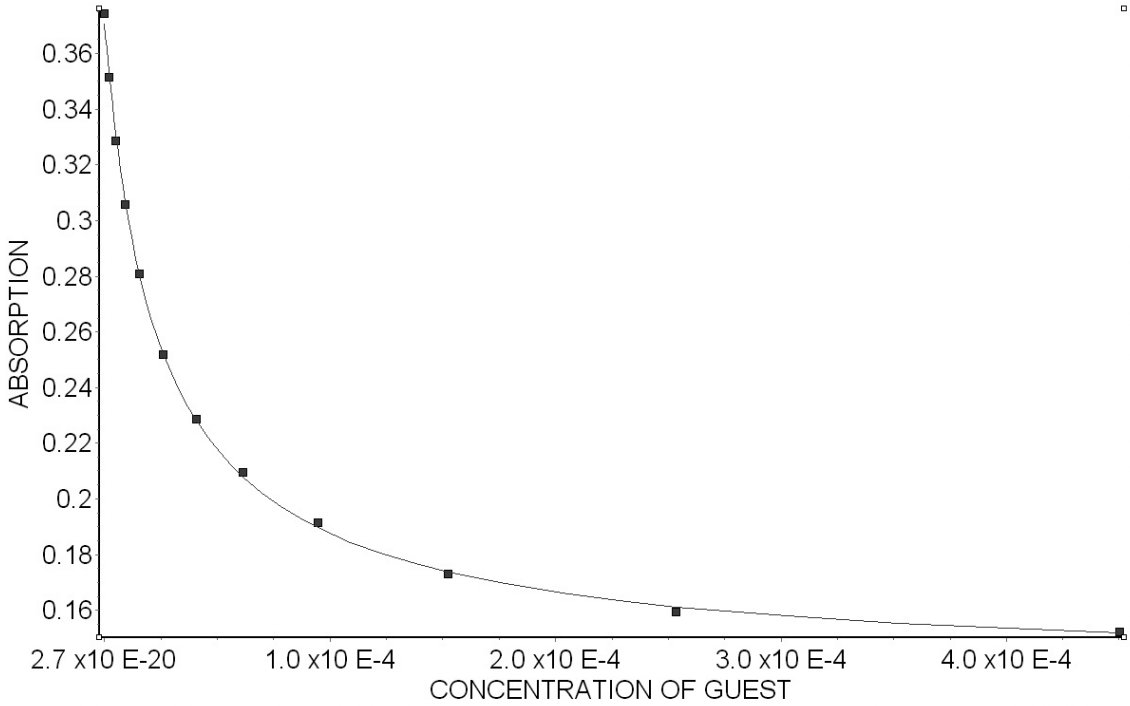

Figure S17. (A) UV/Vis spectra from the titration of **2** (10.1 μM) and Rhodamine 6G (9.96 μM) with guest **26** (0 – 450 μM) in 20 mM NaH_2PO_4 buffer (pH = 7.4); (B) plot of the A_{550} as a function of the concentration of **26**. The solid line represents the best non-linear fit of the data to a competitive binding model ($K_a = (9.8 \pm 0.5) \times 10^5\ M^{-1}$).

(A)

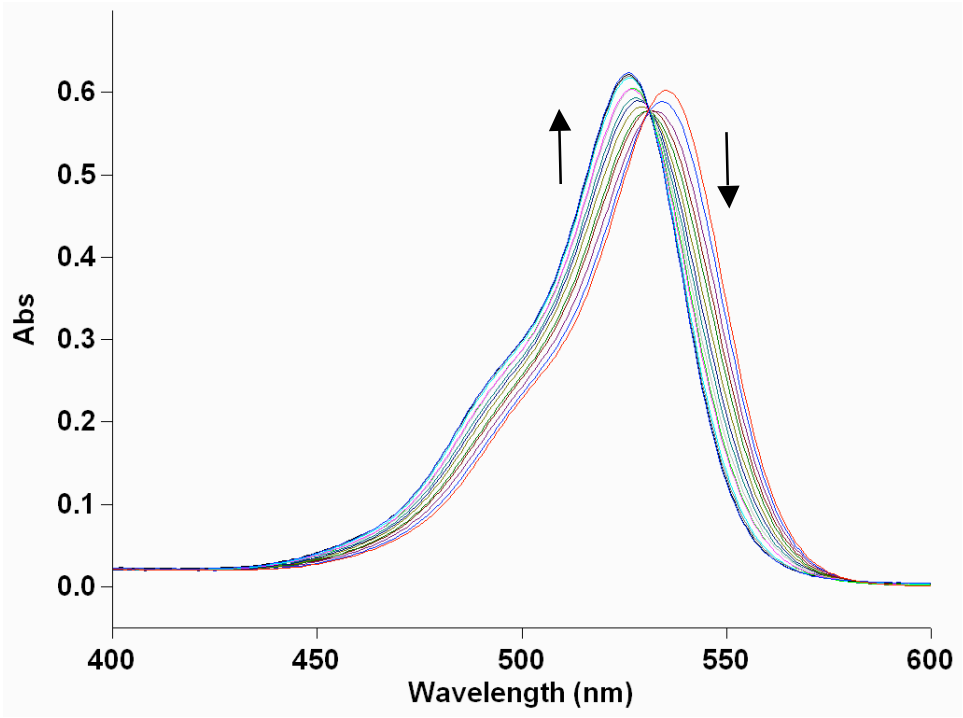

(B)

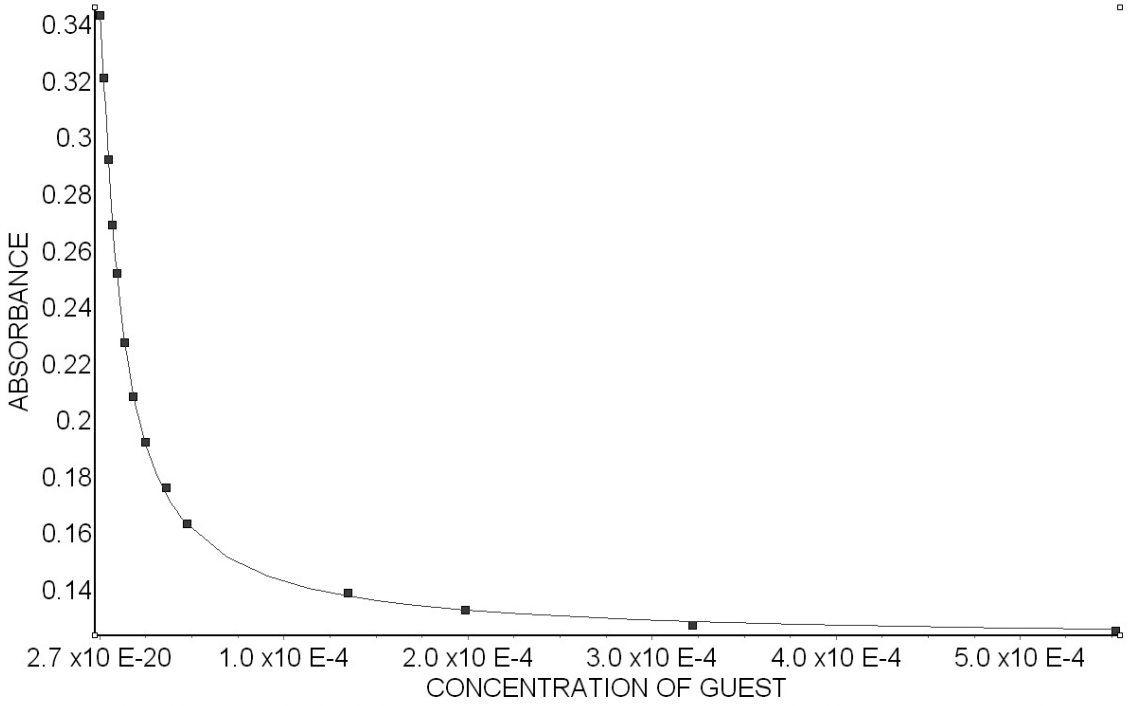

Figure S18. (A) UV/Vis spectra from the titration of **2** (9.92 μM) and Rhodamine 6G (10.0 μM) with guest **27** (0 – 552 μM) in 20 mM NaH_2PO_4 buffer (pH = 7.4); (B) plot of the A_{550} as a function of the concentration of **27**. The solid line represents the best non-linear fit of the data to a competitive binding model ($K_a = (2.8 \pm 0.1) \times 10^6\ M^{-1}$).

(A)

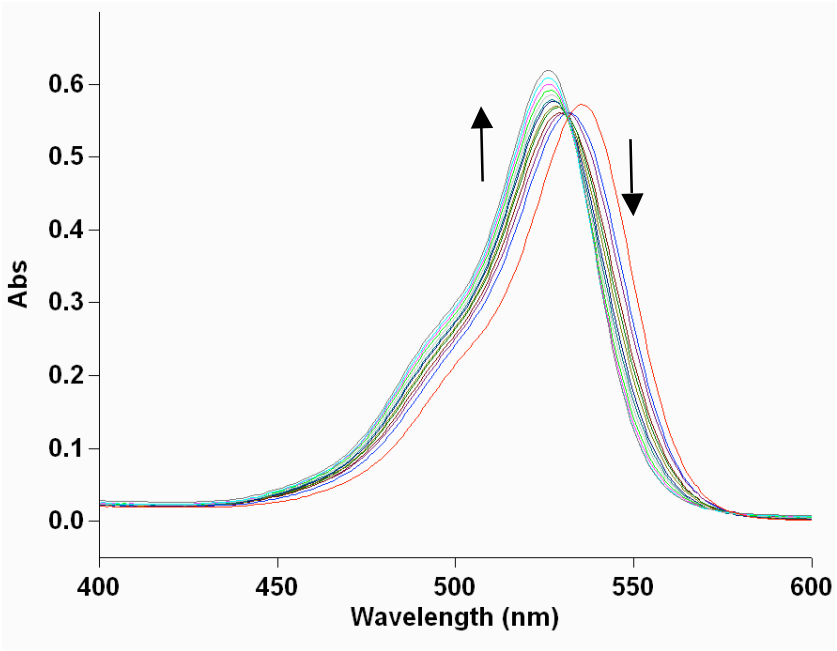

(B)

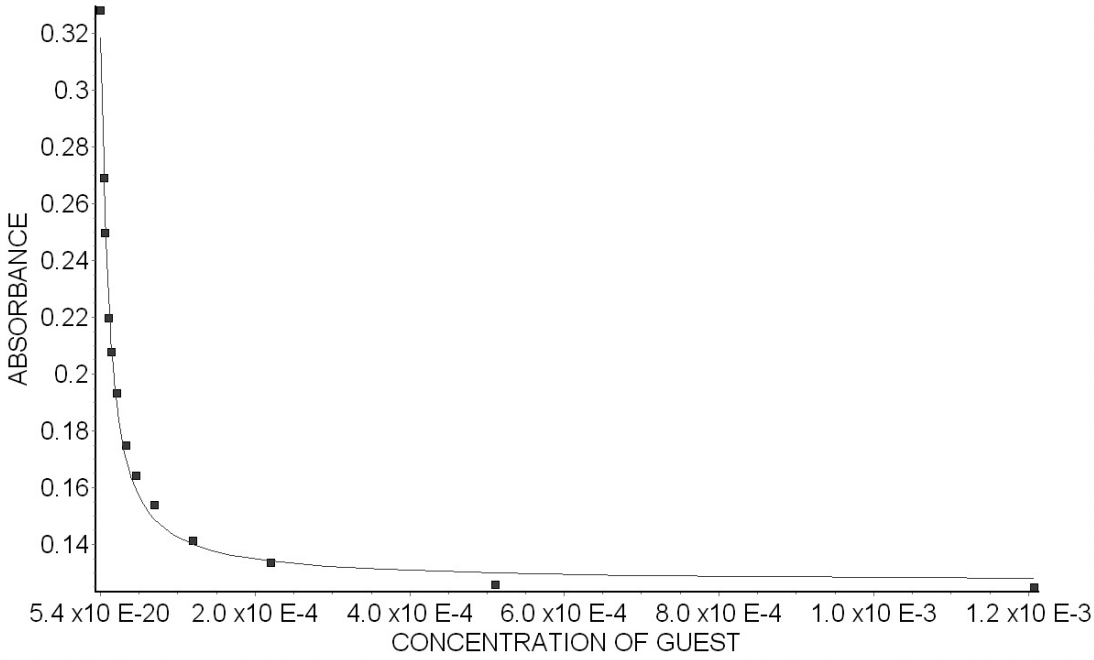

Figure S19. (A) UV/Vis spectra from the titration of **2** (9.92 μM) and Rhodamine 6G (10.0 μM) with guest **28** (0 – 1.21 mM) in 20 mM NaH_2PO_4 buffer (pH = 7.4); (B) plot of the A_{550} as a function of the concentration of **28**. The solid line represents the best non-linear fit of the data to a competitive binding model ($K_a = (3.3 \pm 0.5) \times 10^6\ M^{-1}$).

(A)

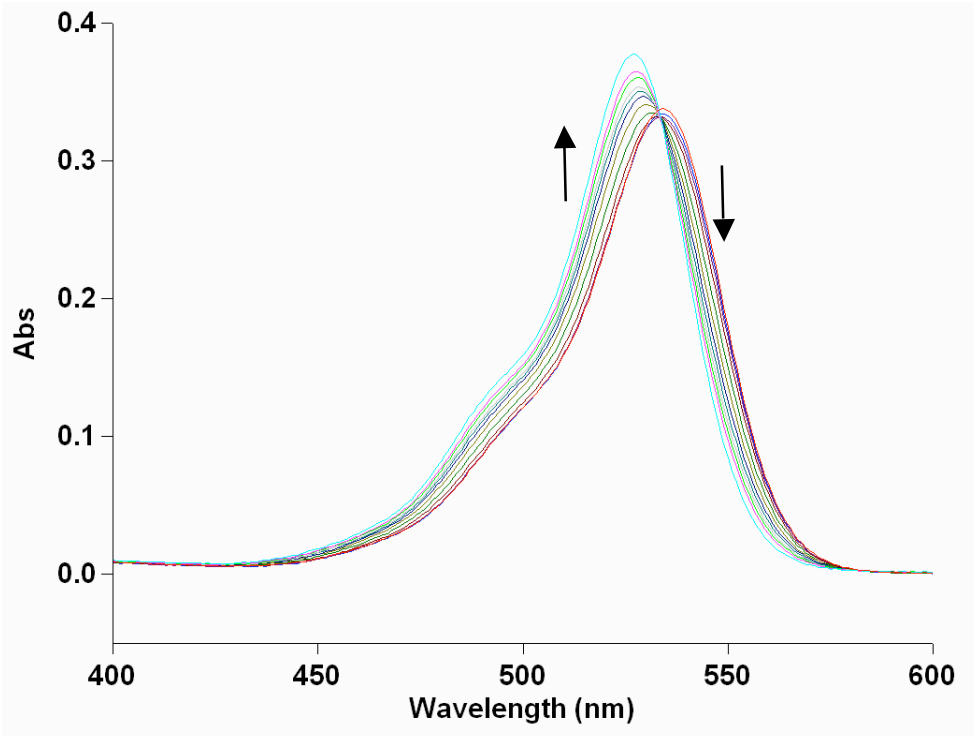

(B)

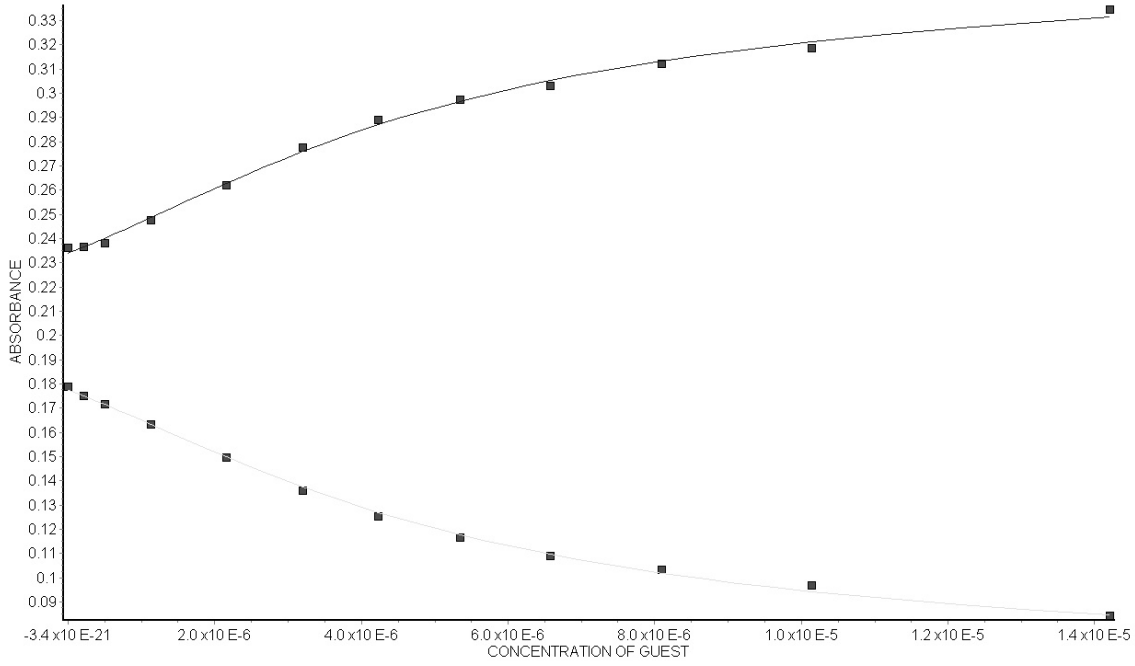

Figure S20. (A) UV/Vis spectra from the titration of **2** (5.07 μM) and Rhodamine 6G (5.01 μM) with guest **29** (0 – 14.2 μM) in 20 mM NaH_2PO_4 buffer (pH = 7.4); (B) plot of the A_{550} as a function of the concentration of **29**. The solid line represents the best non-linear fit of the data to a competitive binding model ($K_a = (4.5 \pm 0.7) \times 10^6$ M^{-1}).

1:1 Binding Models for NMR

Model Fitting Absorbance at One Chemical Shift.

```
// Micromath Scientist Model File
// 1:1 Host:Guest binding model for NMR
//This model assumes the guest concentration is fixed and host concentration is varied
IndVars: ConcHostTot
DepVars: Deltaobs
Params: Ka, ConcGuestTot, Deltasat, Deltazero
Ka = ConcHostGuest/(ConcHostFree*ConcGuestFree)
ConcHostTot=ConcHostFree + ConcHostGuest
ConcGuestTot=ConcGuestFree + ConcHostGuest
Deltaobs = Deltazero + (Deltasat - Deltazero) * (ConcHostGuest/ConcGuestTot)
//Constraints
0 < ConcHostFree < ConcHostTot
0 < Ka
0 < ConcGuestFree < ConcGuestTot
0 < ConcHostGuest < ConcHostTot
***
```

Model Fitting Absorbance at Two Chemical Shifts.

```
// Micromath Scientist Model File
IndVars: ConcHost
DepVars: CSA, CSB
Params: Ka, CSAzero, CSAsat, CSBzero, CSBsat
Ka = ConcHG/(ConcHfree*ConcGfree)
ConcHost=ConcHfree+ConcHG
0.0001=ConcGfree+ConcHG
CSA = CSAzero + ((CSAsat-CSAzero)*(ConcHG/0.0001))
CSB = CSBzero + ((CSBsat-CSBzero)*(ConcHG/0.0001))
0<ConcHfree<ConcHost
0<ConcGfree<0.0001
```

(A)

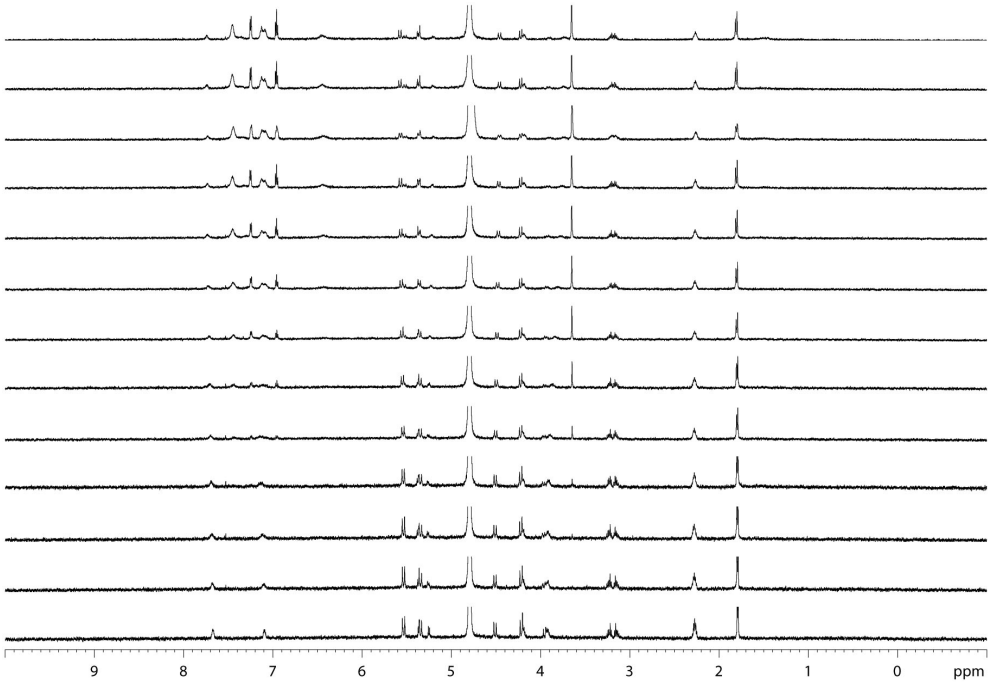

(B)

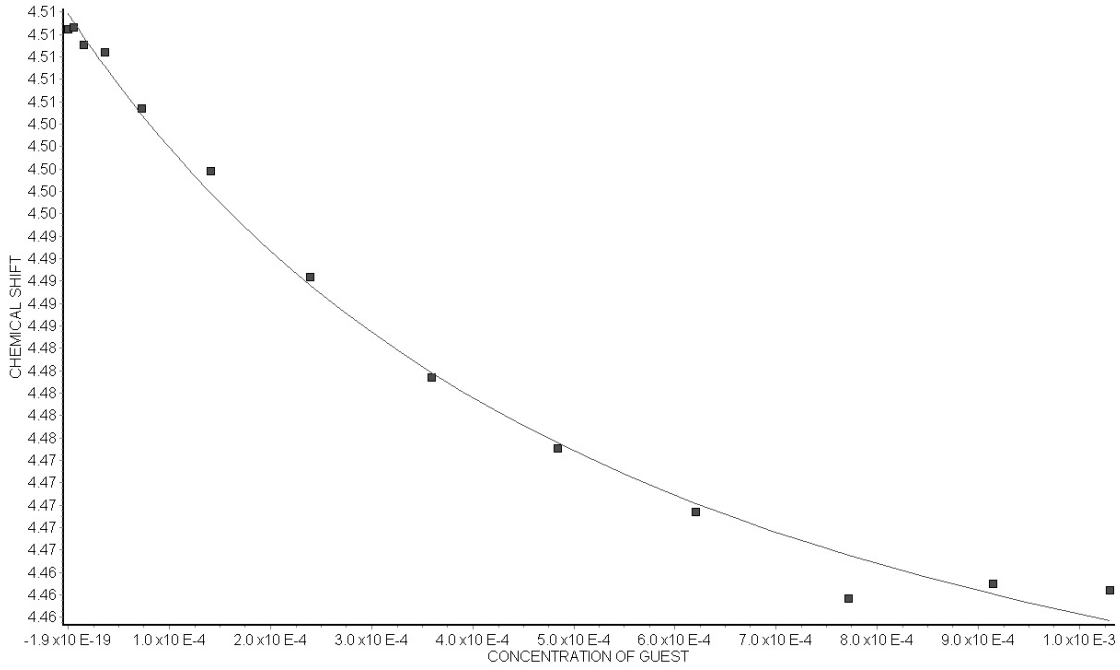

Figure S21. (A) ^{1}H NMR (600 MHz) stack plot of the titration of **2** (0.104 mM) with guest **3** (0 - 1.03 mM) in 20 mM NaH_2PO_4 buffered D_2O (pH = 7.4); (B) plot of the chemical shift at 7.67 ppm as a function of guest concentration. The solid line represents the best non-linear fit of the data to a 1:1 model ($K_a = (2.0 \pm 0.4) \times 10^3$ M^{-1}).

(A)

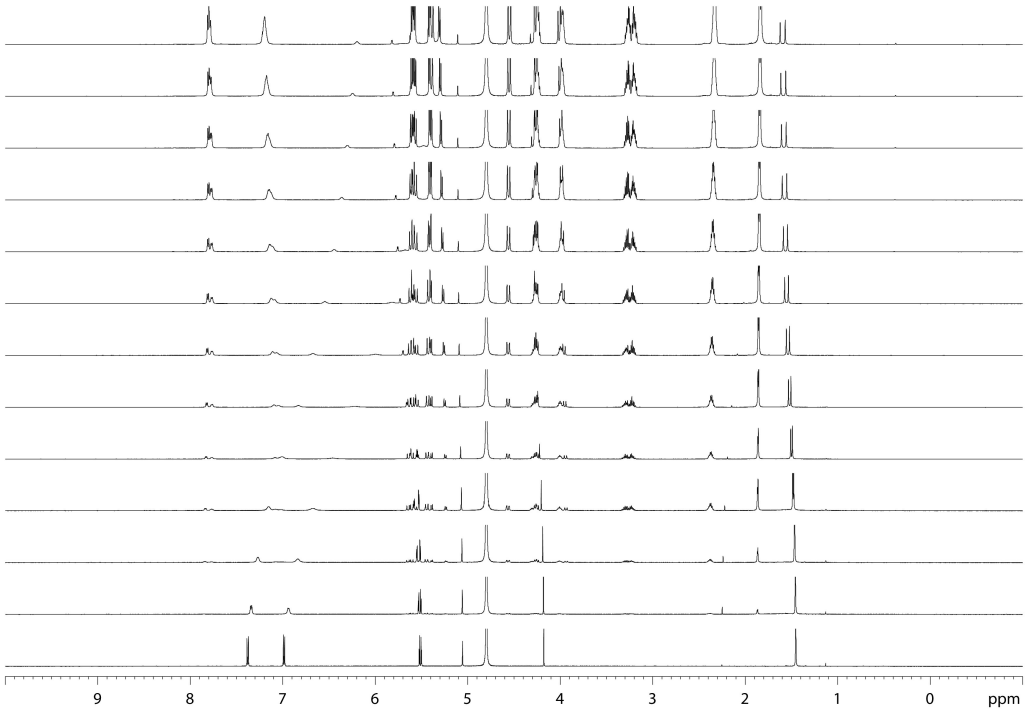

(B)

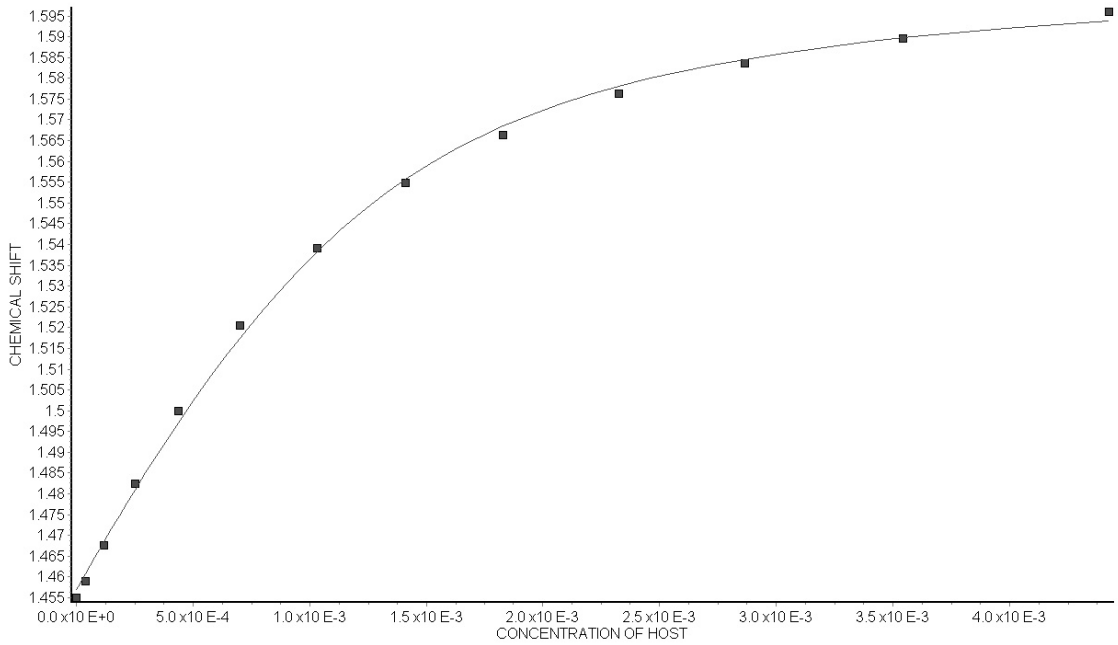

Figure S22. (A) ^{1}H NMR (600 MHz) stack plot of the titration of **2** (0 - 4.5 mM) with guest **5** (1.86 mM) in 20 mM NaH_2PO_4 buffered D_2O (pH = 7.4); (B) plot of the chemical shift at 1.46 ppm as a function of host concentration. The solid line represents the best non-linear fit of the data to a 1:1 model ($K_a = (3.0 \pm 0.4) \times 10^3\ M^{-1}$).

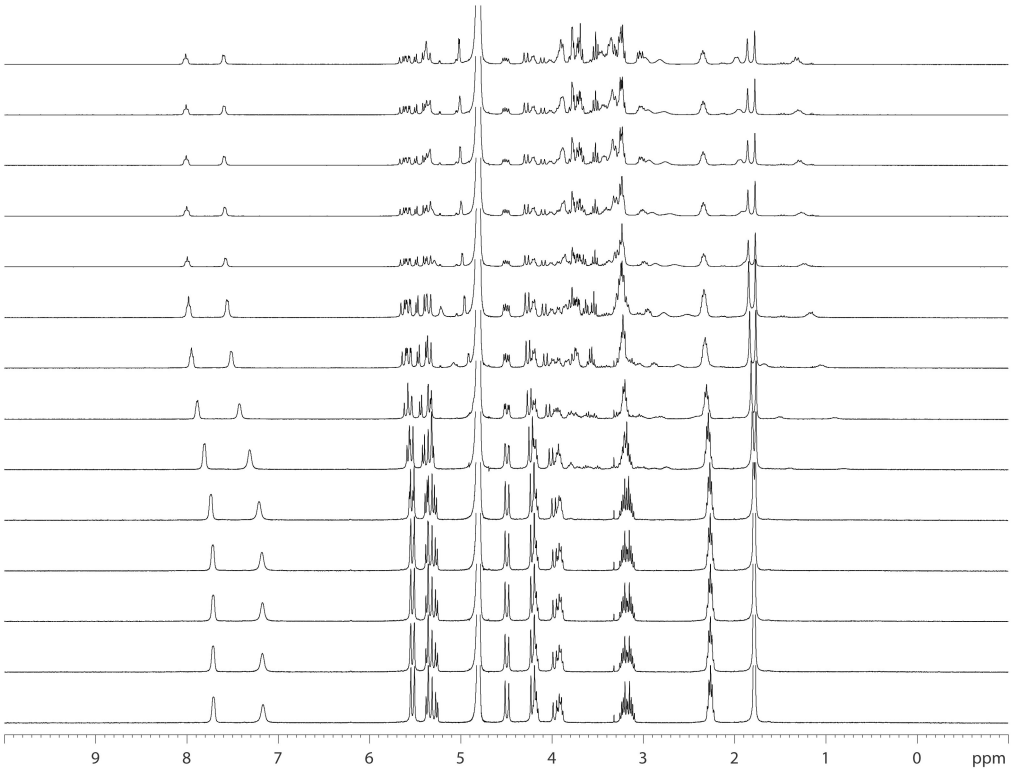

(B)

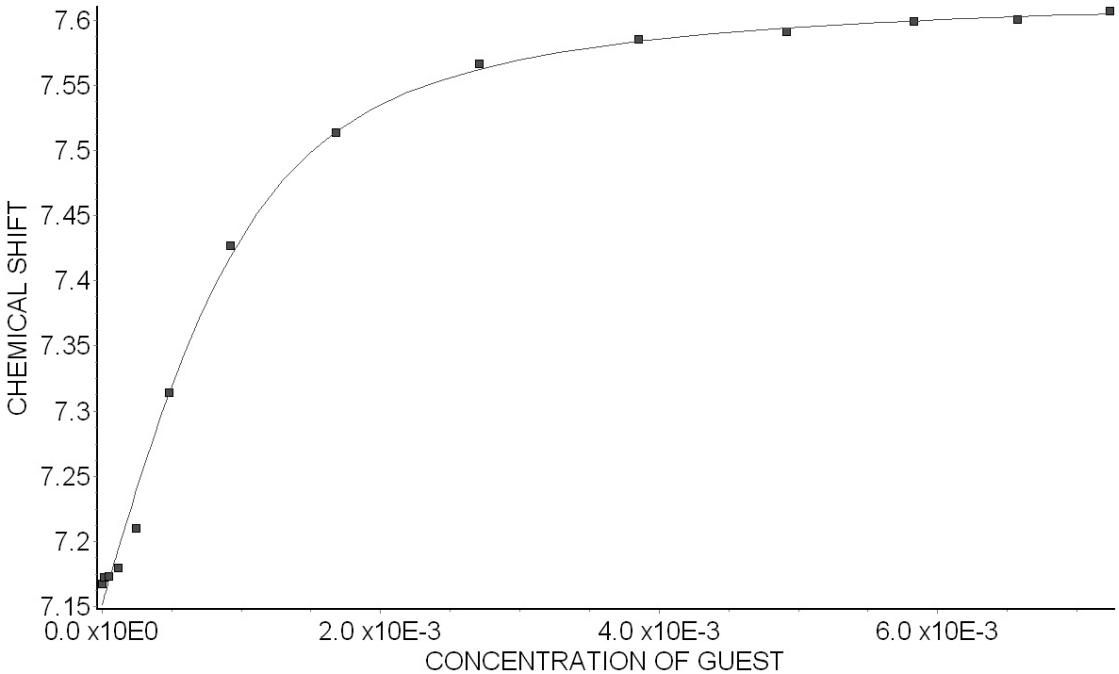

Figure S23. (A) ^{1}H NMR (400 MHz) stack plot of the titration of **2** (0.976 mM) with guest **6** (0 - 7.24 mM) in 20 mM NaH_2PO_4 buffered D_2O (pH = 7.4); (B) plot of the chemical shift at 7.17 ppm as a function of guest concentration. The solid line represents the best non-linear fit of the data to a 1:1 model ($K_a = (3.0 \pm 0.6) \times 10^3$ M^{-1}).

(A)

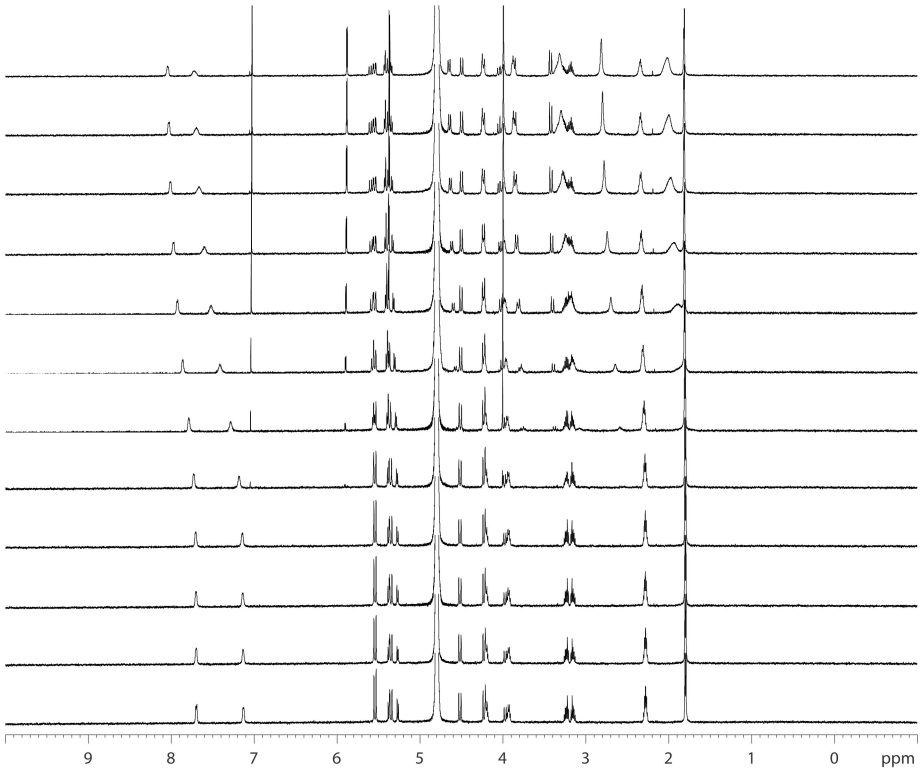

(B)

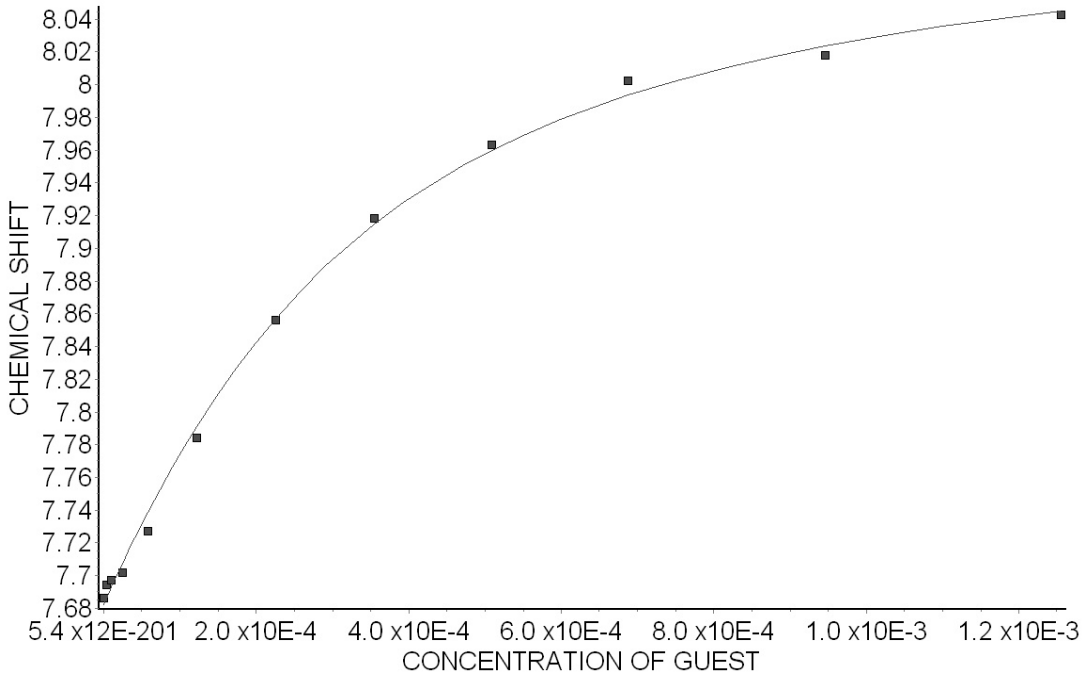

Figure S24. (A) ^{1}H NMR (600 MHz) stack plot of the titration of **2** (0.199 mM) with guest **7** (0 - 1.26 mM) in 20 mM NaH_2PO_4 buffered D_2O (pH = 7.4); (B) plot of the chemical shift at 7.69 ppm as a function of guest concentration. The solid line represents the best non-linear fit of the data to a 1:1 model ($K_a = (4.6 \pm 0.5) \times 10^3$ M^{-1}).

(A)

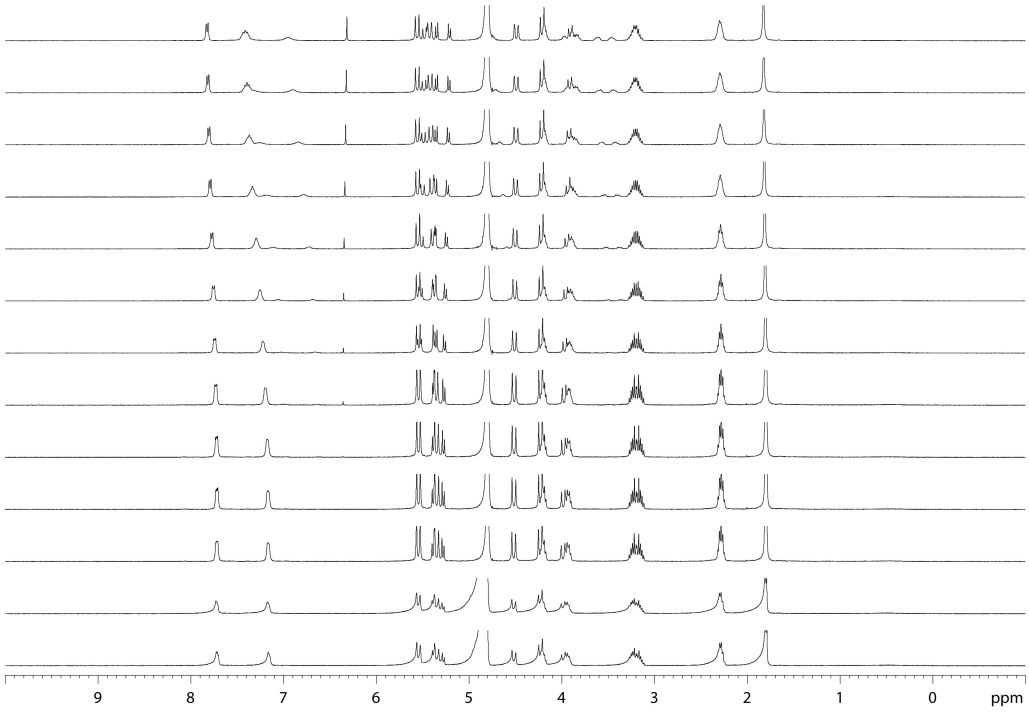

(B)

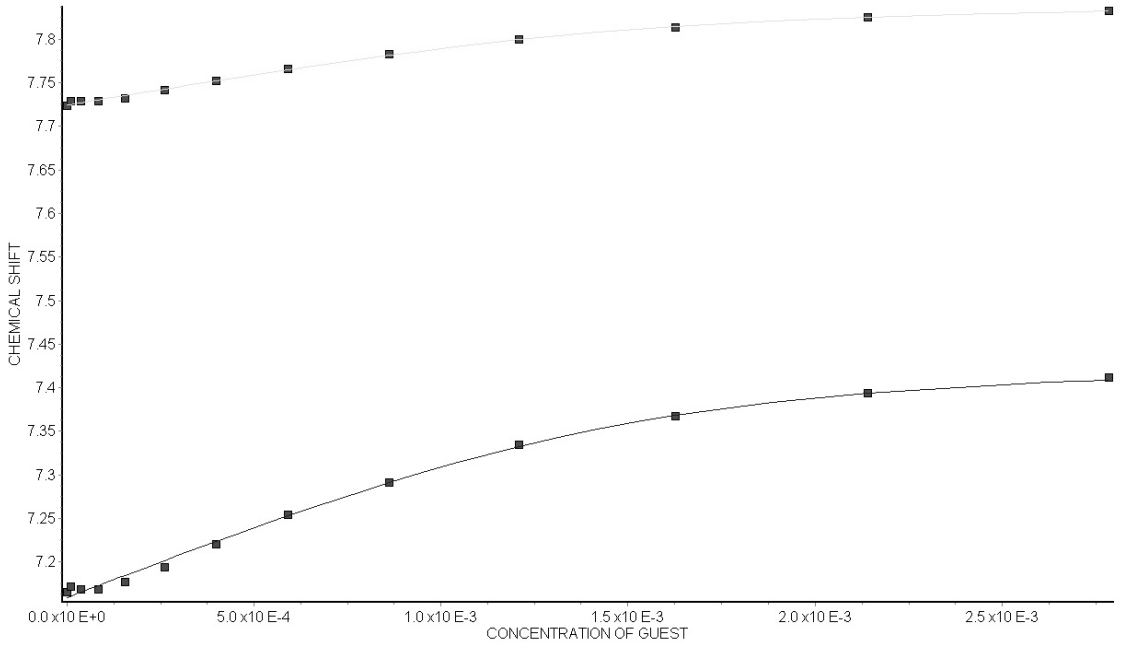

Figure S25. (A) ^{1}H NMR (600 MHz) stack plot of the titration of **2** (1.50 mM) with guest **9** (0 - 2.7 mM) in 20 mM NaH_2PO_4 buffered D_2O (pH = 7.4); (B) plot of the chemical shift at 7.15 and 7.72 ppm as a function of guest concentration. The solid line represents the best non-linear fit of the data to a 1:1 model ($K_a = (5.9 \pm 1.8) \times 10^3\ M^{-1}$).

(A)

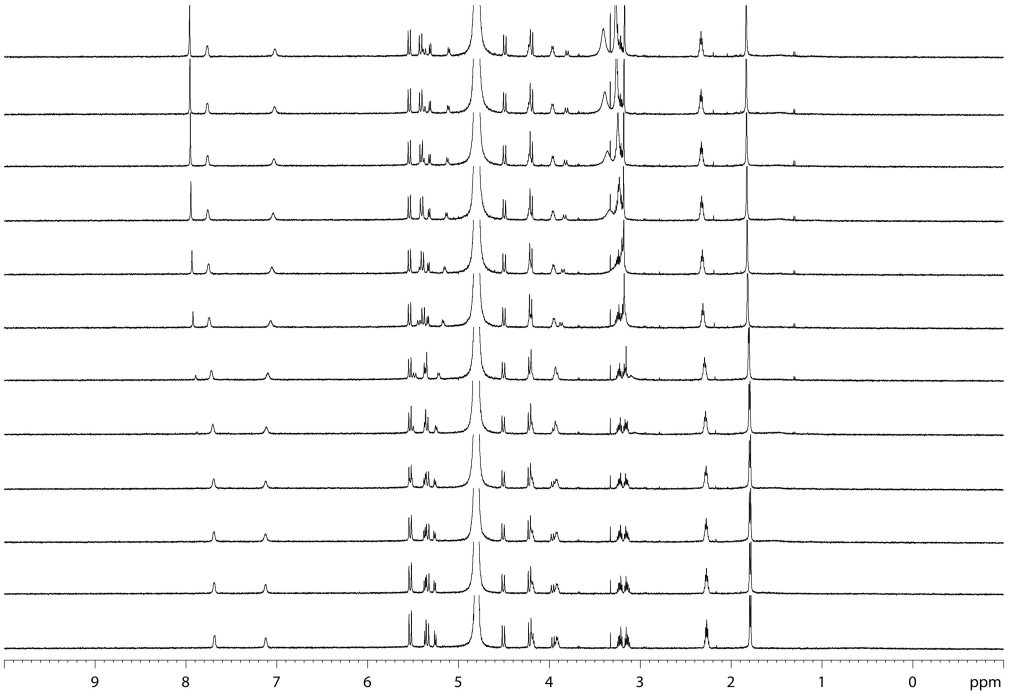

(B)

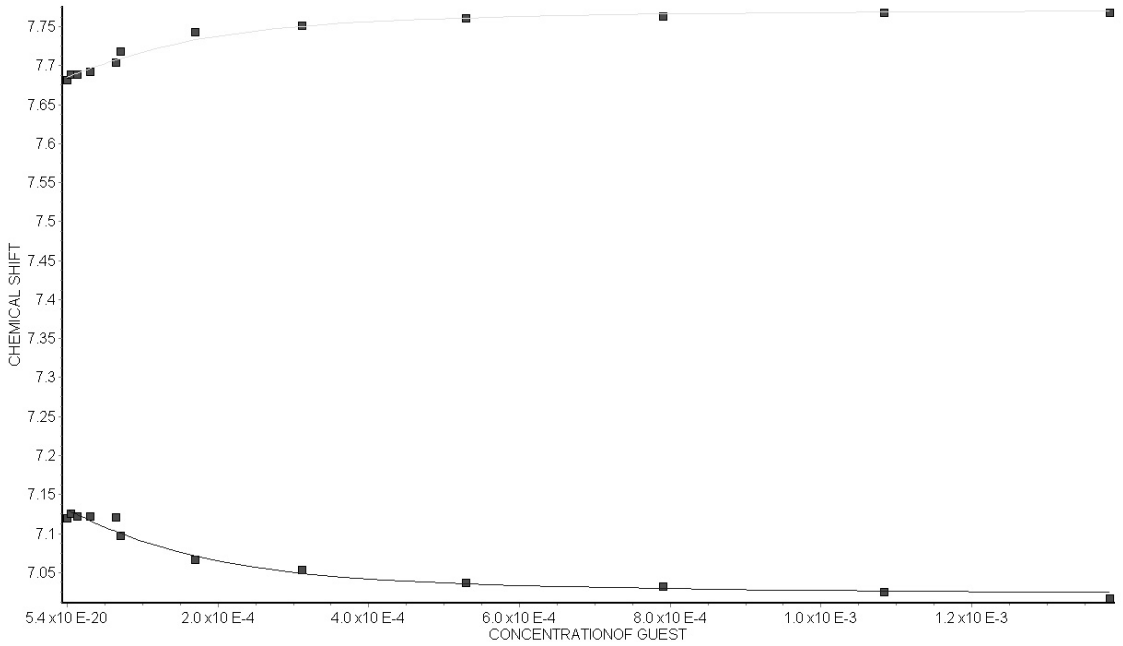

Figure S26. (A) ^{1}H NMR (600 MHz) stack plot of the titration of **2** (0.150 mM) with guest **11** (0 - 1.3 mM) in 20 mM NaH_2PO_4 buffered D_2O (pH = 7.4); (B) plot of the chemical shift at 7.12 and 7.68 ppm as a function of guest concentration. The solid line represents the best non-linear fit of the data to a 1:1 model ($K_a = (1.4 \pm 0.4) \times 10^4$ M^{-1}).

(A)

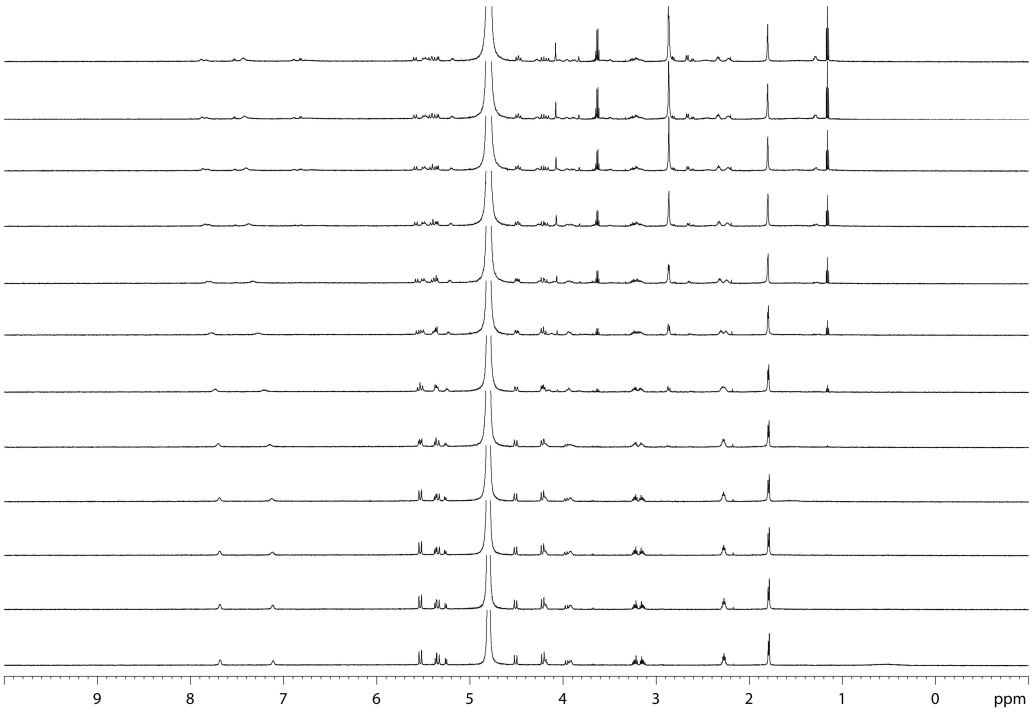

(B)

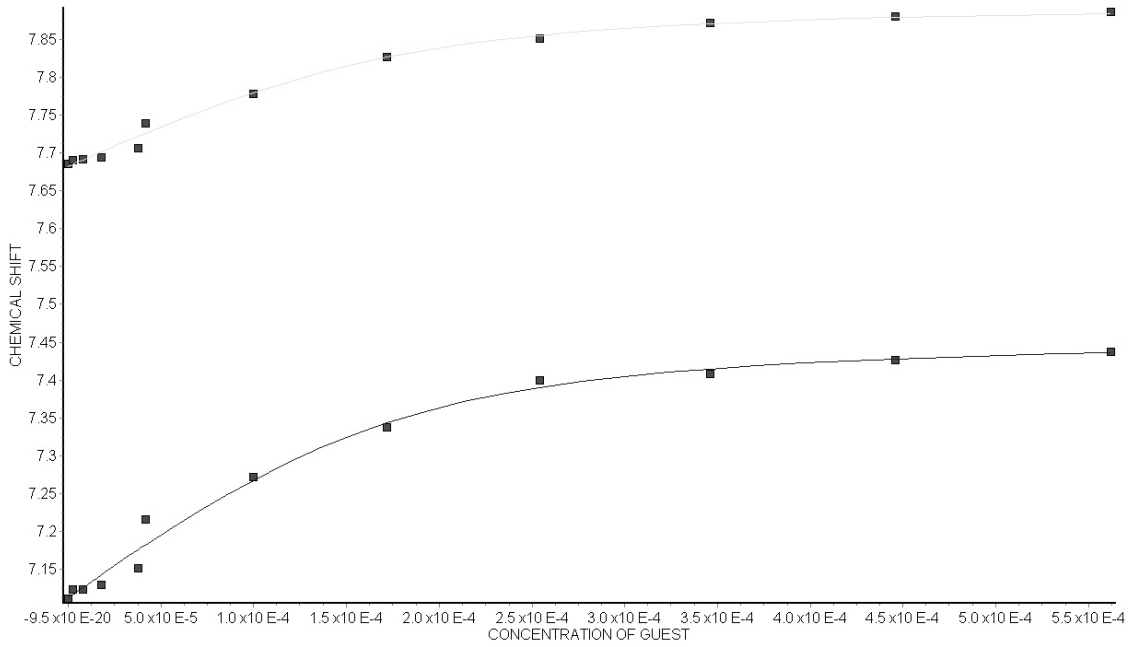

Figure S27. (A) ^{1}H NMR (600 MHz) stack plot of the titration of **2** (0.150 mM) with guest **13** (0 - 1.26 mM) in 20 mM NaH_2PO_4 buffered D_2O (pH = 7.4); (B) plot of the chemical shift at 7.12 and 7.68 ppm as a function of guest concentration. The solid line represents the best non-linear fit of the data to a 1:1 model ($K_a = (3.3 \pm 1.0) \times 10^4\ M^{-1}$).

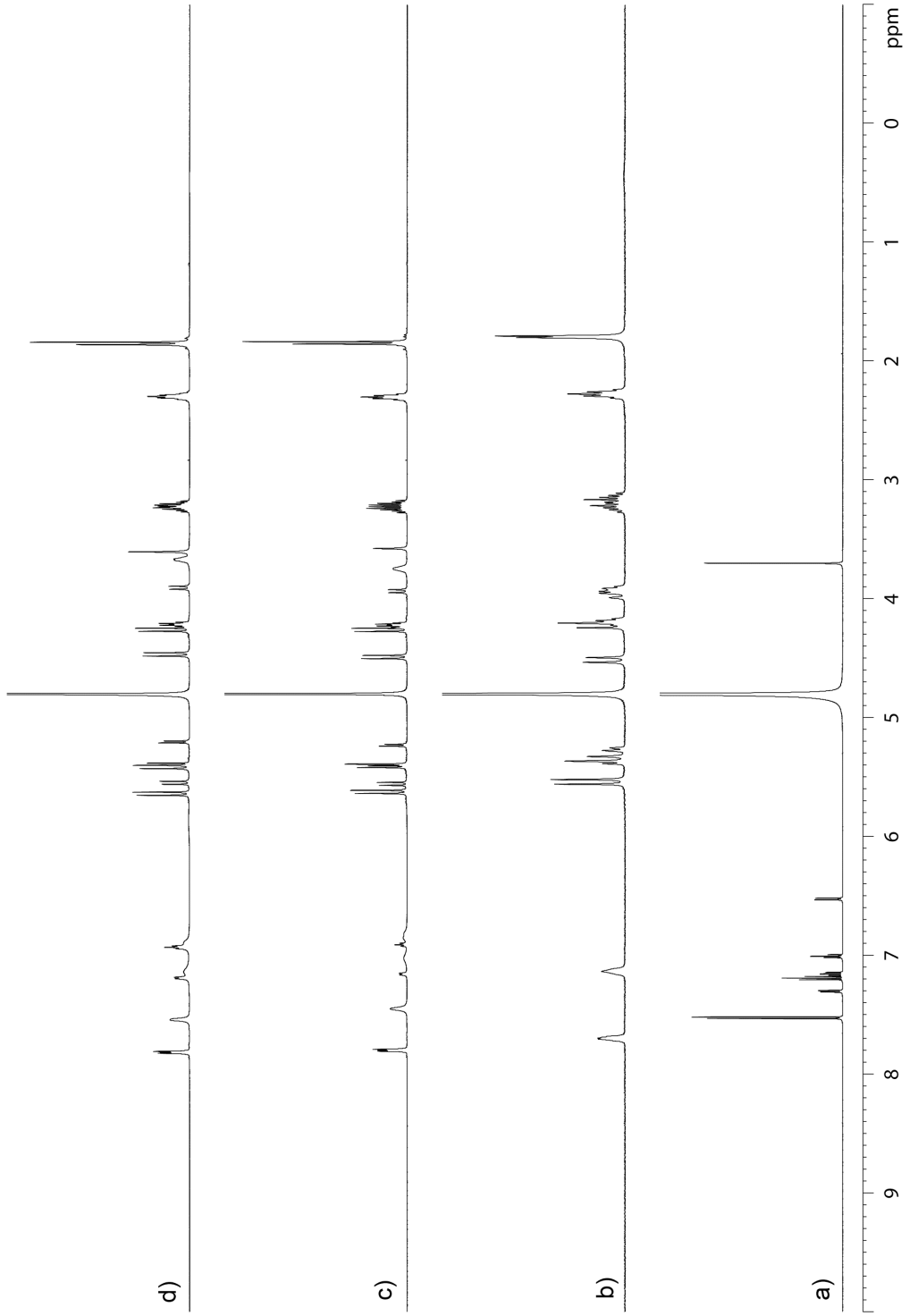

Figure S28. ^{1}H NMR spectra recorded (400 MHz, RT, D_2O) for a) **3**, b) **2**, c) an equimolar mixture of **2** and **3** (5 mM), and d) a 1:2 mixture of **2** (5 mM) and **3** (10 mM).

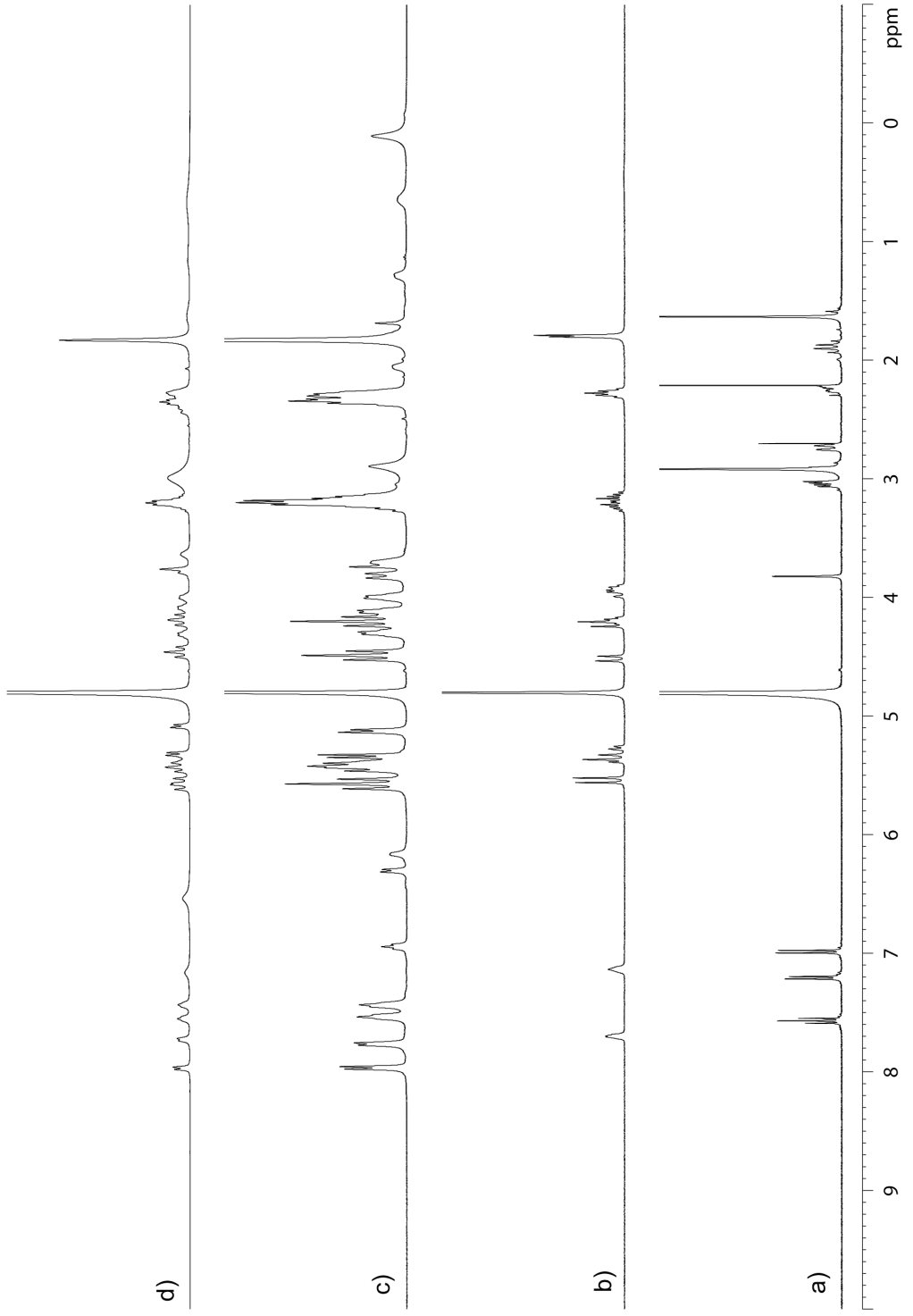

Figure S29. ^{1}H NMR spectra recorded (400 MHz, RT, D_2O) for a) **4**, b) **2**, c) an equimolar mixture of **2** and **4** (12.5 mM), and d) a 1:2 mixture of **2** (12.5 mM) and **4** (25 mM).

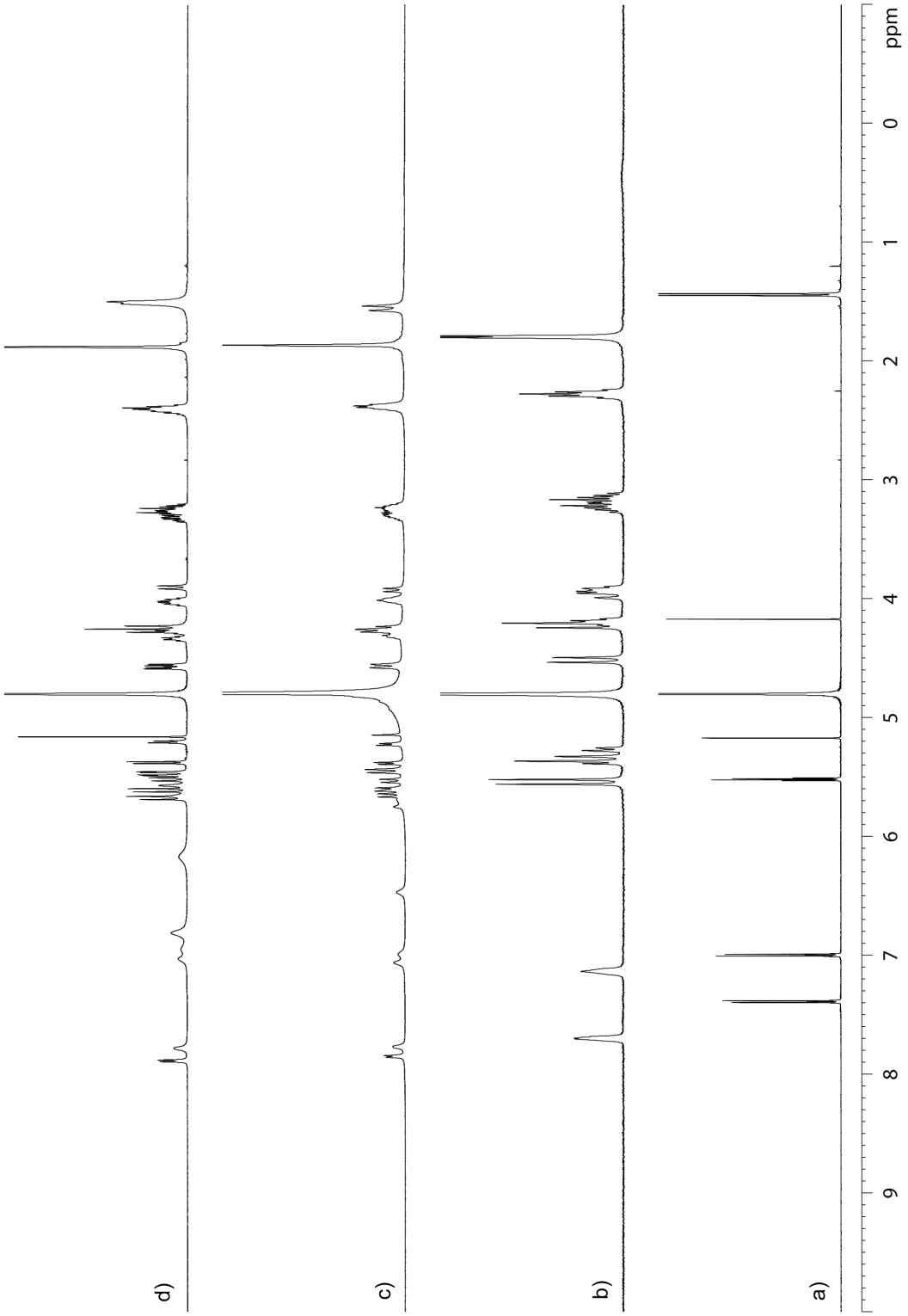

Figure S30. ^{1}H NMR spectra recorded (400 MHz, RT, D_2O) for a) **5**, b) **2**, c) an equimolar mixture of **2** and **5** (5 mM), and d) a 1:2 mixture of **2** (5 mM) and **5** (10 mM).

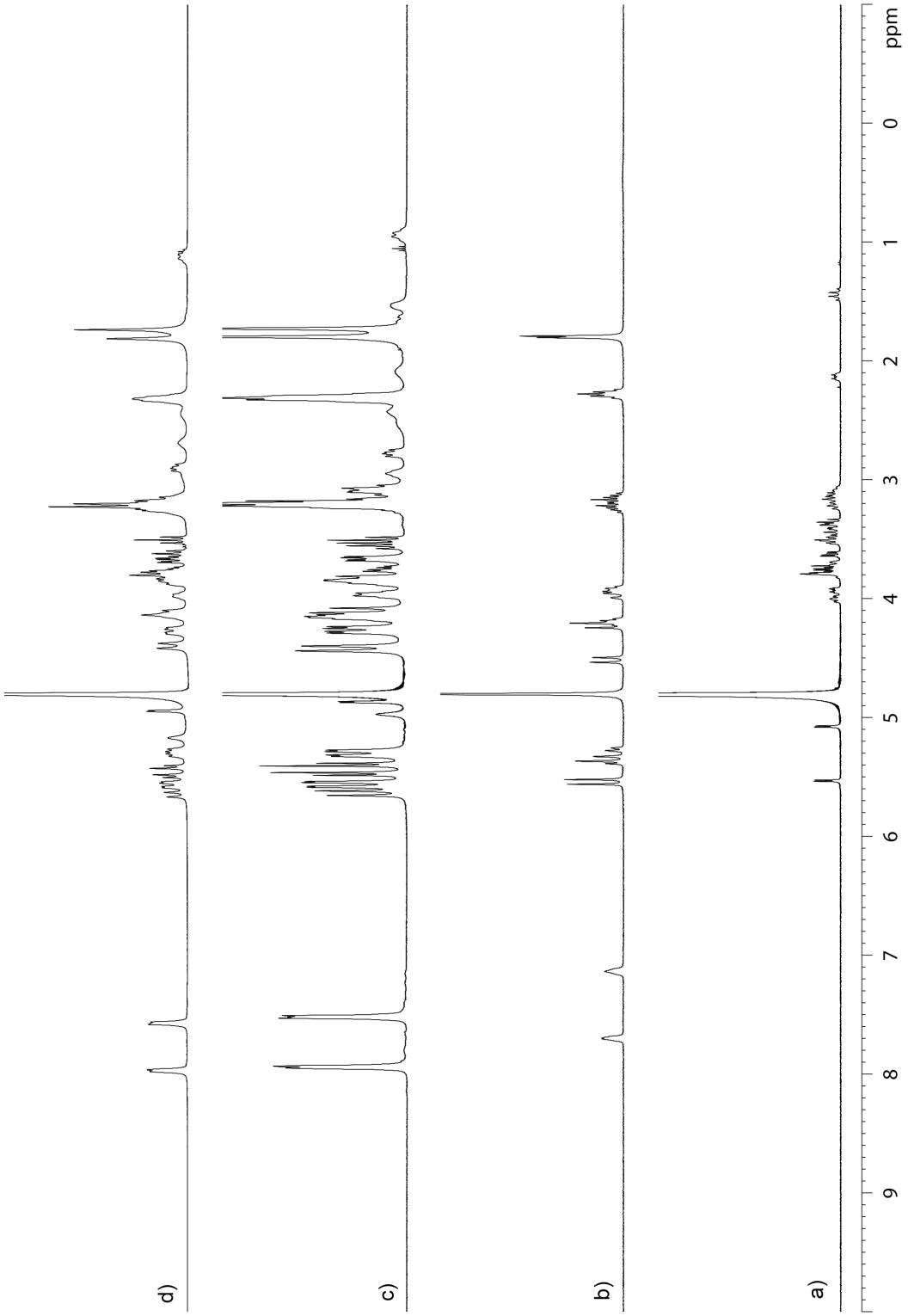

Figure S31. ^{1}H NMR spectra recorded (400 MHz, RT, D_2O) for a) **6**, b) **2**, c) an equimolar mixture of **2** and **6** (12.5 mM), and d) a 1:2 mixture of **2** (12.5 mM) and **6** (25 mM).

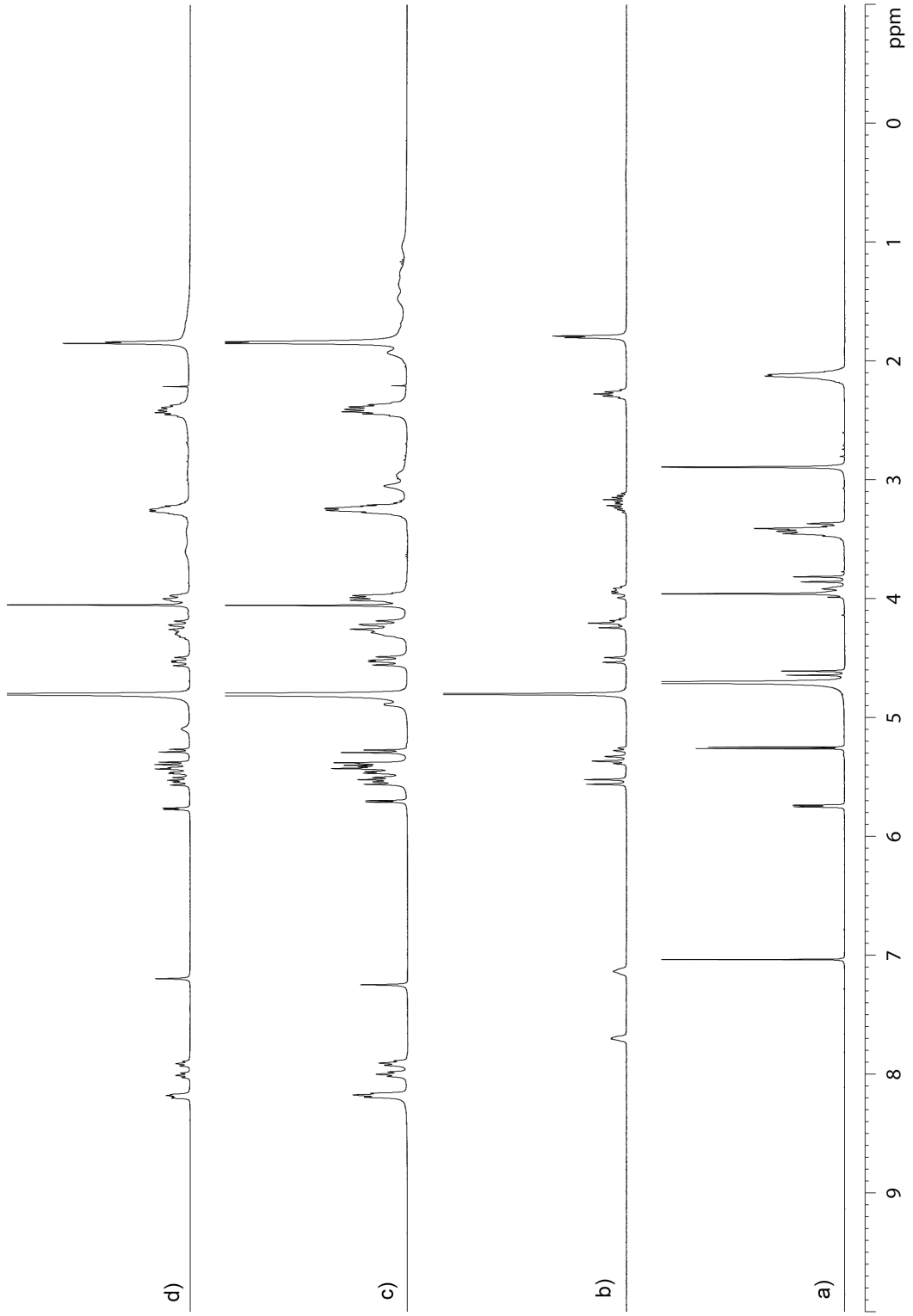

Figure S32. ^{1}H NMR spectra recorded (400 MHz, RT, D_2O) for a) **7**, b) **2**, c) an equimolar mixture of **2** and **7** (5 mM), and d) a 1:2 mixture of **2** (5 mM) and **7** (10 mM).

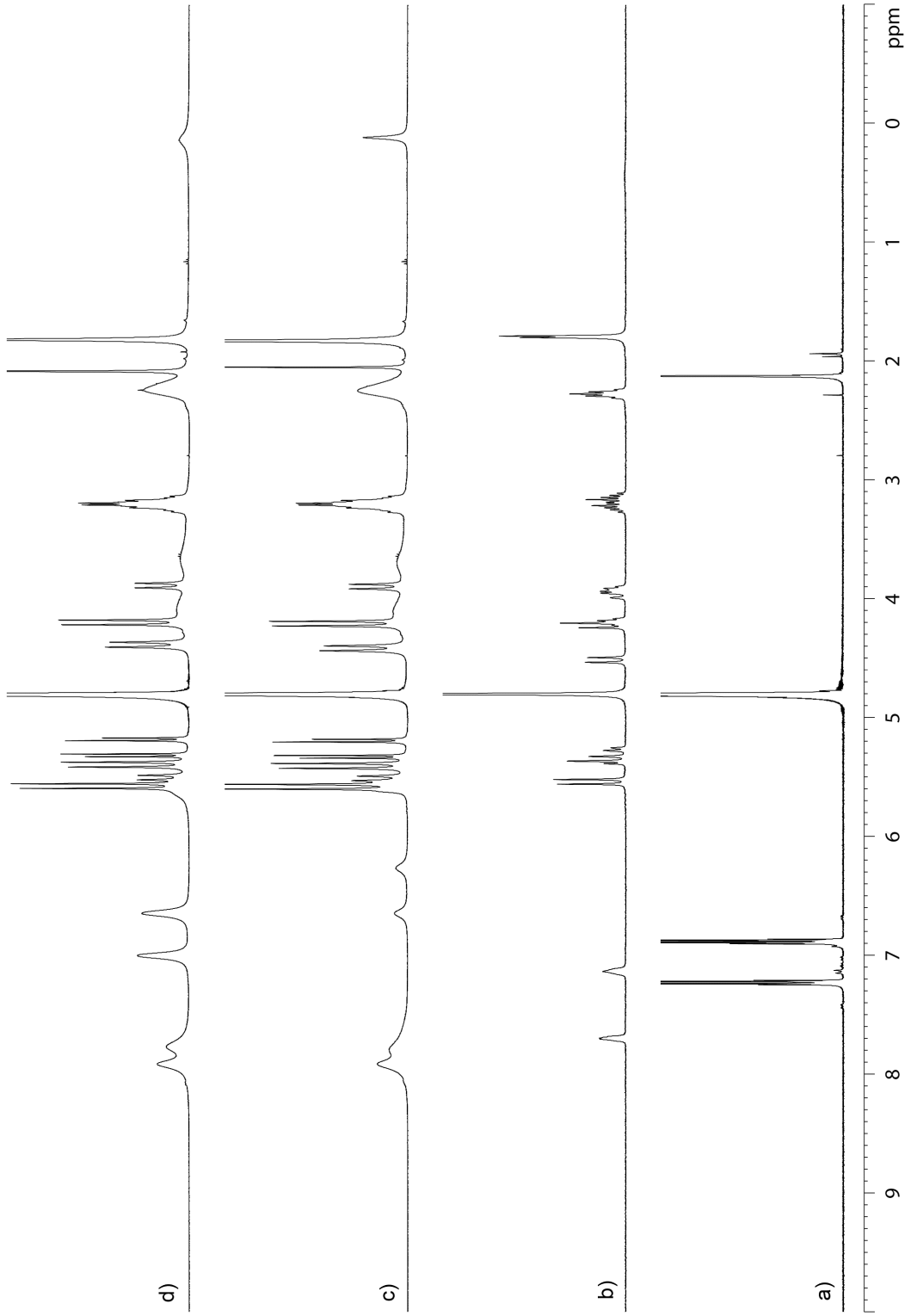

Figure S33. ^{1}H NMR spectra recorded (400 MHz, RT, D_2O) for a) **8**, b) **2**, c) an equimolar mixture of **2** and **8** (5 mM), and d) a 1:2 mixture of **2** (5 mM) and **8** (10 mM).

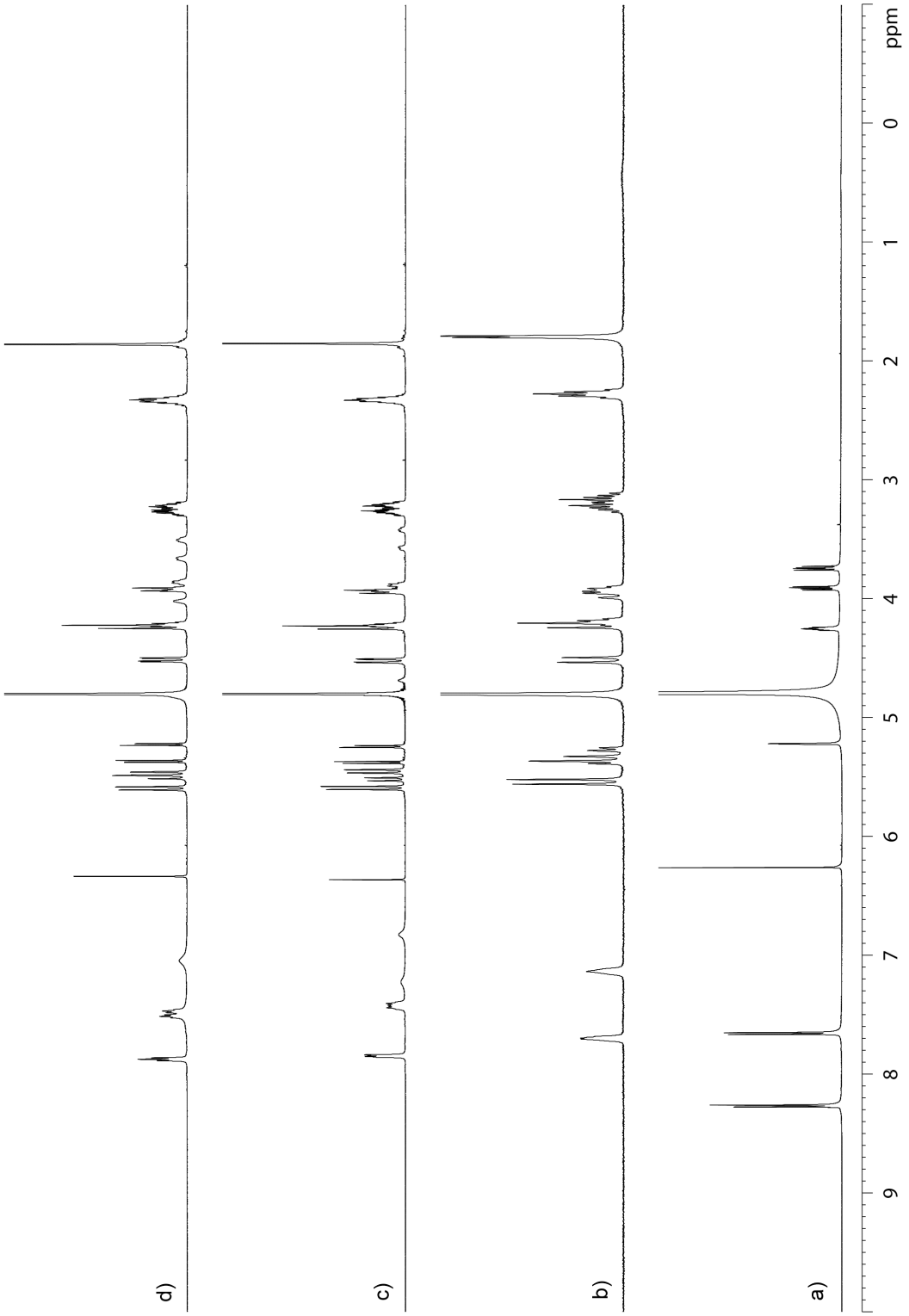

Figure S34. ^{1}H NMR spectra recorded (400 MHz, RT, D_2O) for a) **9**, b) **2**, c) an equimolar mixture of **2** and **9** (5 mM), and d) a 1:2 mixture of **2** (5 mM) and **9** (10 mM).

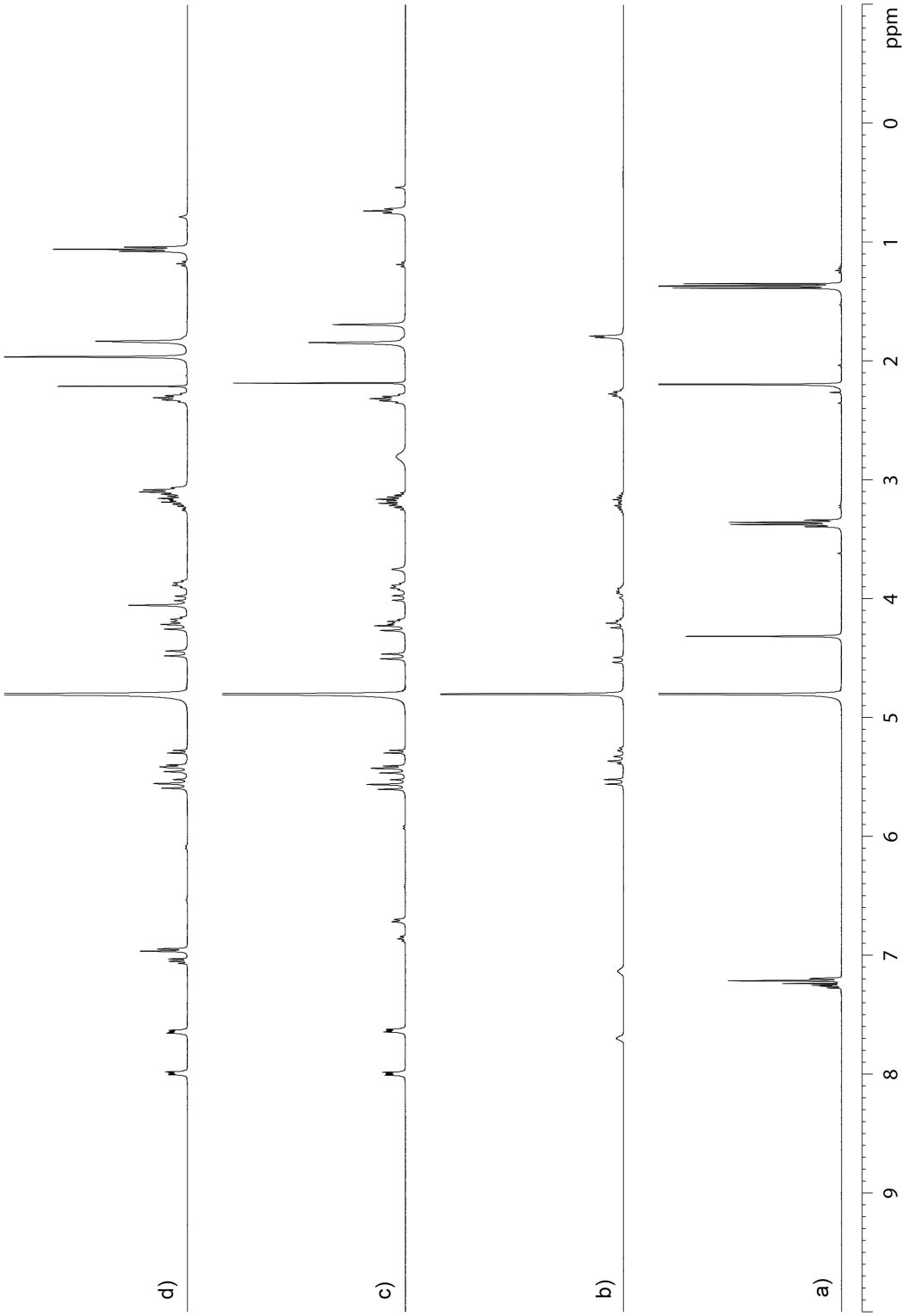

Figure S35. ^{1}H NMR spectra recorded (400 MHz, RT, D_2O) for a) **10**, b) **2**, c) an equimolar mixture of **2** and **10** (4 mM), and d) a 1:2 mixture of **2** (4 mM) and **10** (8 mM).

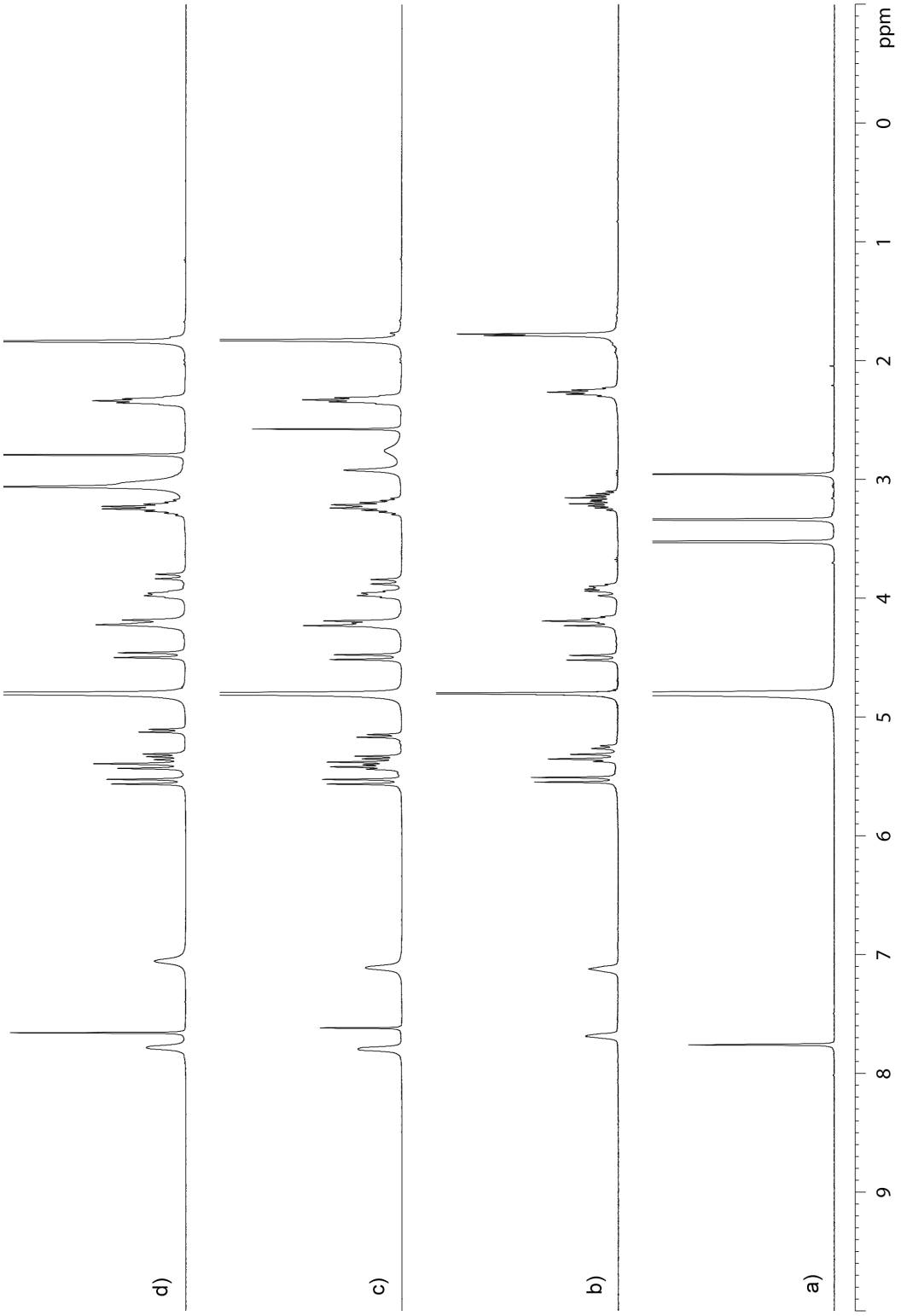

Figure S36. ^{1}H NMR spectra recorded (400 MHz, RT, D_2O) for a) **11**, b) **2**, c) an equimolar mixture of **2** and **11** (4 mM), and d) a 1:2 mixture of **2** (4 mM) and **11** (8 mM).

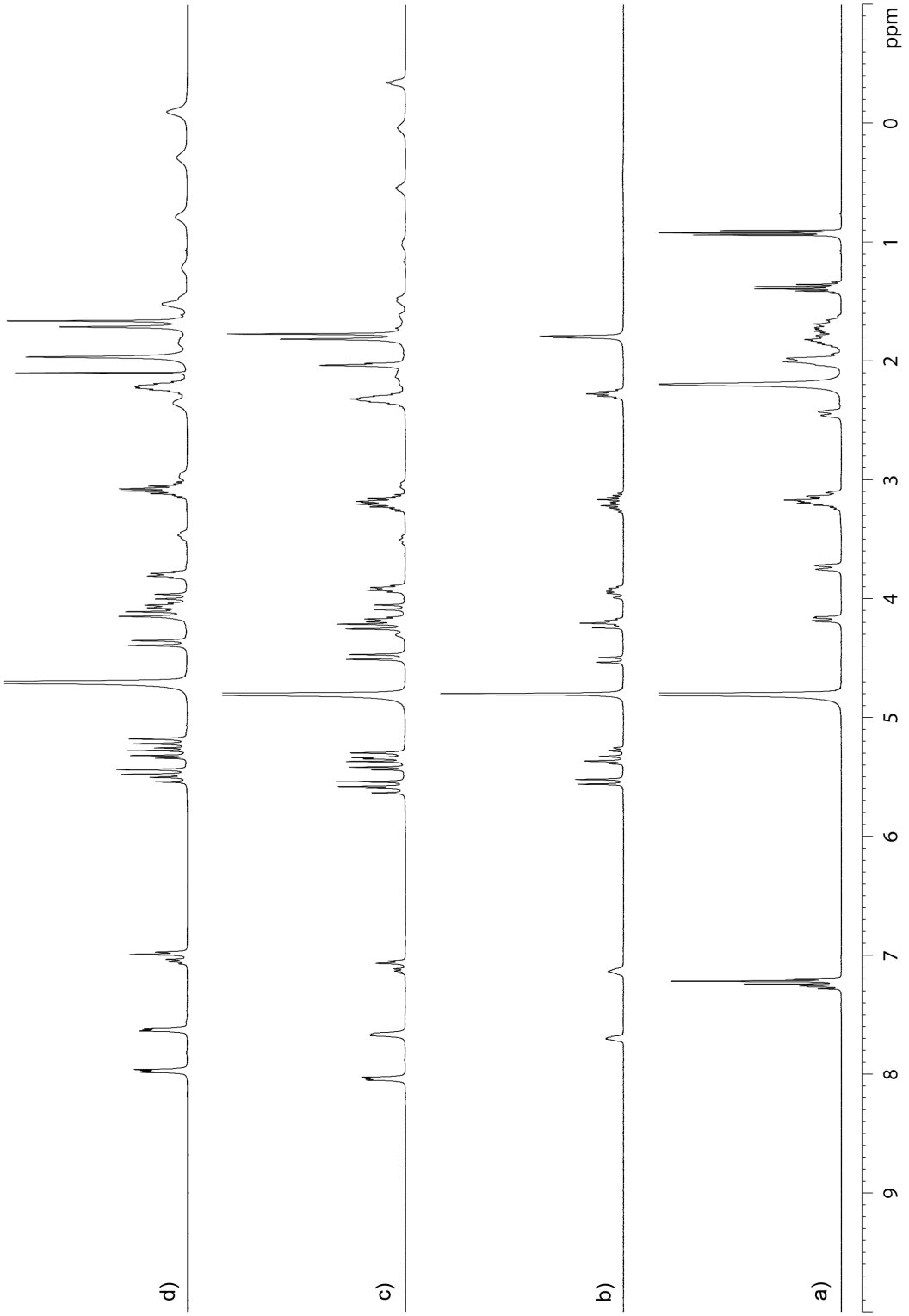

Figure S37. ^{1}H NMR spectra recorded (400 MHz, RT, D_2O) for a) **12**, b) **2**, c) an equimolar mixture of **2** and **12** (4 mM), and d) a 1:2 mixture of **2** (4 mM) and **12** (8 mM).

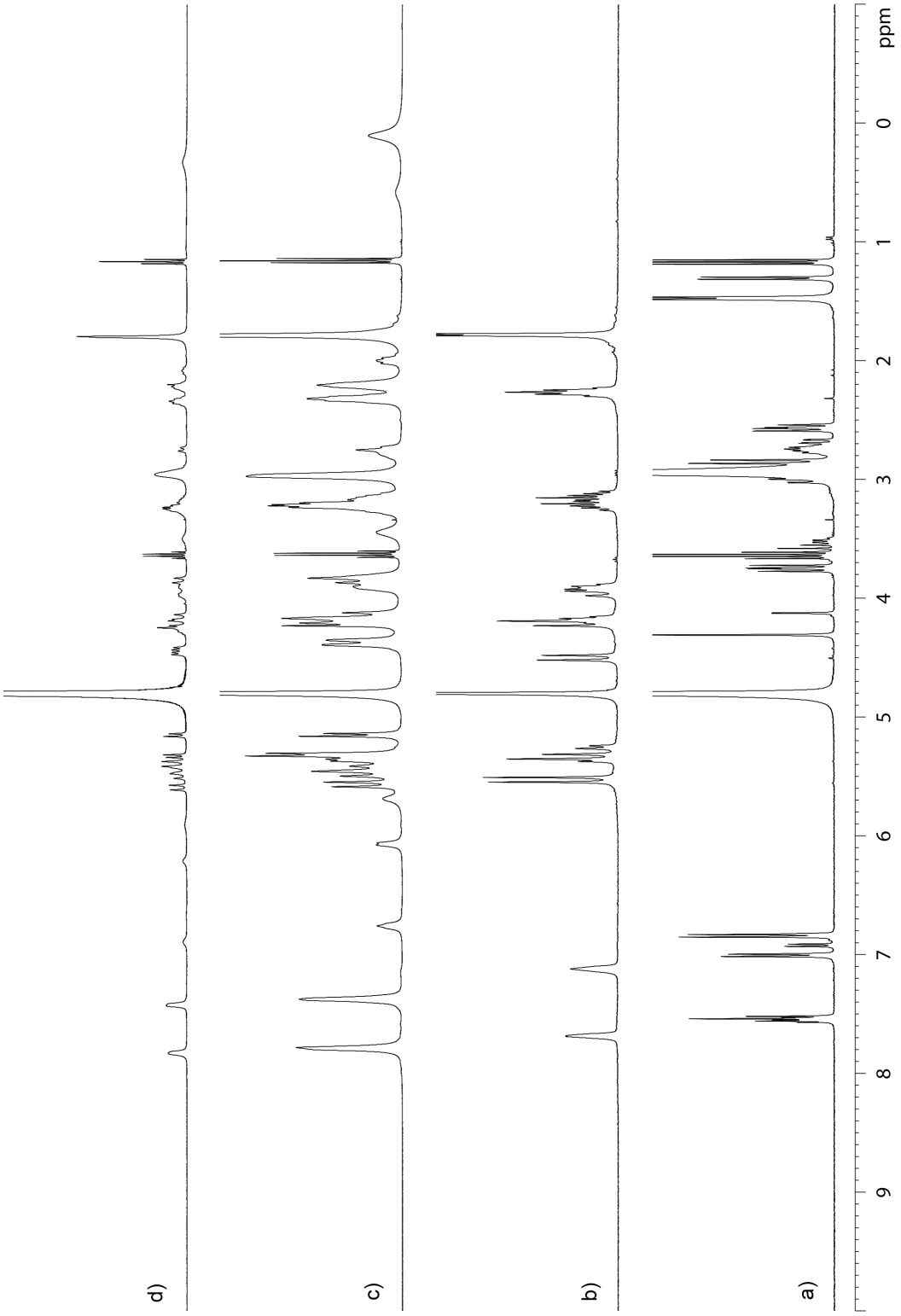

Figure S38. ^{1}H NMR spectra recorded (400 MHz, RT, D_2O) for a) **13**, b) **2**, c) an equimolar mixture of **2** and **13** (12.5 mM), and d) a 1:2 mixture of **2** (4 mM) and **13** (8 mM).

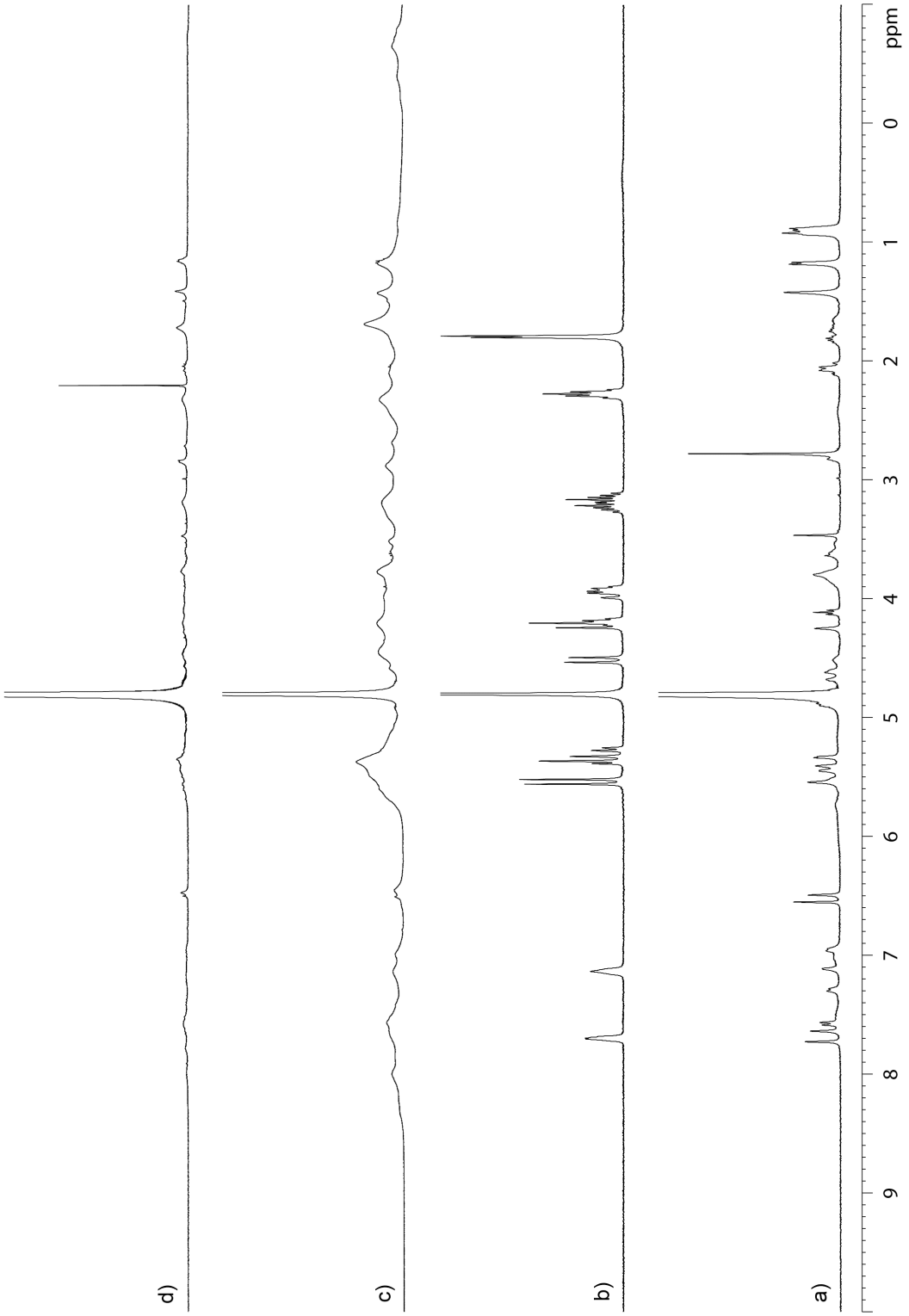

Figure S39. ^{1}H NMR spectra recorded (400 MHz, RT, D_2O) for a) **14**, b) **2**, c) an equimolar mixture of **2** and **14** (4 mM), and d) a 1:2 mixture of **2** (1 mM) and **14** (2 mM).

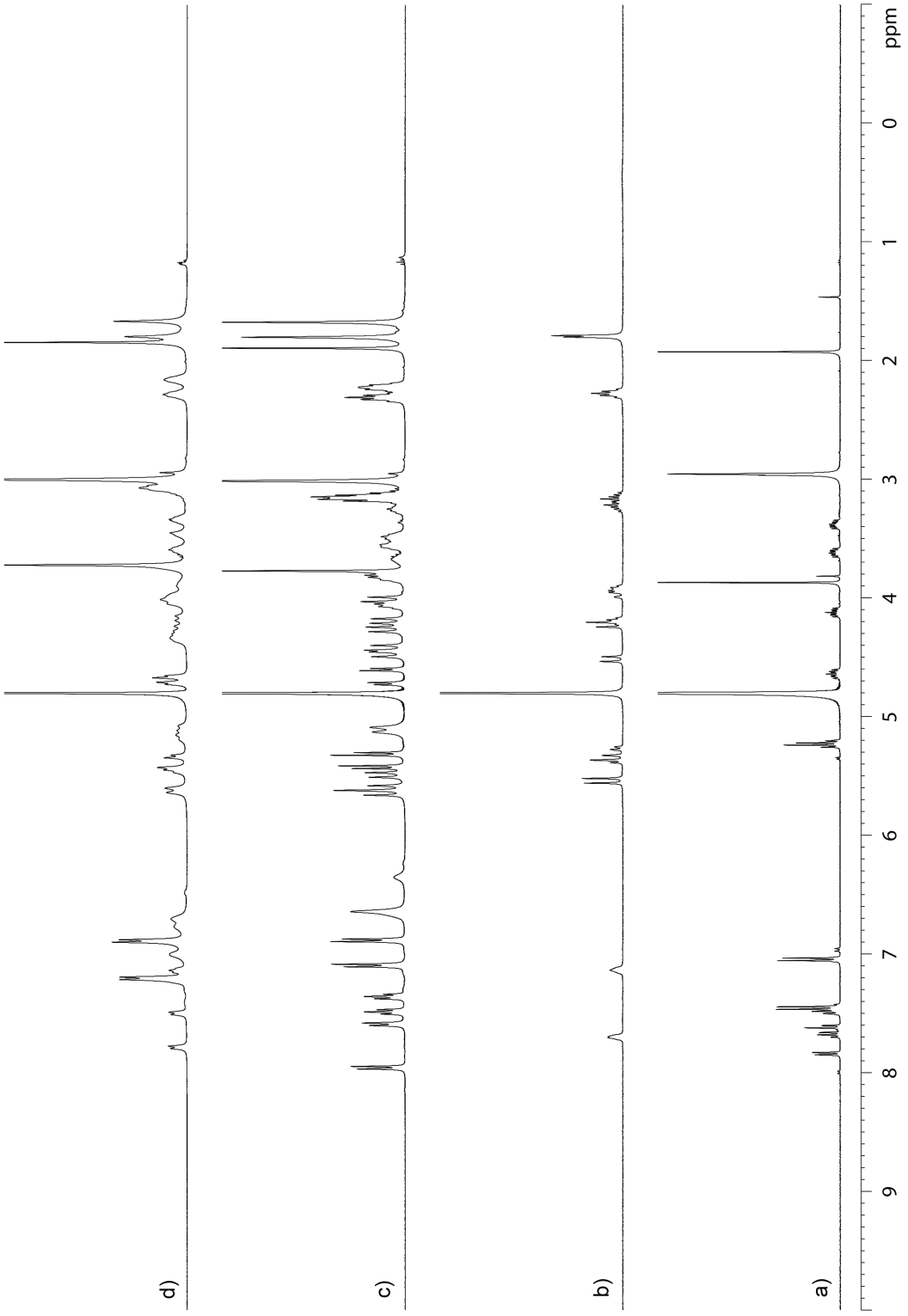

Figure S40. ^{1}H NMR spectra recorded (400 MHz, RT, D_2O) for a) **15**, b) **2**, c) an equimolar mixture of **2** and **15** (12.5 mM), and d) a 1:2 mixture of **2** (12.5 mM) and **15** (25 mM).

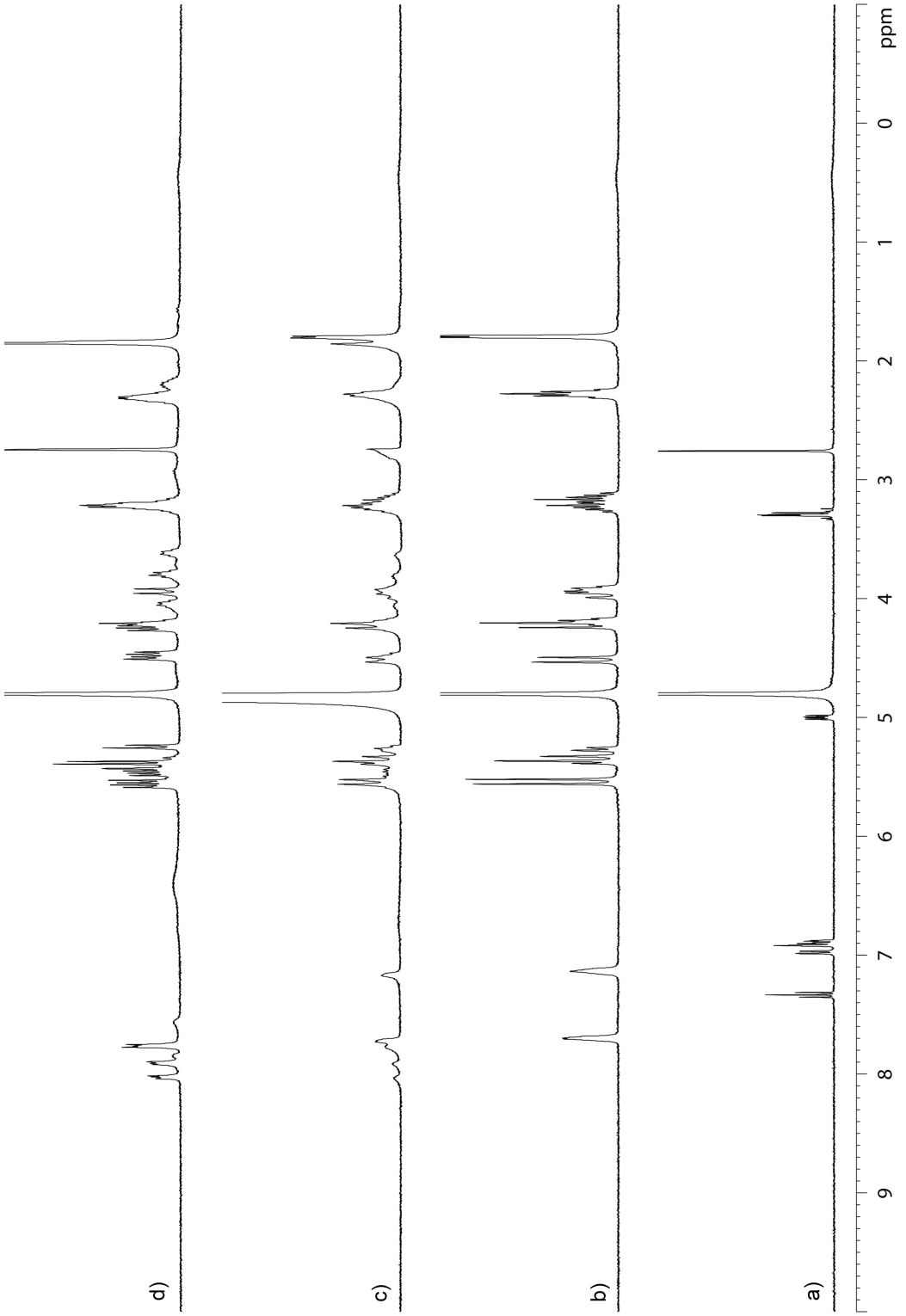

Figure S41. ^{1}H NMR spectra recorded (400 MHz, RT, D_2O) for a) **16**, b) **2**, and c) an equimolar mixture of **2** and **16** (2 mM), and d) a 1:2 mixture of **2** (0.7 mM) and **16** (1.3 mM).

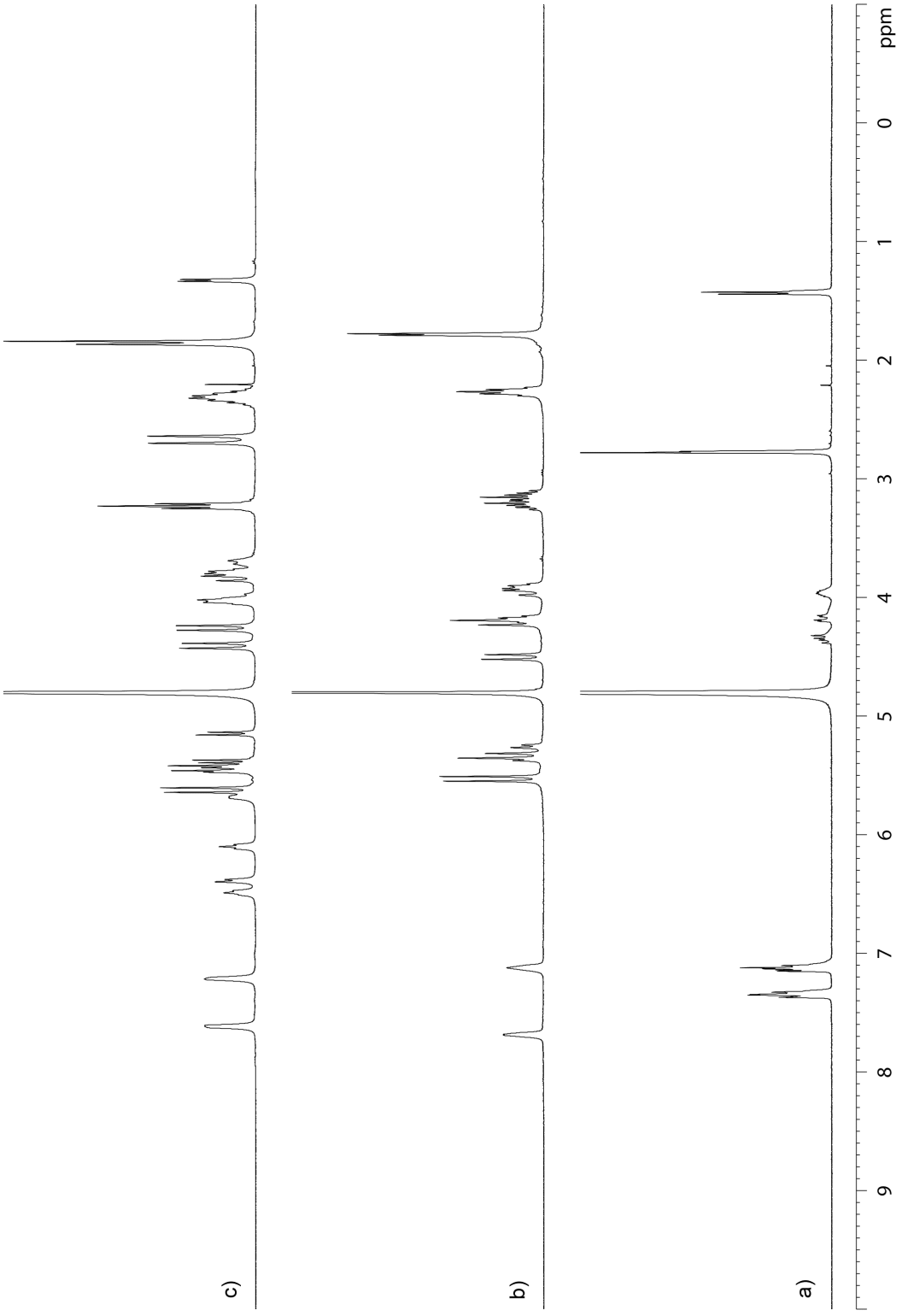

Figure S42. ^{1}H NMR spectra recorded (400 MHz, RT, D_2O) for a) **17**, b) **2**, and c) an equimolar mixture of **2** and **17** (4 mM).

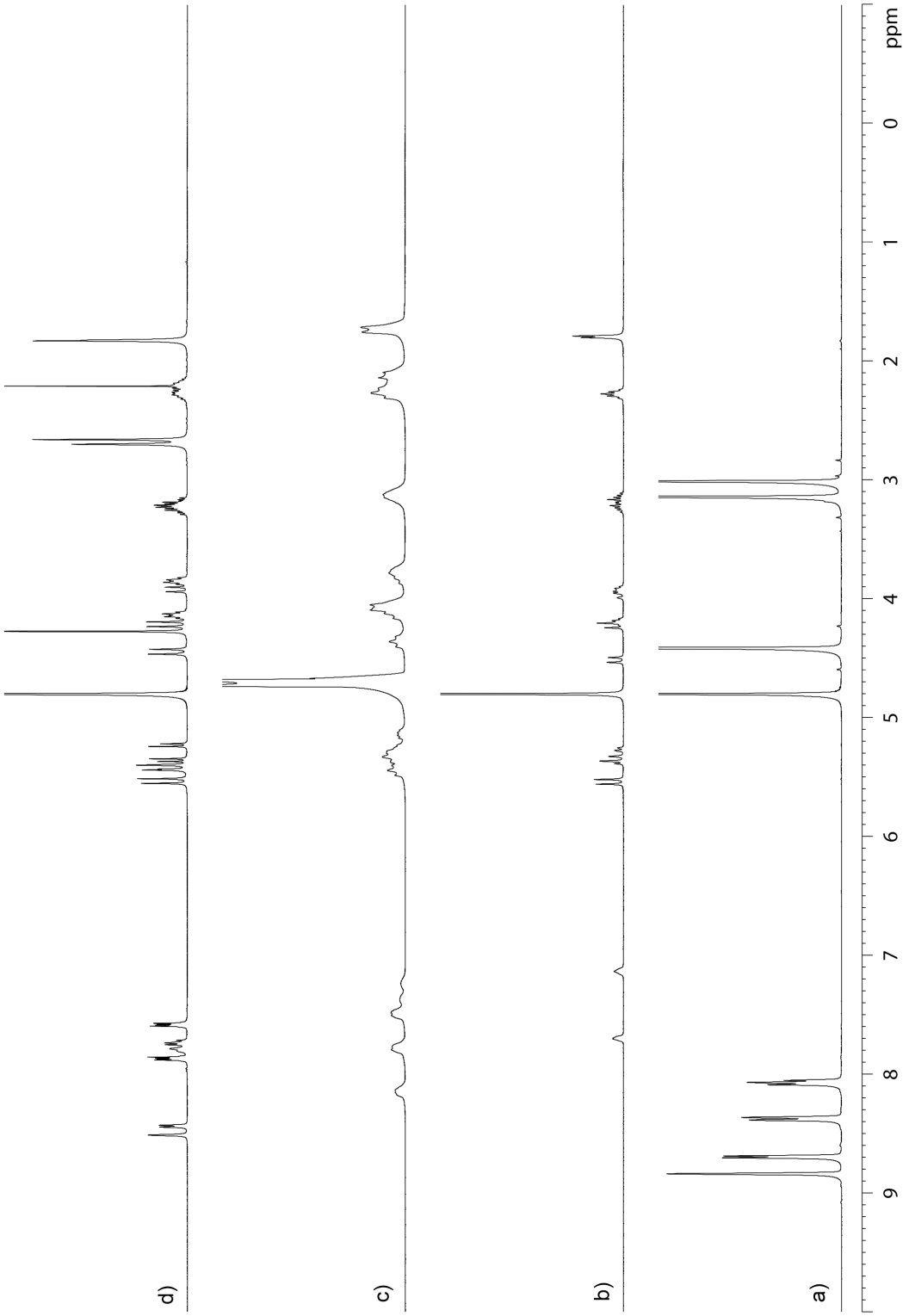

Figure S43. ^{1}H NMR spectra recorded (400 MHz, RT, D_2O) for a) **18**, b) **2**, c) an equimolar mixture of **2** and **18** (4 mM), and d) a 1:2 mixture of **2** (4 mM) and **18** (8 mM).

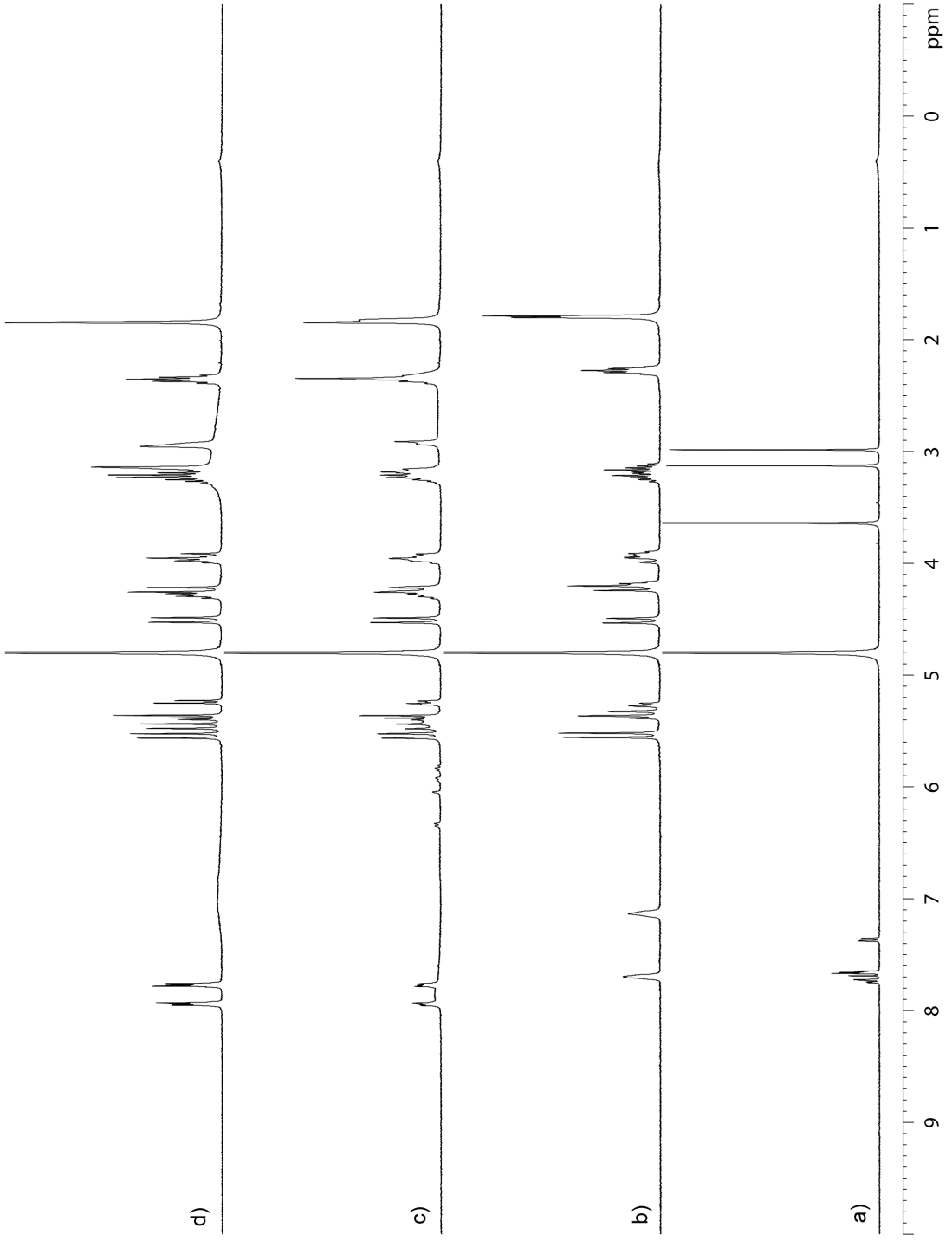

Figure S44. ^{1}H NMR spectra recorded (400 MHz, RT, D_2O) for a) **19**, b) **2**, c) an equimolar mixture of **2** and **19** (4 mM), and d) a 1:2 mixture of **2** (4 mM) and **19** (8 mM).

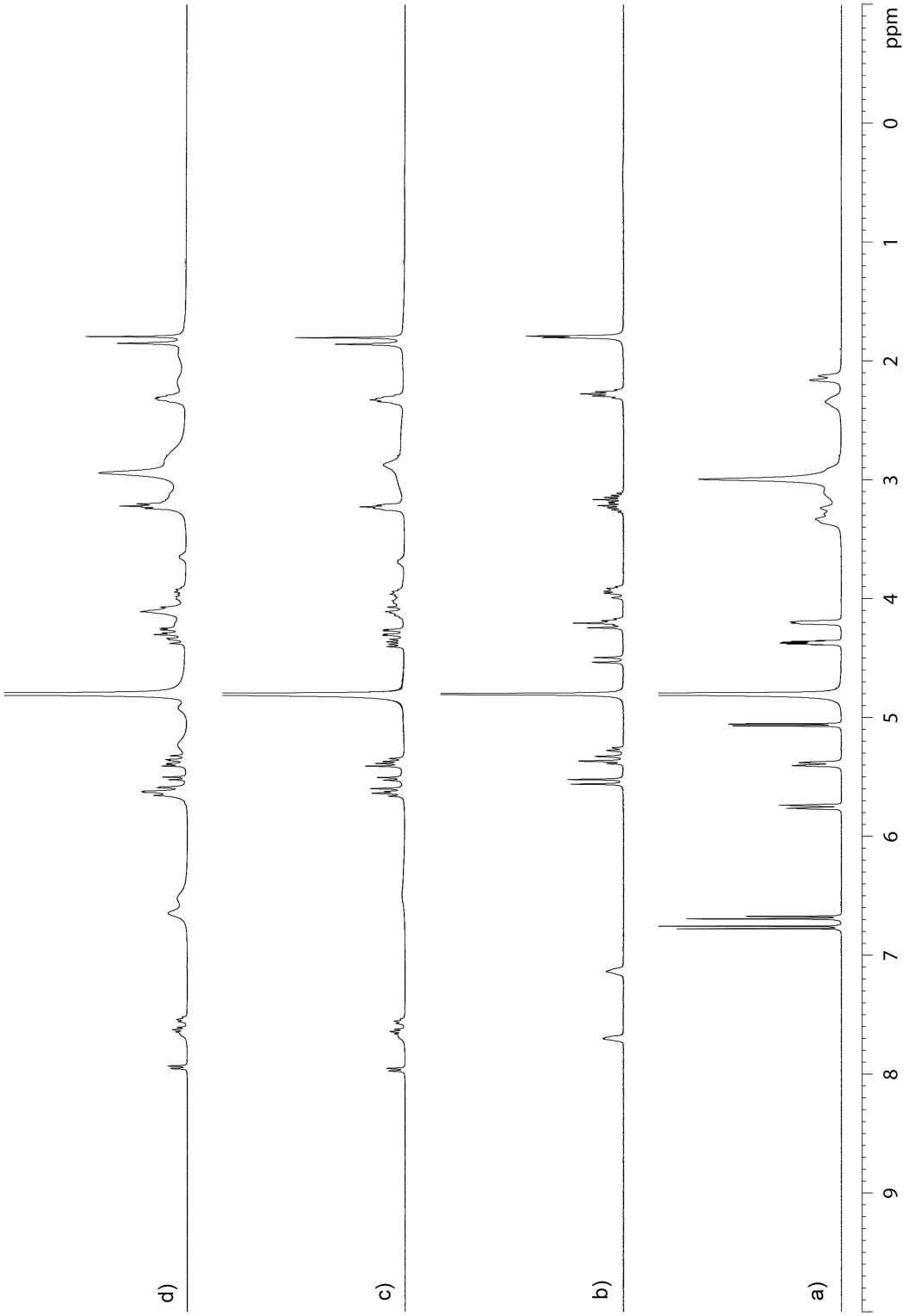

Figure S45. ^{1}H NMR spectra recorded (400 MHz, RT, D_2O) for a) **20**, b) **2**, c) an equimolar mixture of **2** and **20** (5 mM), and d) a 1:2 mixture of **2** (5 mM) and **20** (10 mM).

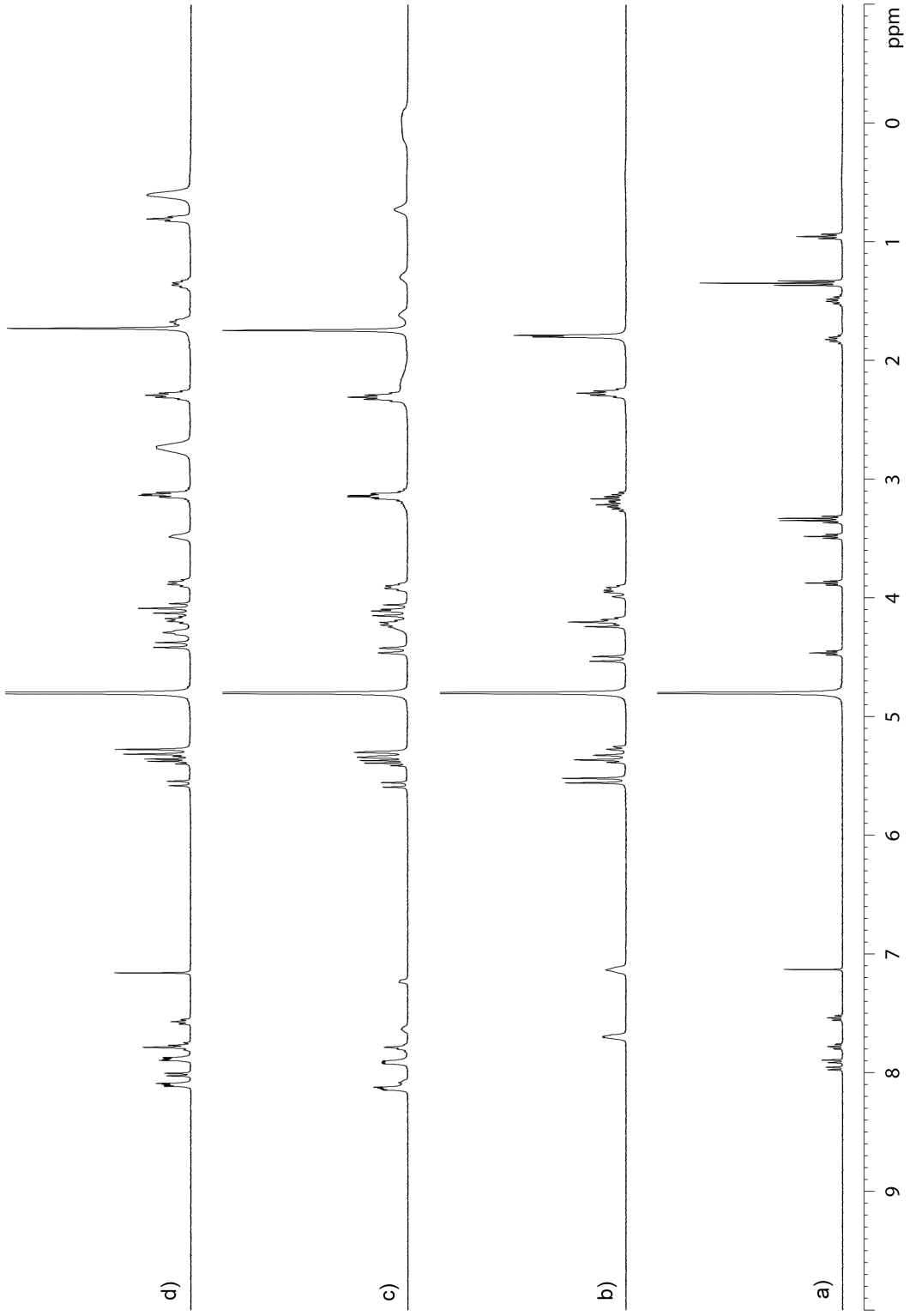

Figure S46. ^{1}H NMR spectra recorded (400 MHz, RT, D_2O) for a) **21**, b) **2**, and c) an equimolar mixture of **2** and **21** (4 mM), and d) a 1:2 mixture of **2** (2 mM) and **21** (4 mM).

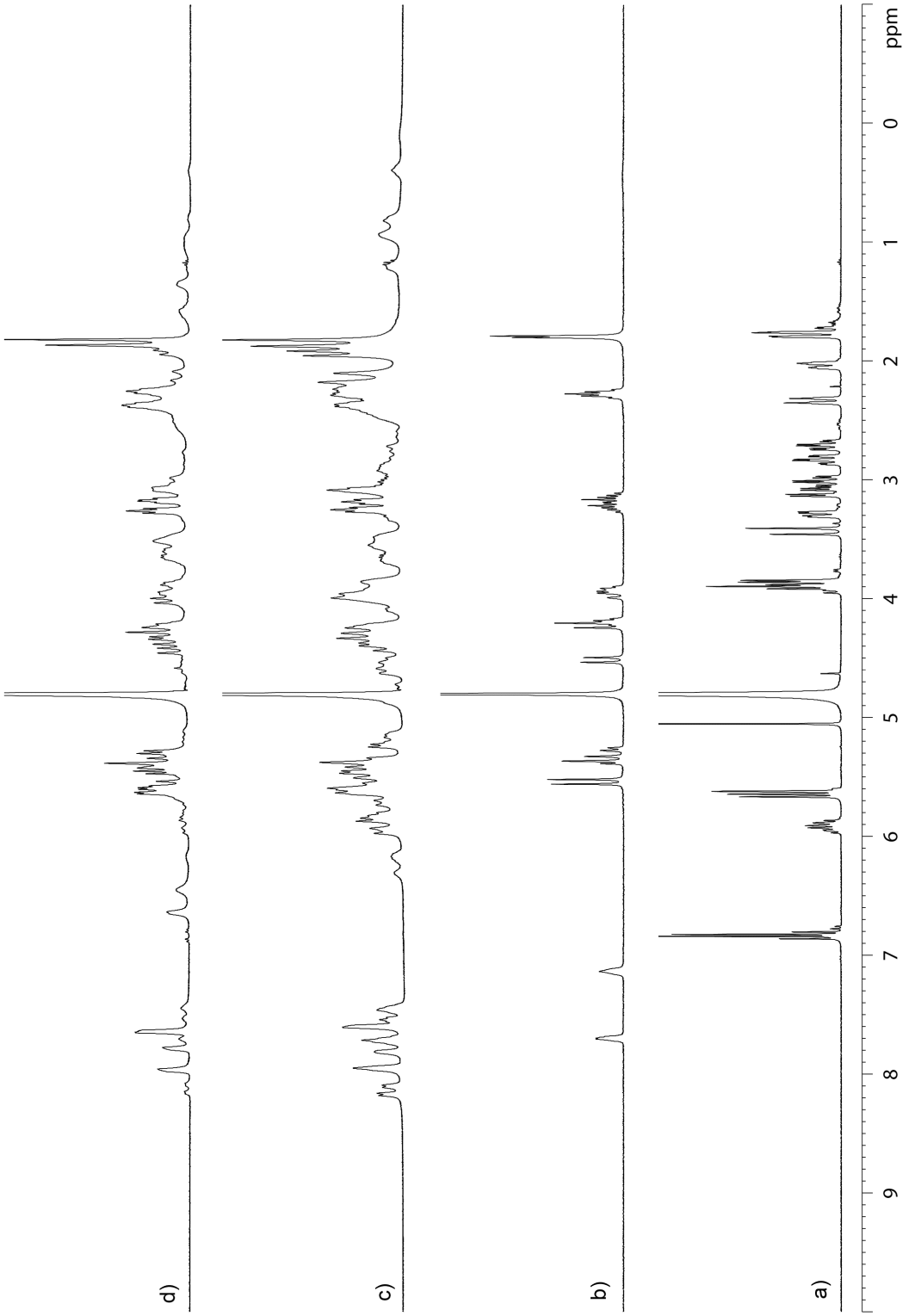

Figure 47. ^{1}H NMR spectra recorded (400 MHz, RT, D_2O) for a) **22**, b) **2**, c) an equimolar mixture of **2** and **22** (12.5 mM), and d) a 1:2 mixture of **2** (6.25 mM) and **22** (12.5 mM).

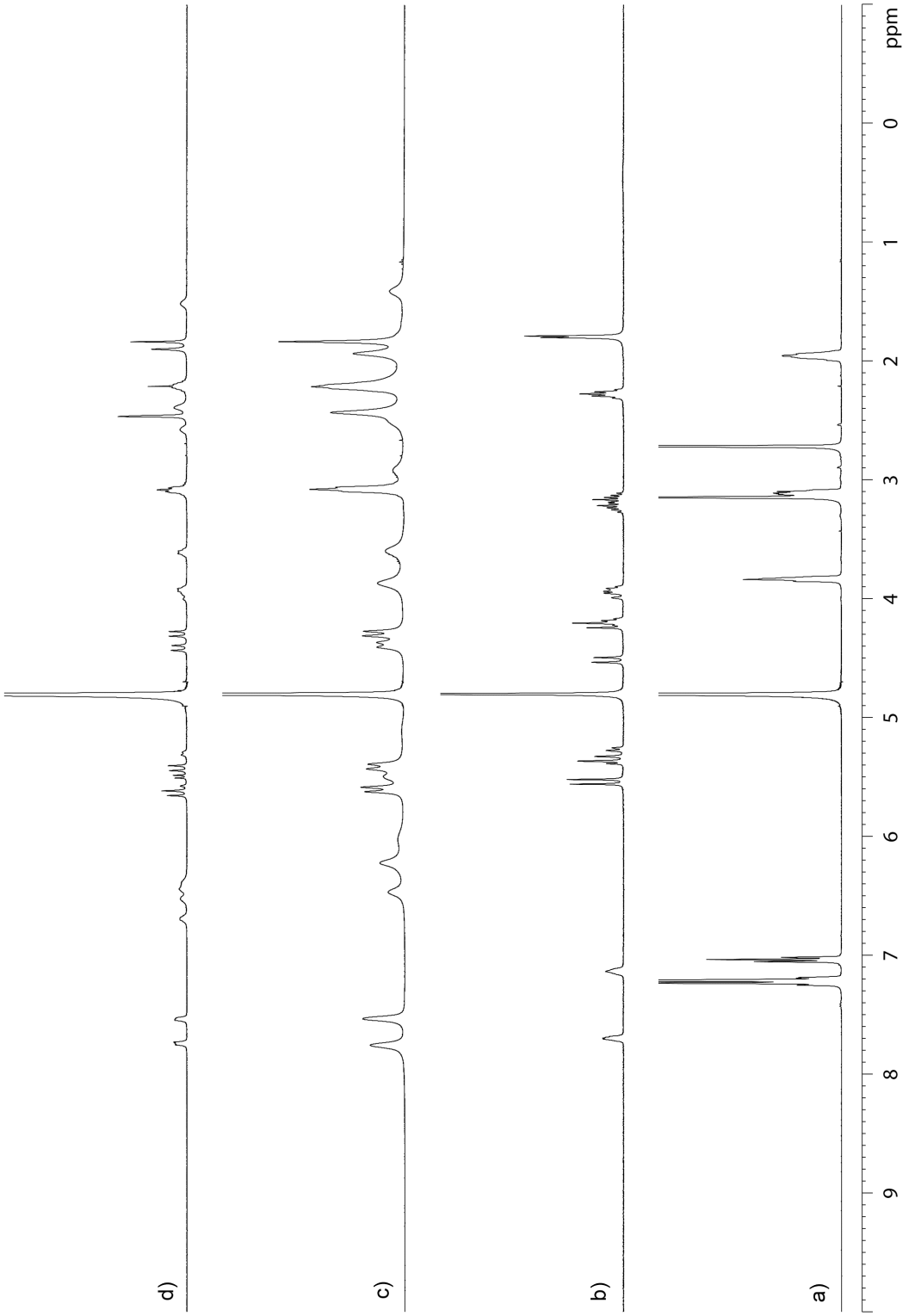

Figure S48. ^{1}H NMR spectra recorded (400 MHz, RT, D_2O) for a) **23**, b) **2**, c) an equimolar mixture of **2** and **23** (5 mM), and d) a 1:2 mixture of **2** (5 mM) and **23** (10 mM).

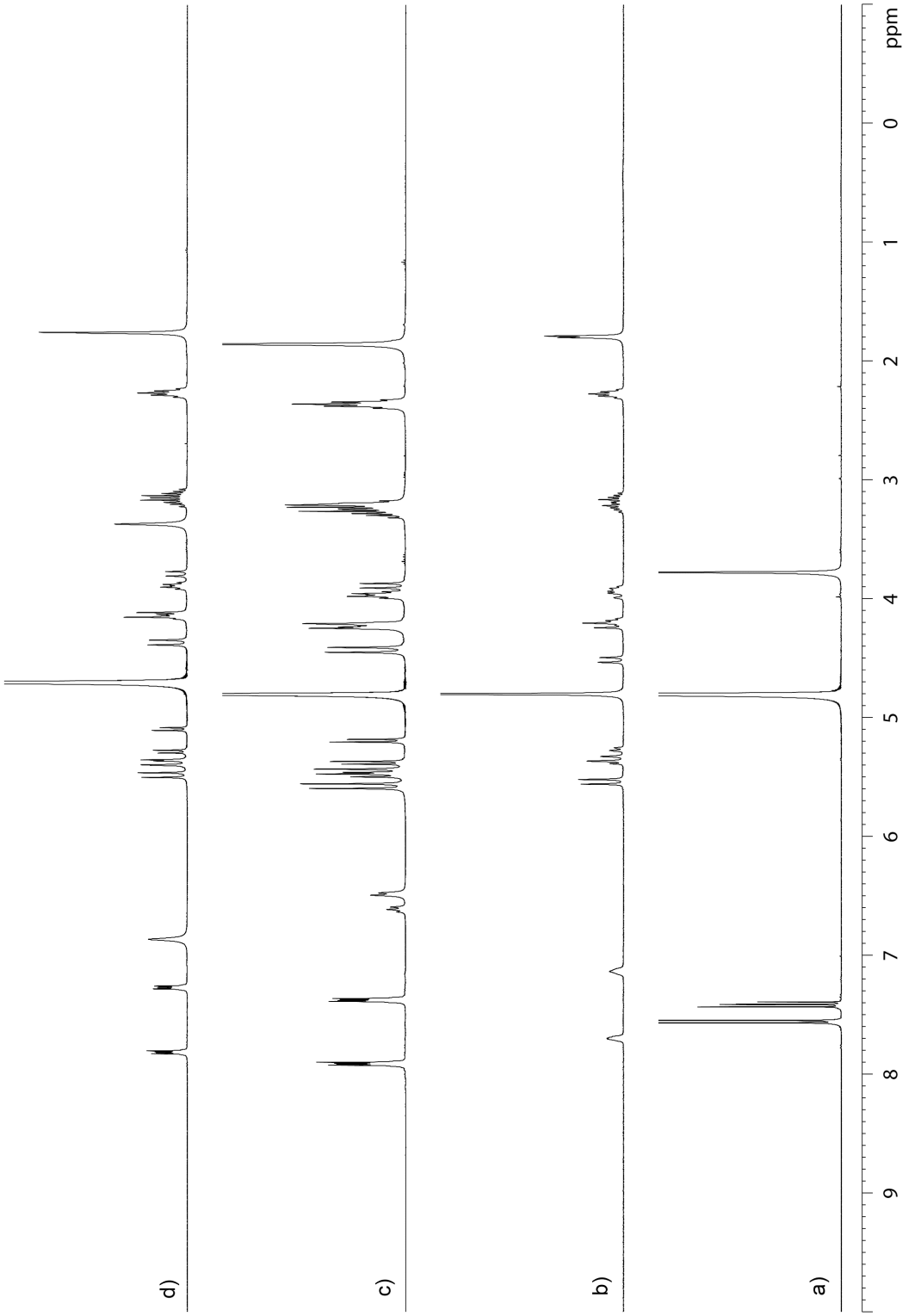

Figure S49. ^{1}H NMR spectra recorded (400 MHz, RT, D_2O) for a) **24**, b) **2**, c) an equimolar mixture of **2** and **24** (5 mM), and d) a 1:2 mixture of **2** (5 mM) and **24** (10 mM).

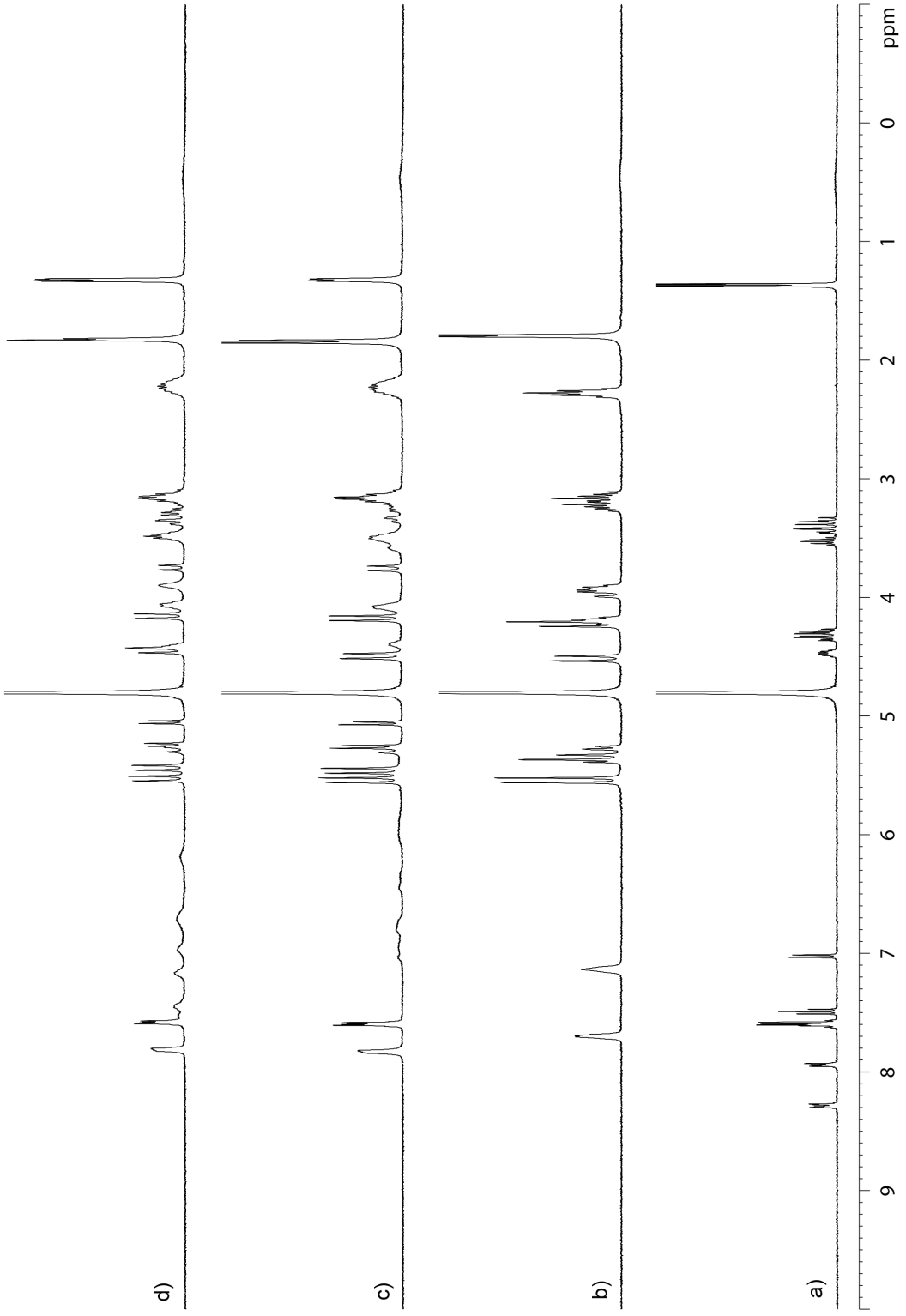

Figure S50. ^{1}H NMR spectra recorded (400 MHz, RT, D_2O) for a) **25**, b) **2**, and c) an equimolar mixture of **2** and **25** (2 mM), and d) a 1:2 mixture of **2** (0.7 mM) and **25** (1.3 mM).

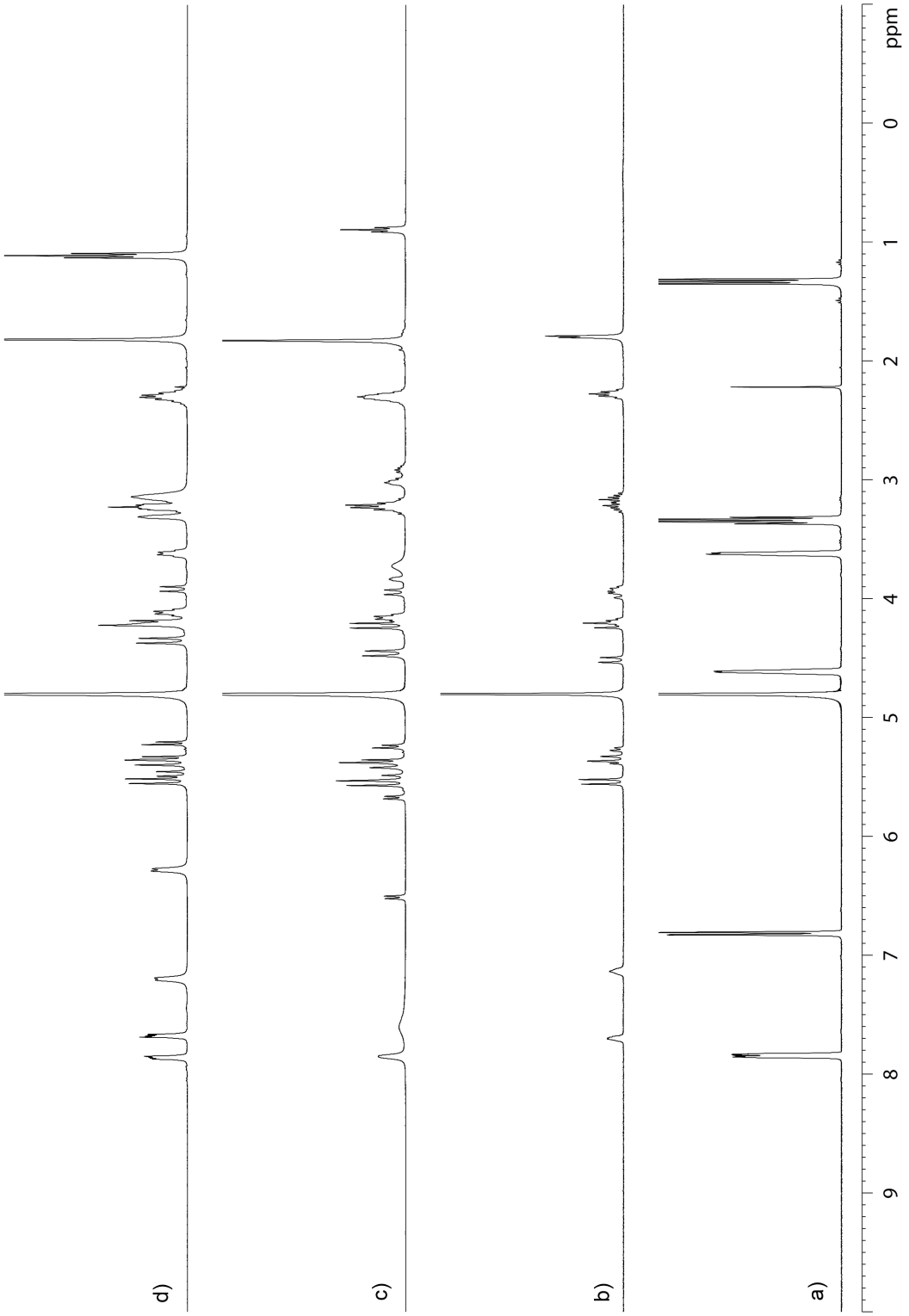

Figure S51. ^{1}H NMR spectra recorded (400 MHz, RT, D_2O) for a) **26**, b) **2**, c) an equimolar mixture of **2** and **26** (4 mM), and d) a 1:2 mixture of **2** (4 mM) and **26** (8 mM).

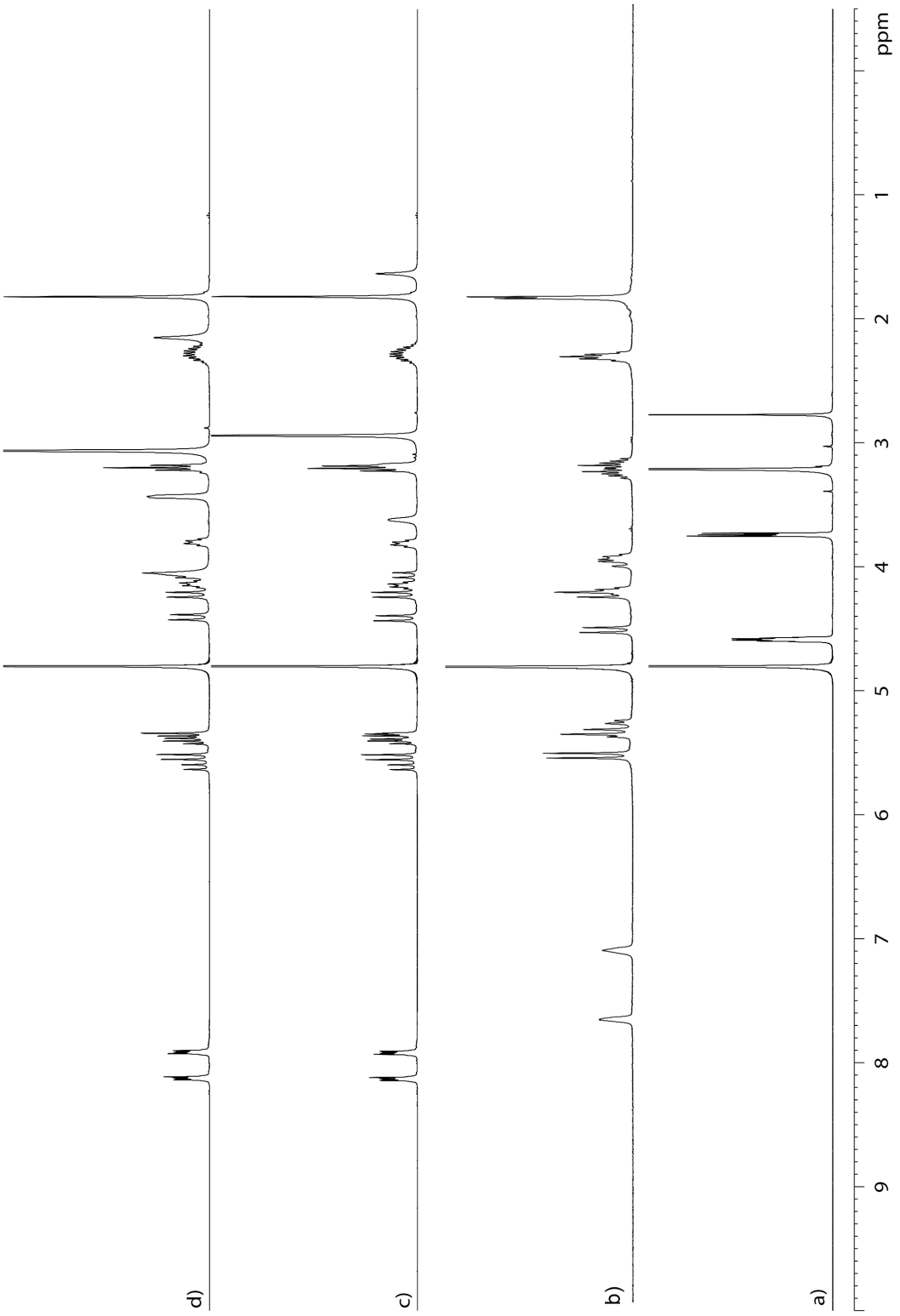

Figure S52. ^{1}H NMR spectra recorded (400 MHz, RT, D_2O) for a) **27**, b) **2**, c) an equimolar mixture of **2** and **27** (5 mM), and d) a 1:2 mixture of **2** (5 mM) and **27** (10 mM).

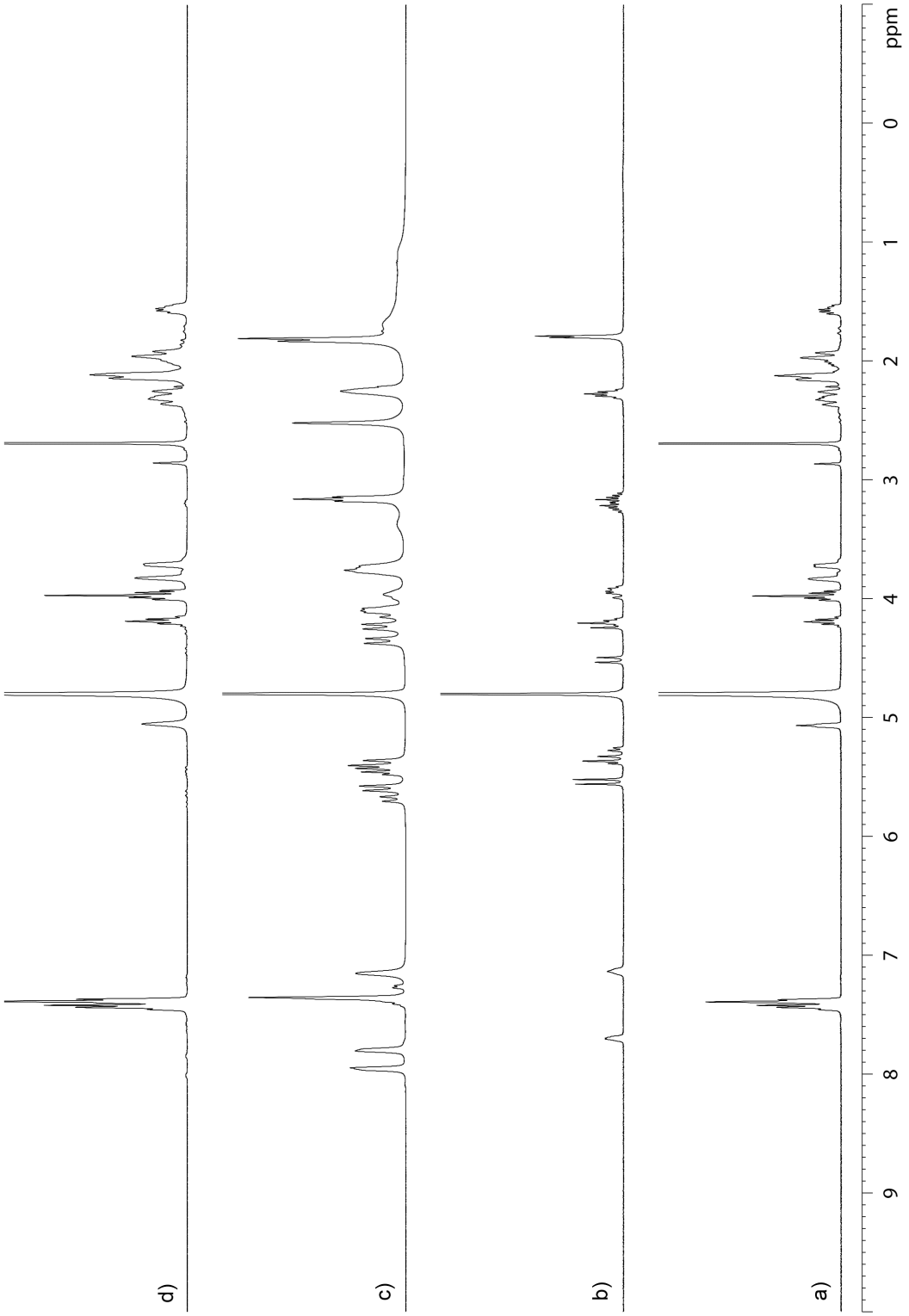

Figure S53. ^{1}H NMR spectra recorded (400 MHz, RT, D_2O) for a) **28**, b) **2**, c) an equimolar mixture of **2** and **28** (12.5 mM), and d) a 1:2 mixture of **2** (12.5 mM) and **28** (25 mM).

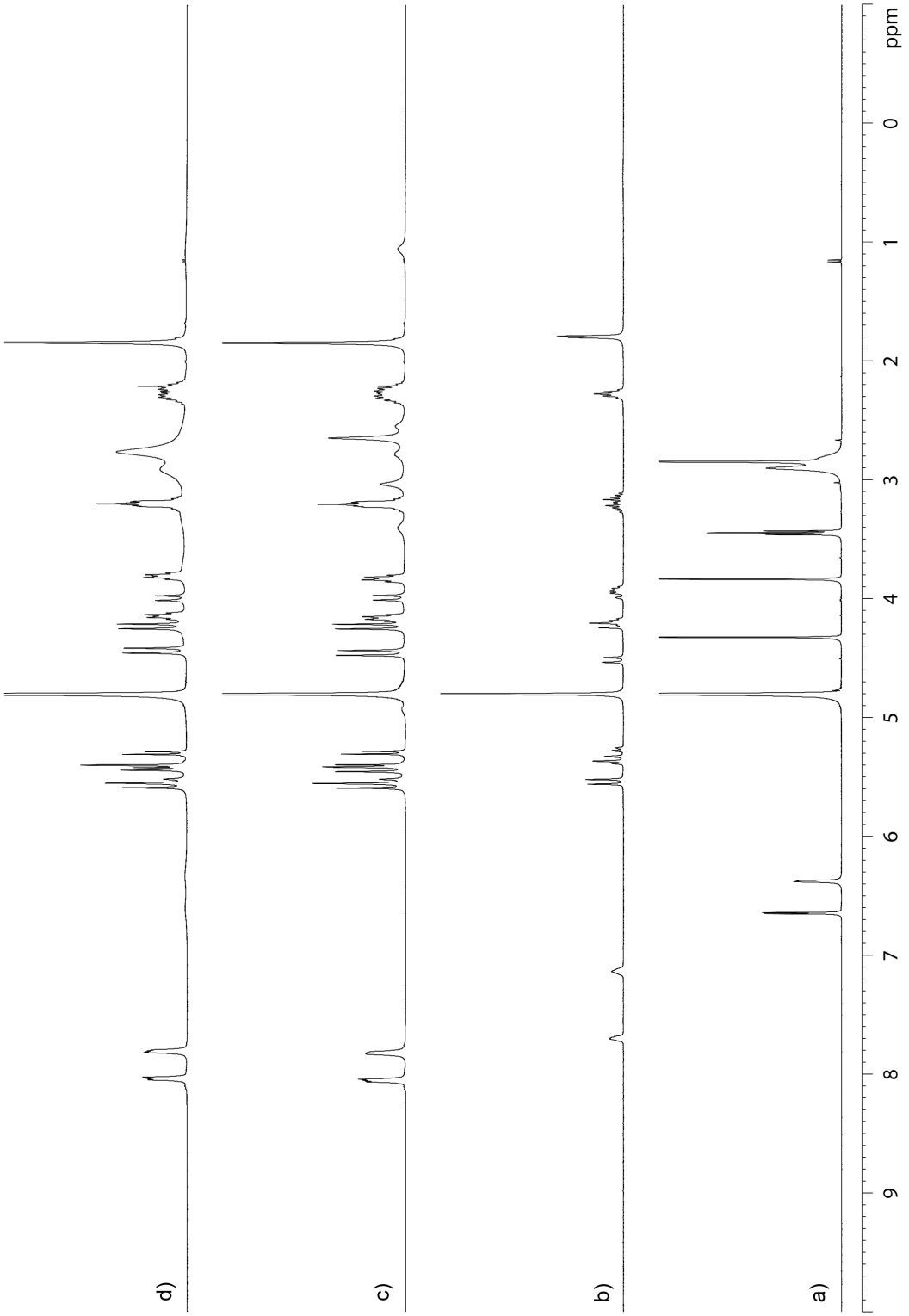

Figure S54. ^{1}H NMR spectra recorded (400 MHz, RT, D_2O) for a) **29**, b) **2**, c) an equimolar mixture of **2** and **29** (5 mM), and d) a 1:2 mixture of **2** (5 mM) and **29** (10 mM).

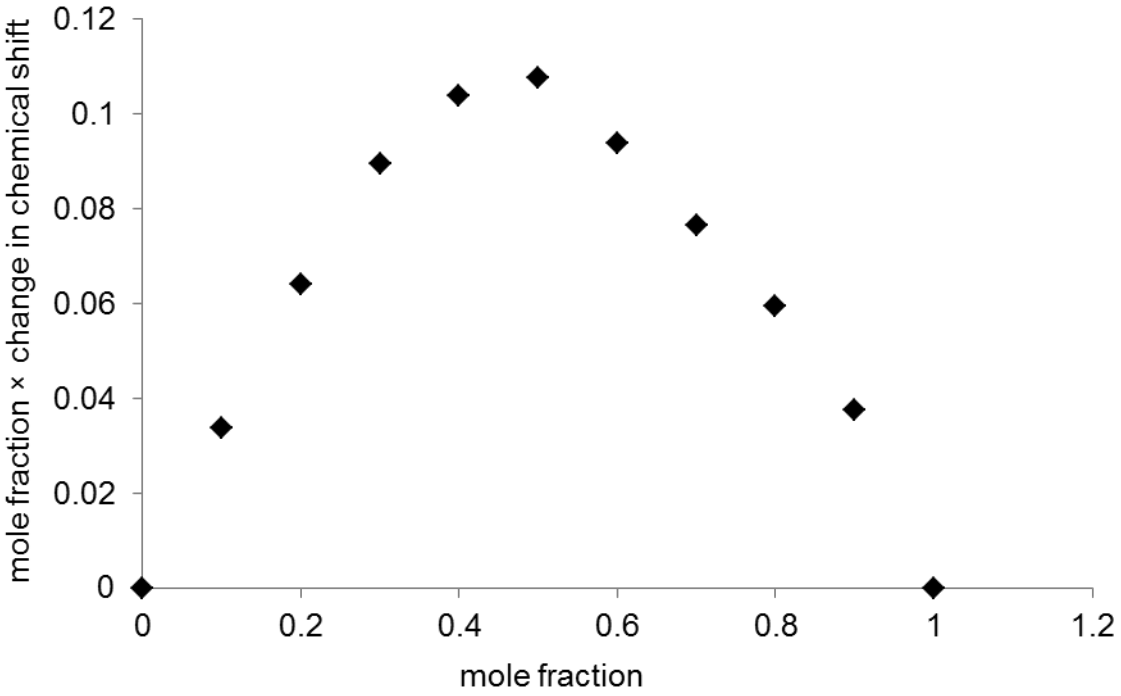

Figure S55. Job plot establishing 1:1 binding of **6** (0 - 1 mM) with **2** (0 - 1 mM) based on change in chemical shift of ^{1}H NMR (400 MHz, D_2O).

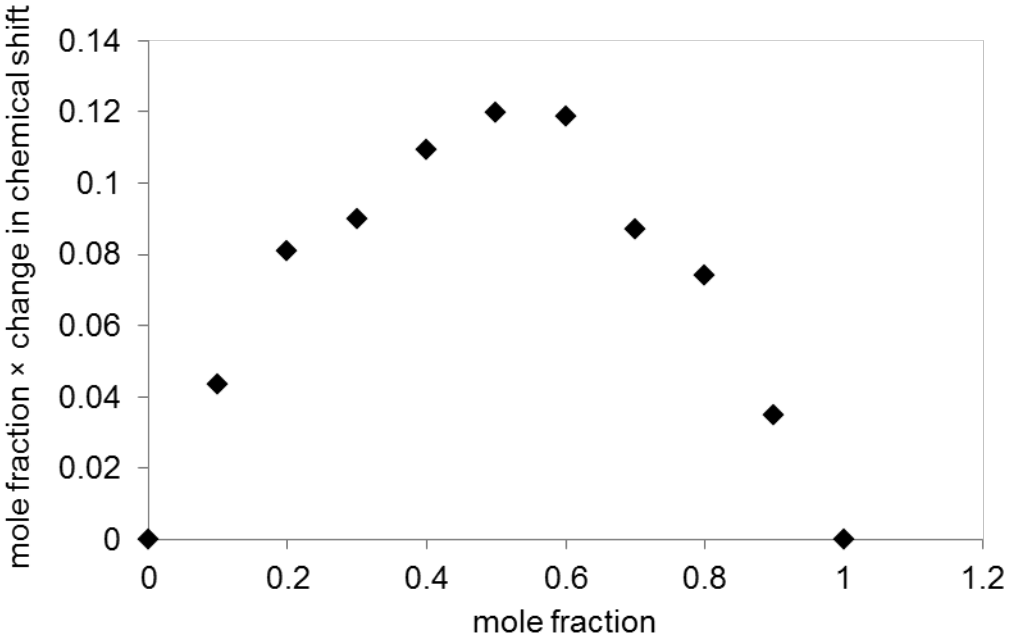

Figure S56. Job plot establishing 1:1 binding of **7** (0 - 1 mM) with **2** (0 - 1 mM) based on change in chemical shift of ^{1}H NMR (400 MHz, D_2O).

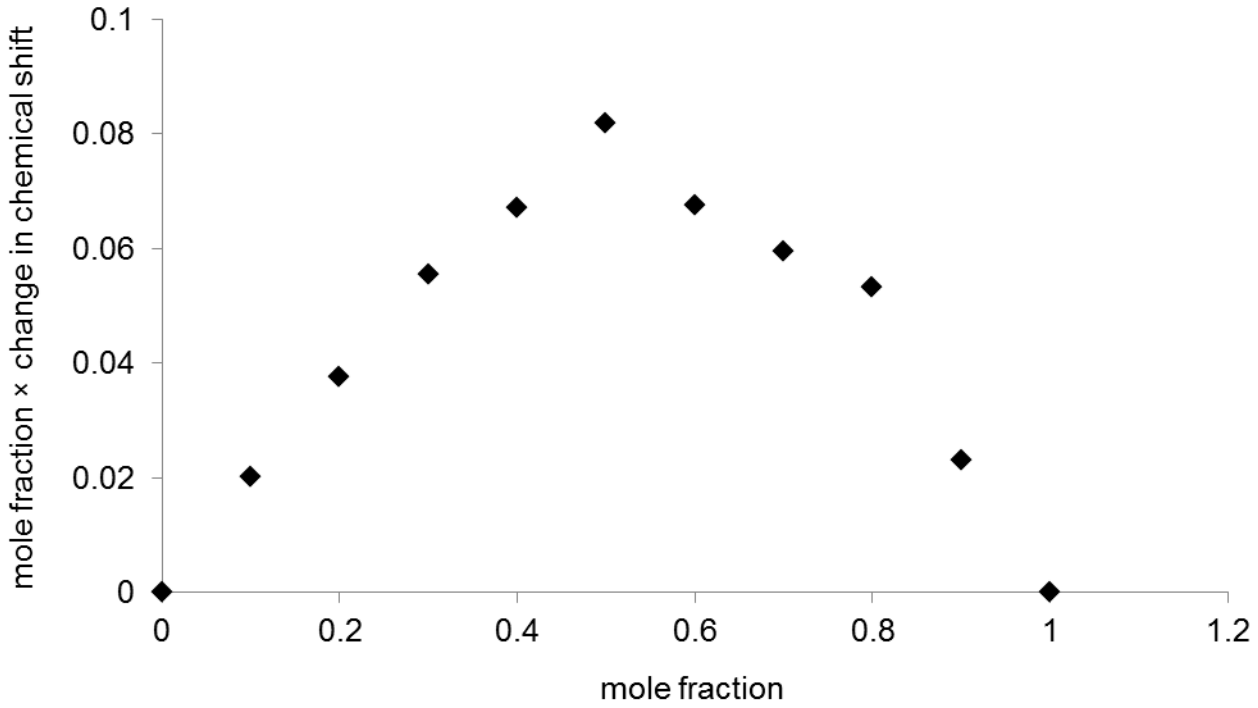

Figure S57. Job plot establishing 1:1 binding of **13** (0 - 1 mM) with **2** (0 - 1 mM) based on change in chemical shift of ^{1}H NMR (400 MHz, D_2O).

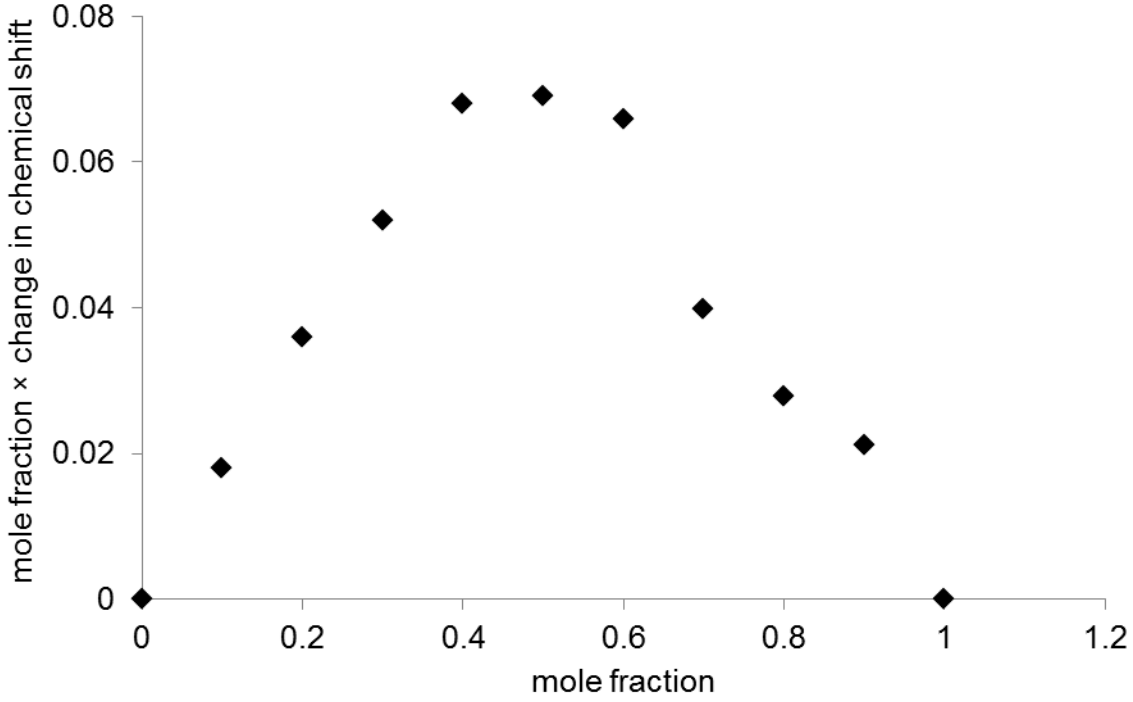

Figure S58. Job plot establishing 1:1 binding of **15** (0 - 1 mM) with **2** (0 - 1 mM) based on change in chemical shift of ^{1}H NMR (400 MHz, D_2O).

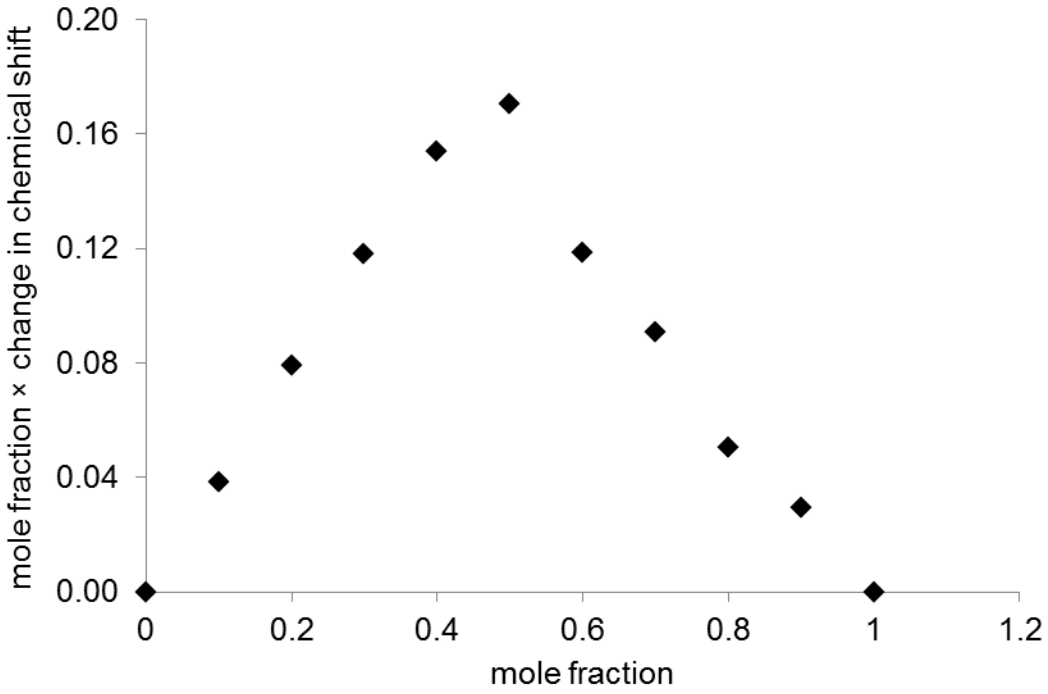

Figure S59. Job plot establishing 1:1 binding of **20** (0 - 1 mM) with **2** (0 - 1 mM) based on change in chemical shift of ^{1}H NMR (400 MHz, D_2O).

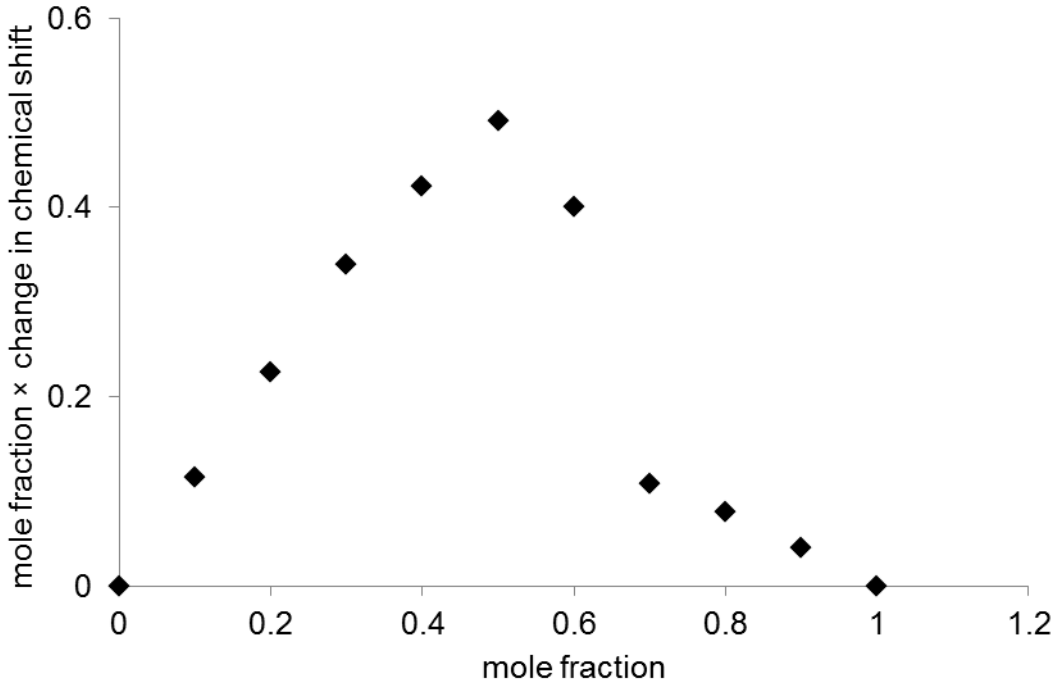

Figure S60. Job plot establishing 1:1 binding of **21** (0 - 1 mM) with **2** (0 - 1 mM) based on change in chemical shift of ^{1}H NMR (400 MHz, D_2O).

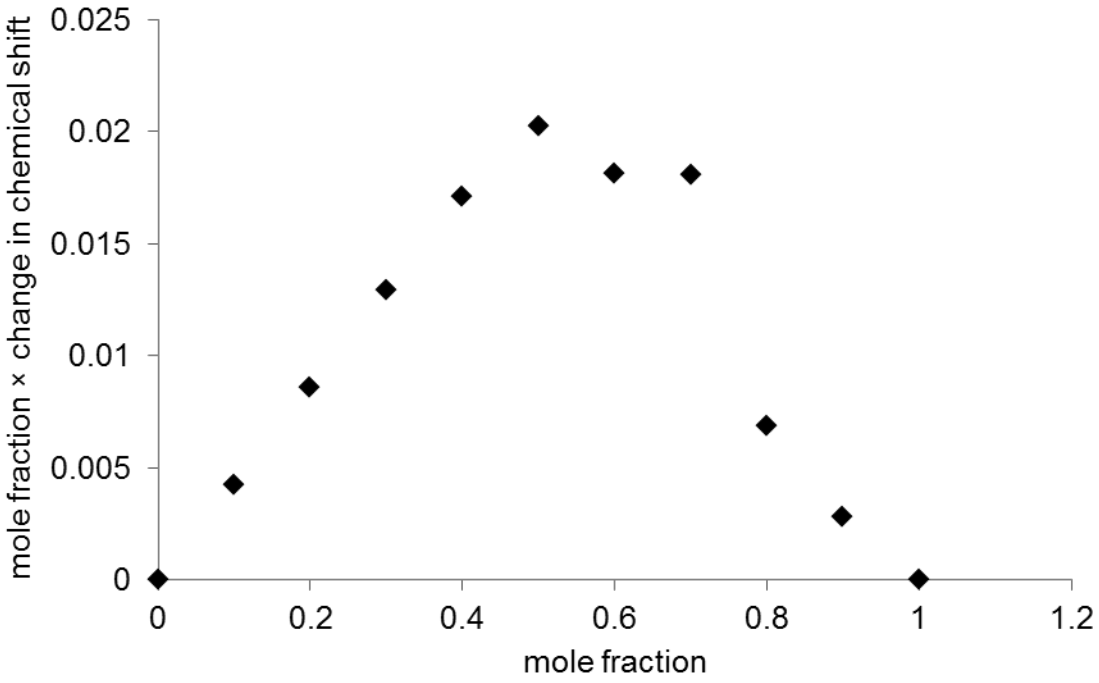

Figure S61. Job plot establishing 1:1 binding of **22** (0 - 1 mM) with **2** (0 - 1 mM) based on change in chemical shift of ^{1}H NMR (400 MHz, D_2O).

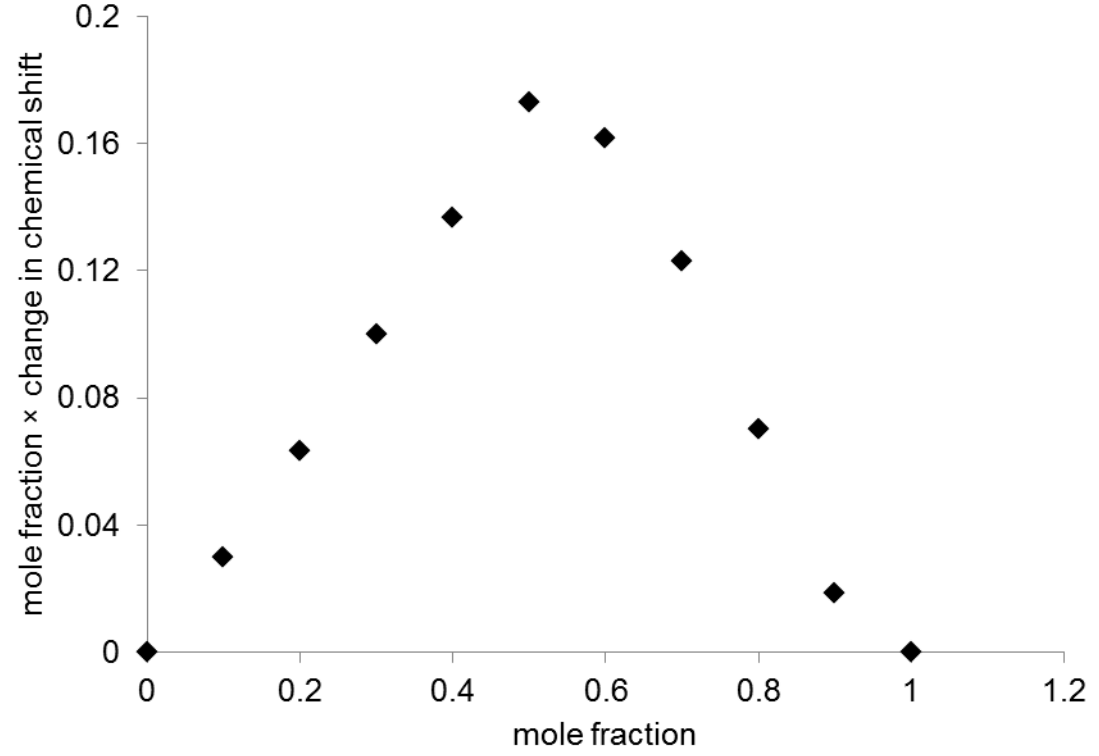

Figure S62. Job plot establishing 1:1 binding of **23** (0 - 1 mM) with **2** (0 - 1 mM) based on change in chemical shift of ^{1}H NMR (400 MHz, D_2O).

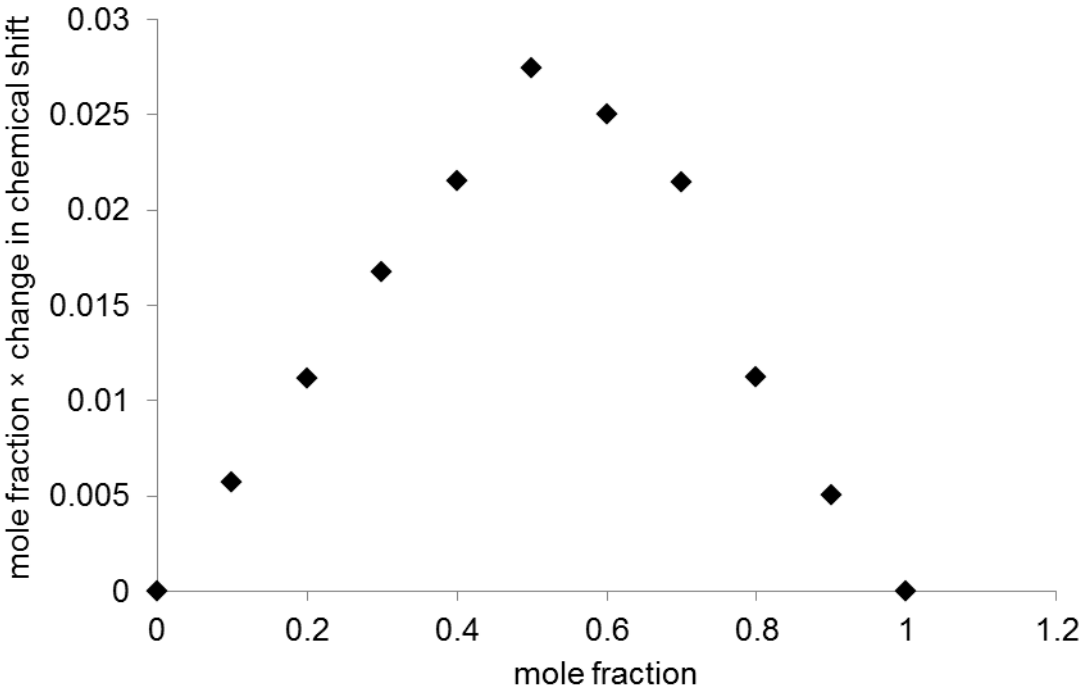

Figure S63. Job plot establishing 1:1 binding of **28** (0 - 1 mM) with **2** (0 - 1 mM) based on change in chemical shift of ^{1}H NMR (400 MHz, D_2O).

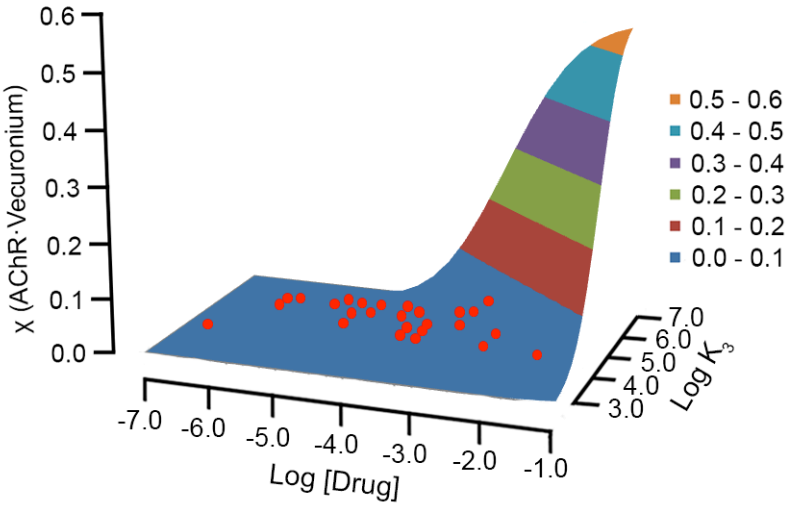

Figure S64. Three dimensional surface plot of the equilibrium mole fraction of AChR•vecuronium versus log [Drug] and log K_3 for vecuronium at [Vecuronium] = [AChR] = 27 μM, [**2**] = 54 μM (2 eqv.), $K_1 = 10^5$ M^{-1}, $K_2 = 1.6 \times 10^9$ M^{-1}. The red dots mark the points corresponding to each of the 27 drugs (**2** – **29**).

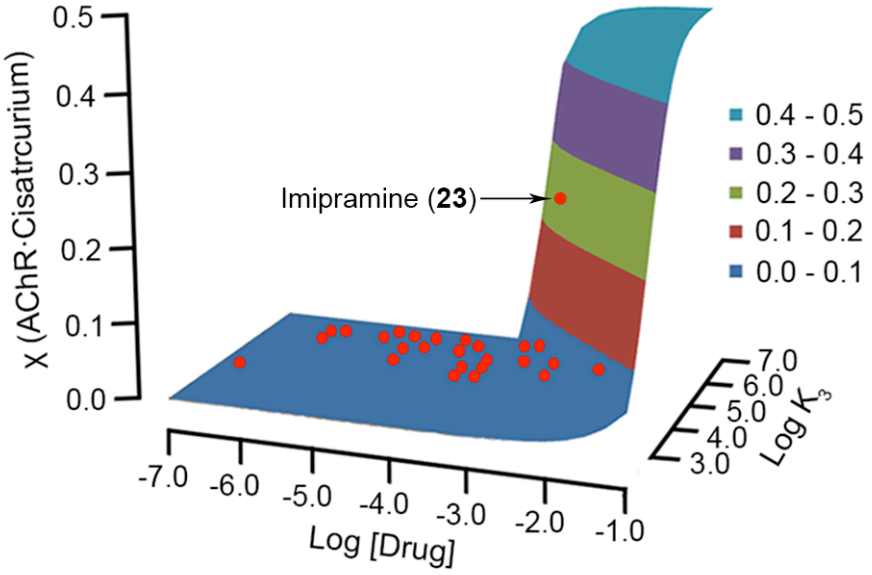

Figure S65. Three dimensional surface plot of the equilibrium mole fraction of AChR•cisatracurium versus log [Drug] and log K_3 at [Cisatracurium] = [AChR] = 18 μM, [**2**] = 576 μM (32 eqv.), $K_1 = 10^5$ M^{-1}, $K_2 = 4.8 \times 10^6$ M^{-1}. The red dots mark the points corresponding to each of the 27 drugs (**2** – **29**).

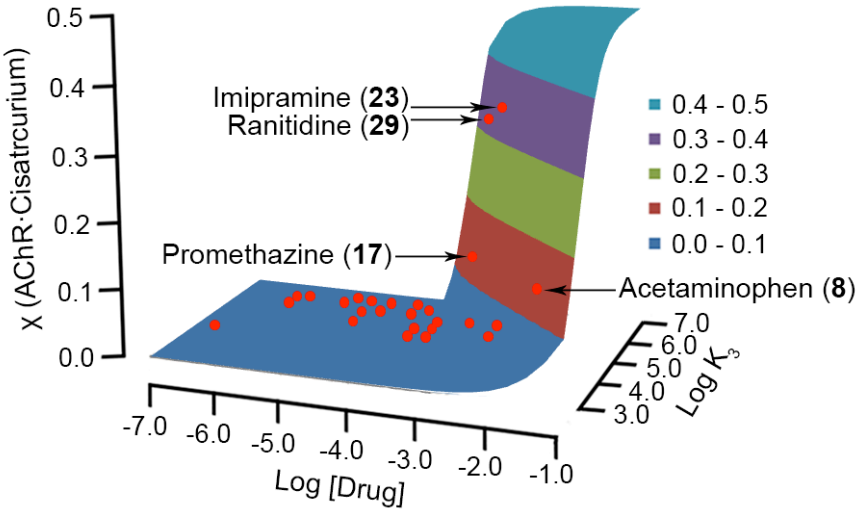

Figure S66. Three dimensional surface plot of the equilibrium mole fraction of AChR•cistracurium versus log [Drug] and log K_3 at [Cisatracurium] = [AChR] = 18 μM, [**2**] = 288 μM (16 eqv.), $K_1 = 10^5$ M^{-1}, $K_2 = 4.8 \times 10^6$ M^{-1}. The red dots mark the points corresponding to each of the 27 drugs (**2** – **29**).